

Biomedical &
Life Sciences

Lancaster
University



Repurposing glucagon-like peptide-1 (GLP-1) receptor agonists for the treatment of intestinal helminth infection

Master's by Research Thesis

Jessica Macluskie BSc (Hons)

Lancaster University

March 2025

I, Jessica Macluskie, confirm that the work presented in this thesis is my own and has not been submitted in substantially the same form for the award of a higher degree elsewhere,

Where information has been derived from other sources, I confirm that this has been indicated in the thesis.

Submitted in part fulfilment of the requirements for the degree of Master's by Research.

Table of Contents

<i>Acknowledgements</i>	5
1. <i>Abstract</i>	6
2. <i>Literature Review</i>	7
2.1 Gastrointestinal Parasites.....	7
2.2 Current Treatments	8
2.3 <i>Trichuris trichiura</i>	9
2.4 <i>Trichinella spiralis</i>	11
2.5 <i>Trichuris muris</i>	14
2.6 The Immune Response to Helminths; Worm Expulsion vs Chronic Infection.....	14
2.7 The Intestinal Epithelium in Helminth Infection.....	16
2.7.2 Tuft cells.....	17
2.7.3 Goblet Cells and Mucins.....	18
2.7.4 Enteroendocrine Cells.....	19
2.7.5 Intestinal Muscle Contractility.....	21
2.7.6 Epithelial Turnover.....	21
2.7.7 Intraepithelial Lymphocytes.....	23
2.8 GLP-1.....	24
2.9 GLP-1 Receptor Agonists.....	27
2.10 Aims.....	28
3. <i>Methods</i>	28
3.1. Animals.....	28
3.1.1 Small Intestinal Epithelial Organoid Culture.....	29
3.1.2 Immunofluorescent Staining of Small Intestinal Epithelial Organoids.....	29
3.1.3 GLP-1 Secretion Assay.....	29
3.1.4 GLP-1 ELISA.....	30

3.1.5 <i>T. muris</i> Infection, Faecal Egg Counts and Determination of Worm Burden.....	30
3.1.6 High Dose Chronic Infection.....	30
3.1.7 GLP-1 Receptor Agonist Treatment.....	30
3.1.8 T Cell Transfer.....	30
3.2. Parasite-Specific Enzyme Linked Immunosorbent Assay (ELISA).....	31
3.3. Histology.....	31
3.3.1 Alcian Blue-PAS for Goblet Cells.....	31
3.3.2 BrdU Pulse-Chase Experiment for Epithelial Turnover.....	31
3.4 Mesenteric Lymph Node Cell Isolation and Restimulation.....	32
3.5 Flow Cytometry.....	32
3.6 Statistical Analysis.....	33
4. Results	34
4.1 Organoid culture represents expected GLP-1 ⁺ EEC spatiotemporal ratio and development pathways.....	34
4.2 Helminth antigen increases secretion of GLP-1 without direct influence on GLP-1 ⁺ EEC development.....	37
4.3 The influence of GLP-1rA treatment on a trickle <i>T. muris</i> reinfection.....	40
4.4 Lixisenatide treatment decreases worm burden in <i>T. muris</i> -infected RAG mice reconstituted with T cells following GLP-1rA treatment.....	54
4.5 Lixisenatide reduced worm burden in chronic, high-dose <i>T. muris</i> infection.....	63
5. Discussion	73
5.1 Helminth antigen increases GLP-1 secretion without direct influence on GLP-1 ⁺ EEC frequency.....	74
5.2 The effect of GLP-1rA treatment on a trickle <i>T. muris</i> infection remains inconclusive.....	76
5.3 Adoptive transfer of CD4 ⁺ T cells from lixisenatide-treated mice provides some protection against challenge <i>T. muris</i> infection.....	78

5.4 GLP-1rA treatment reduces worm burden in chronic, high-dose <i>T. muris</i> infection	81
5.5 GLP-1rA treatment increased intestinal epithelial turnover.....	83
5.6 GLP-1rA has no effect on caecal crypt structure.....	84
5.7 Limitations	85
5.8 Importance of the work.....	86
5.9 Conclusions.....	88
6. Appendix: Exploring the potential use of QuCCi reporter mice to investigate intestinal epithelial turnover in <i>T. muris</i> infection	90
7. References	92

Acknowledgements

I would like to express my appreciation to my supervisor, Dr John Worthington for affording me the opportunity to pursue this research project under his supervision and for his continuous support, guidance, and encouragement throughout the course of my project.

I would also like to recognise my family for their support throughout my project; to my fiancé for pushing me to pursue this project in the first instance, for his endless love, patience and understanding throughout this project, and for driving me to the lab at all times of the day and night so that I could complete my work, thank you! To my parents, Ian and Margaret, and to Maighdlin, William and Ann, for their continued love, support and encouragement.

1. Abstract

Soil-transmitted helminth infections are neglected tropical diseases, afflicting over 1.5 billion people in developing countries. Children often endure the heaviest parasite burdens, suffering from malnutrition, stunted growth and cognitive impairment. The widespread use of anthelmintic drugs as preventative chemotherapy has accentuated low cure rates, high reinfection rates and increasing prevalence of anthelmintic-resistant species, particularly in *Trichuris* infection, highlighting an urgent need for novel treatments. Intestinal helminth infections are associated with changes in enteroendocrine cell (EEC) development and peptide hormone secretion. Furthermore, intraepithelial lymphocytes, found at the parasite intestinal barrier niche, have been shown to express receptors for the EEC derived incretin peptide hormone, glucagon-like peptide-1 (GLP-1). Recently GLP-1 receptor agonist (GLP-1rA) treatment has been shown to induce expulsion of a chronic low-dose *Trichuris muris* infection via the adaptive immune system and accelerated intestinal epithelial turnover. However, the effects of intestinal helminths on endogenous GLP-1 secretion are currently unknown. Furthermore, the efficacy of GLP-1rA treatment in individuals with high infection intensity, and against challenge infection, is yet to be investigated. A small intestinal organoid platform was used to investigate the effects of intestinal helminth antigen on GLP-1 secretion. The mouse model of human trichuriasis, *Trichuris muris*, was employed to investigate the potential for the GLP-1rA, lixisenatide to induce protective effects against challenge infection, and, via rIL-12-pretreatment, to investigate the efficacy of lixisenatide against a chronic high-dose infection. *Trichinella spiralis* was shown to increase GLP-1 secretion from EECs in the small intestine through a mechanism mediated by bitter taste receptors. *In vivo* experimentation demonstrated that lixisenatide treatment drives a reduction in worm burden in a chronic, high-dose *T. muris* infection, and induces CD4⁺ T cell-mediated protection against challenge infection. These data provide further evidence that this treatment may provide an exciting novel option for the treatment of intestinal STH infection, with efficacy in reducing high intensity infection and providing some protection against reinfection, crucial effects that current anthelmintic treatments lack. GLP-1rAs are already approved for the treatment of type 2 diabetes mellitus and obesity, which would allow for rapid and straightforward repurposing of this drug class for the treatment of Trichuriasis afflicting livestock and humans worldwide.

2. Literature review

2.1 Gastrointestinal Parasites

Despite continued advancements in sanitation and drug regimens, parasitic infections remain a key cause of morbidity and mortality in both humans and animals throughout the world (Wright 2012). A common site of primary parasitic involvement is the gastrointestinal (GI) tract, associated with parasites of protozoan or helminthic natures; protozoan parasites are more prevalent in developed countries than helminths, which are much more commonplace in developing countries (Sinha *et al.* 2012; Taghipour *et al.* 2021).

Soil-transmitted helminths (STHs) are parasitic worms which are transmitted by the faecal-oral route, following the contamination of the environment by egg-containing faeces from infected individuals (World Health Organisation 2023). STH infections are currently believed to afflict almost 25% of the world's population (Palmeirim *et al.*, 2018), with their prevalence reportedly highest in Asia, South America and sub-Saharan Africa (Figure 2.1). The four major nematode species afflicting humans include the whipworm (*Trichuris trichiura*), roundworm (*Ascaris lumbricoides* and *Trichinella spiralis*), hookworms (*Ancylostoma duodenale* and *Necator americanus*) and threadworm (*Strongyloides stercoralis*) (Loukas *et al.* 2021). In general, STH infections are not associated with mortality but are diseases of severe morbidity; with moderate- and high-intensity infections associated with symptoms including weight loss, diarrhoea and malnourishment (Mascarini-Serra 2011, Ngwese *et al.*, 2020). STH infections, therefore, have intense impacts on quality of life, and were reportedly responsible for the loss of over 5 million disability-adjusted life-years (DALYs) worldwide in 2010, and are therefore involved in the maintenance of an impoverished community (Hay *et al.* 2017, Hotez *et al.* 2014).

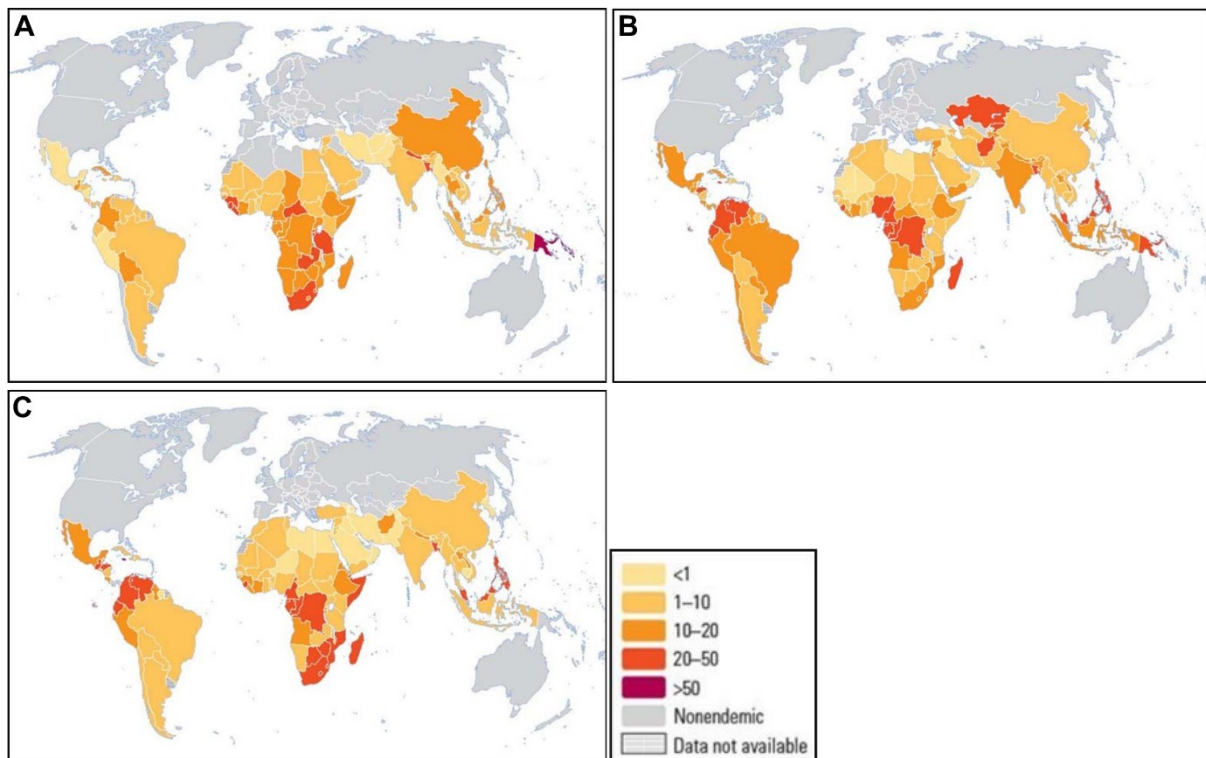


Figure 2.1: Global Distribution of Soil Transmitted Helminth infection by species, in pre-school and school-age children in 2015. Prevalence (%) of (A) Hookworm (B) Roundworm and (C) Whipworm infection, showing greater transmission of whipworm and roundworm infection in urban areas, but greater hookworm transmission in rural areas. Figure adapted from Bundy *et al.* 2017.

While low-intensity infections, characterised by low worm burden, are often asymptomatic, moderate- and high-intensity infections are associated with severe morbidity and clinical manifestations including weight loss, diarrhoea, anaemia and abdominal pain, with children also showing stunted growth, clubbing of the fingers and malnourishment (Mascarini-Serra 2011).

Pregnant women are at increased risk of STH infection compared to the wider population; however, children of school age are the most vulnerable to infection (Adegnika *et al.* 2007; Bethony *et al.* 2006). Children often present with high worm burdens and suffer with symptoms including stunted growth, cognitive impairment, malnutrition, anaemia, and intestinal blockage (Bethony *et al.* 2006). Despite donations of anthelmintic drugs to endemic countries, many children still lack access to treatment with only half of at-risk children receiving treatment in 2016 through mass drug administration programmes. Furthermore, these programmes aim to reduce infection intensity, rather than eradicating infection (Jourdan *et al.* 2018).

2.2 Current Treatments

Broad-spectrum anthelmintic (AH) drugs are the basis of the treatment and management of infection caused by STHs; treatment of infection and preventative chemotherapy utilises a small number of drugs belonging to three major drug classes, namely benzimidazoles (BZs), cholinergic agonists and macrocyclic lactones (MLs) (Fissiha *et al.* 2021; Prangthip *et al.* 2023) BZs, such as albendazole and

mebendazole, are the most commonly used in humans (Chai *et al.* 2021). In countries where STH infections are endemic, prevention of infection through provision of adequate sanitation is not always possible, and so preventative chemotherapy is often implemented for individuals who are deemed at-risk. In general, children of preschool and school age, women of reproductive age, women in the second or third trimester of pregnancy and adult groups with high risk of exposure are administered 400mg albendazole or 500mg mebendazole as a single dose to be taken once or twice per year (World Health Organisation 2017), with the aim of reducing infection intensity. Preventative chemotherapy is not used in 'developed' countries where STH infections are rare; STH infections in the UK are not currently commonplace, likely due to widespread provision of high-quality sanitation and improvements in hygiene education and food preparation (Ryan *et al.* 2022), although NHS guidelines suggest that mebendazole administration twice daily for three days is sufficient for the treatment of whipworm, roundworm, and hookworm infections (NHS 2019).

Preventative chemotherapy (PC) has shown some efficacy in endemic countries; the WHO estimates that the implementation of PC averted over 44% of STH-associated DALYs that would have been caused in children in 2015 (Montresor *et al.* 2017). However, efficacy of these mass drug administration programmes in the treatment and prevention of trichuriasis, the disease caused by *Trichuris trichiura*, is limited by low cure rates and high rates of reinfection; randomised controlled trials in the analysis of anthelmintic efficacy have shown that mebendazole shows the highest efficacy against *T. trichiura*, although with a cure rate of only 25.9-60.2% (Hotez 2017; Moser *et al.* 2017; Speich *et al.* 2014).

Furthermore, the high-intensity use of anthelmintic agents in livestock has demonstrated a rapid emergence of anthelmintic-resistant (AR) populations, as particularly evident in small ruminant livestock nematode infections (Kaplan 2004). Although helminth infection in livestock presents a significant burden on animal health and welfare and agricultural productivity (Kaplan 2004; Fissiha *et al.* 2021) as well as potentially increasing greenhouse gas outputs of these rumen (Fox *et al.* 2018; Kenyon *et al.* 2013), routine use of AH agents selects strongly for AH resistance. Kenyon *et al.* (2013) showed that regular treatment of livestock with AH therapies increased the number of animals that reached their slaughter weight in 5 years compared to those treated only upon evidence of parasitism, however, this 4-weekly use of ivermectin resulted in a 33.4% reduction in efficacy over 5 years. Moser *et al.* (2017) also showed a reduction in the efficacy albendazole in *T. trichiura* infection by 29.2% between 1995 and 2015.

The alarming rate of anthelmintic resistance in animals, and low efficacy in the prevention of trichuriasis in humans, highlights a grave situation and calls into question the long-term efficacy of PC. Therefore, increasing our understanding of these helminths and the immune response to helminth infection is key to identifying novel therapeutic targets.

2.3 *Trichuris trichiura*

Colloquially referred to as 'whipworm', *Trichuris trichiura* is one of the most prevalent STH infections in humans, currently believed to afflict more than 600 million people worldwide (Centers for Disease Control and Prevention 2023). Trichuriasis disproportionately affects populations in impoverished areas

where access to quality sanitation is poor, with greatest prevalence in Latin America and Caribbean regions, as well as South-Eastern Asia and Sub-Saharan Africa (Else *et al.* 2020; Behniafar *et al.* 2024). Children between the ages of 5 and 15 bear the highest infection prevalence within endemic communities, and this age group also suffer with most significant clinical manifestations associated with highest worm burdens (McDowell and Rafaty 2014; Else *et al.* 2020). Symptoms of trichuriasis associated with high worm burden include gastrointestinal pain and bleeding, malnutrition, and anaemia (OK *et al.* 2009, Stephenson *et al.* 2000, Speich *et al.* 2014). In children, even low-intensity infection is associated with stunted growth and malnutrition, and increased worm burden associated with *Trichuris* dysentery-syndrome (TDS), characterised by chronic dysentery, rectal prolapse, anaemia, stunted growth and clubbing of the fingers (Bundy & Cooper 1989; Stephenson *et al.* 2000).

Transmission of *T. trichiura* occurs through the faecal-oral route (Fig. 2.2); following ingestion, physical interaction of bacterial species of the host gut microbiota triggers larval activation, and serine proteases of both larval and bacterial origins degrade a polar plug of the ovum, facilitating larval rupture from the egg in the proximal colon (Hayes *et al.* 2010; Goulding *et al.* 2025). This hatching dependent upon physical bacterial interaction is best-characterised, however there has since been evidence to suggest that hatching can occur independently of direct contact (Koyama 2015) and, in the S strain of *T. trichiura*, independently of bacteria altogether (Koyama 2013). Following hatching, L1 larvae emerge and burrow into the epithelial layer at the base of the crypts to form syncytial tunnels (Cliffe and Grecis, 2004). Within this niche, L1 larvae grow and progress through four larval stages and subsequent adult stages where they can persist for up to 8 years; the posterior end of L3, L4 and adult worms protrudes into the intestinal lumen allowing for copulation and oviposition (Else *et al.* 2020). Fertilised females can release up to 8000 eggs per day (Pike 1969; Else *et al.* 2020); these unembryonated eggs are shed in the faeces and passed into the environment where embryonation can occur at temperatures between 0-37°C (Else *et al.* 2020). It is reported that these eggs can remain infective in the environment for at least 5 years (Brown 1927).

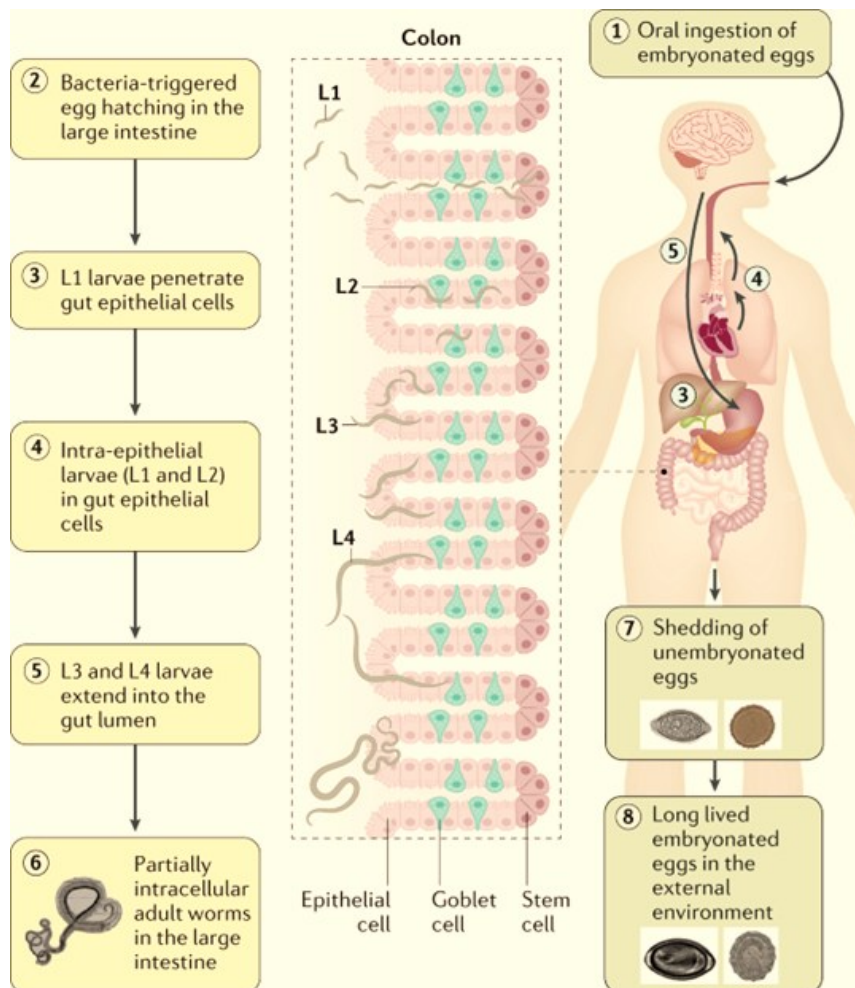


Figure 2.2: The life cycle of *Trichuris trichiura*. Infection begins when embryonated eggs are ingested. Eggs hatch in the large intestine in response to resident bacteria, releasing L1 larvae which burrow into the epithelium of the intestinal crypts. Here, the larvae grow and undergo a series of moults (L2-L4) before a final moult reveals the adult worms. Sexually mature adult worms mate and females produce unembryonated eggs which are released into the gut lumen and shed in the faeces. These eggs develop and become embryonated under sufficient moisture and temperature conditions. Figure adapted from Else *et al.* 2020.

Key to increasing our understanding of *Trichuris* infection has been use of the murine parasite, *Trichuris muris*; use of this rodent model of trichuriasis has allowed for the elucidation of the host-parasite interactions and the immune responses underpinning susceptible and resistant phenotypes (Klementowicz *et al.* 2012).

2.4 *Trichinella spiralis*

Trichinosis, caused by parasitic roundworms of the genus *Trichinella*, is a foodborne parasitic disease transmitted through the consumption of raw or undercooked meat of infected mammals, birds and reptiles. *Trichinella spiralis* is ubiquitous in its distribution, infecting most warm-blooded vertebrates, but

is a significant parasite afflicting humans and is most often transmitted through the consumption of raw or undercooked pork and horse meat (Gottstein *et al.* 2009). Trichinosis is most prevalent in parts of Europe and the United States, (Centers for Disease Control, 2024) leading to approximately 10 000 cases per year (Murrell & Pozio 2000; Pozio 2007) worldwide. Epidemiology of *T. spiralis* infection is strongly associated with culturally associated consumption of traditional dishes based on raw or undercooked meat (Murrell *et al.* 2000).

The initial, enteral phase of infection occurs following ingestion of contaminated meat containing collagen-encapsulated muscle larvae from the domestic or sylvatic cycle (Fig. 2.3). Gastric digestion releases the encapsulated *T. spiralis* larvae which invade the small intestinal mucosa and undergo a series of four rapid moults before maturing to adulthood. This process of maturation is complete within 48 hours of ingestion. Once mature, male and female worms copulate and between 5- and 7-days post-infection and females begin to release immature larvae, with females producing up to 1500 larvae during their lifespan. The parenteral, muscular phase of infection occurs when these newborn larvae migrate to highly oxygenated striated muscle tissue via the lymphatics and circulation. Alterations in infected muscle cell apoptosis leads to transformation of the muscle cells into encapsulated nurse cells within approximately 15 days of infection (Despommier *et al.* 1995; Gottstein *et al.* 2009). These infective larvae have been known to survive in humans for up to 40 years (Fröscher *et al.* 1988). Given that *T. spiralis* completes its life cycle within a single host, it is ideal for utilisation as a model to observe and quantify the efficacy of anthelmintic agents (El-Sayad *et al.* 2023). Furthermore, given the ability of all mouse strains to expel enteral *T. spiralis* this helminth is a commonly utilised model of a transient enteric infection (Bell & Liu 1988).

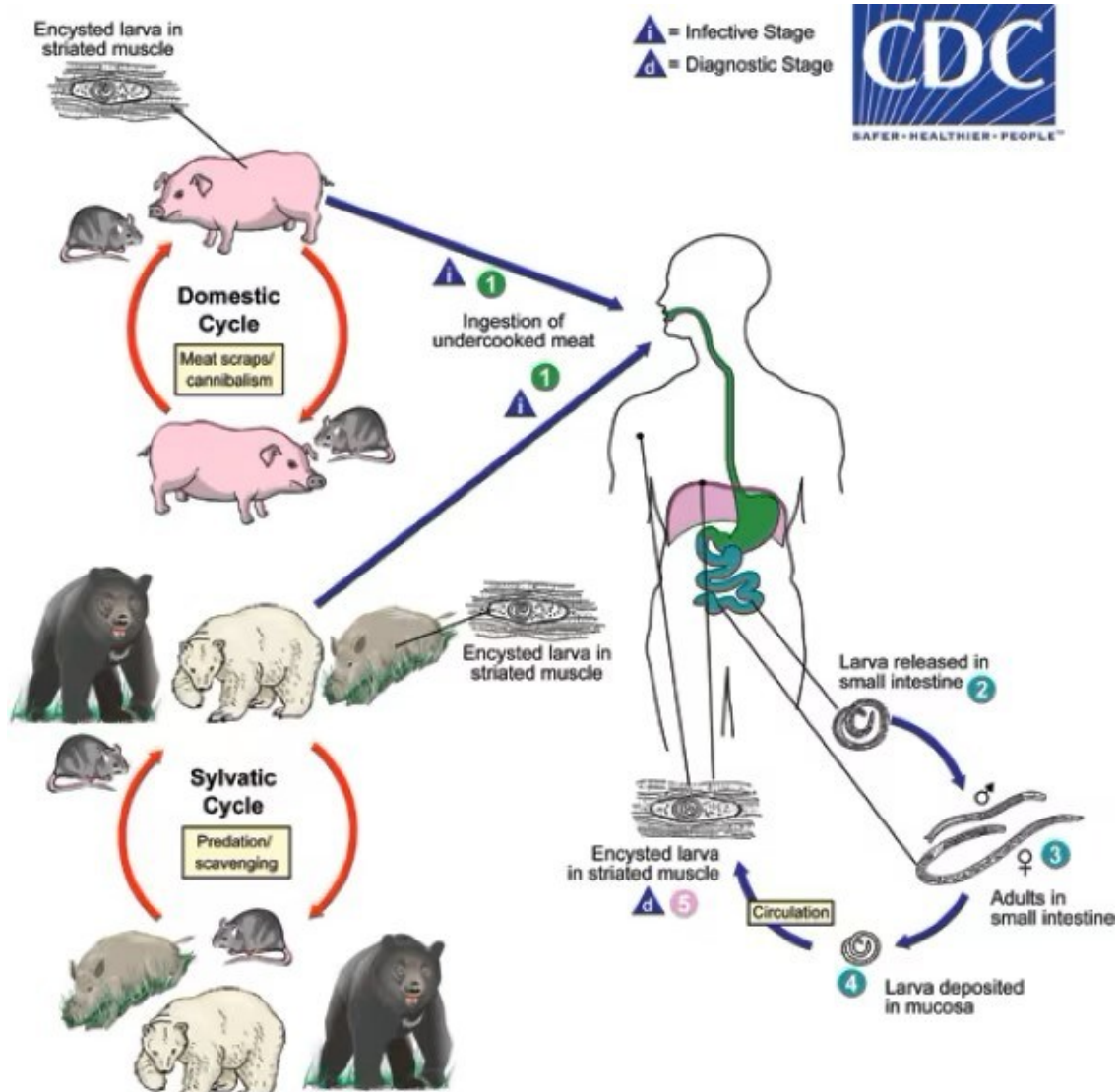


Figure 2.3: *Trichinella spiralis* life cycle. 1) Animals that are fed other animals (domestic cycle) or eat other animals (sylvatic cycle), such as pigs and bears, respectively, become infected through the consumption of meat containing tissue-encysted larvae. Humans become infected through the consumption of raw or undercooked meat containing tissue-encysted larvae. 2) Following pepsin and gastric acid exposure, larvae are released from the cysts in the small intestine and penetrate the intestinal mucosa. 3) Larvae undergo a series of moults and develop into adult worms. 4) After 1 week, females release larvae that migrate to striated muscles where they become encysted. 5) The life cycle continues when a tissue containing encysted larvae is ingested by another carnivore. Image adapted from Centers for Disease Control, 2024.

Diagnosis of trichinosis is often delayed due to a lack of pathognomonic symptoms; low intensity infections often remain asymptomatic, although higher intestinal worm burden can cause acute gastroenteritis, pyrexia and malaise early in infection. Periorbital and/or facial oedema and myalgia are principal manifestations of the parenteral phase of trichinosis, which is also associated with

complications including encephalitis and myocarditis, (Capo & Despommier 1996) and secondary infections such as sepsis. Though rare, these complications can be fatal, with trichinosis associated with a mortality rate of 0.2% (Pozio 2007; Gottstein *et al.* 2009).

T. spiralis is a self-limiting intestinal infection; although infection induces a complex mixed T-helper (T_h)-1/T_h2 response, a predominance in polarisation towards T_h2 induces expulsion of adult worms in the intestine. Given the self-limiting nature of infection, mild infections are generally treated symptomatically using anti-pyretic and anti-inflammatory agents. Cases of trichinosis resulting in systemic complications, and therefore requiring diagnosis, are routinely treated using anthelmintic agents (often albendazole or mebendazole) and corticosteroids (Gottstein *et al.* 2009). However, the efficacy of chemotherapy using anthelmintics is strongly dependent upon time of administration; drug administration during the first 3 days post-infection induces intestinal worm expulsion and prevents muscular invasion. However, efficacy of these agents against the tissue-encysted larvae is variable (Pozio *et al.* 2001; Codina *et al.* 2015).

2.5 *Trichuris muris*

T. muris exists as a natural chronic infection of wild rodents. Sharing high levels of morphology, antigenic cross-reactivity and niche with the human parasite, this murine helminth is utilised as a laboratory model for human trichuriasis which has allowed the characterisation of the nature of host immune polarisation in promoting chronic infection or parasite expulsion (Zaph *et al.* 2014; Yousefi *et al.* 2021). Our understanding of the expulsion mechanisms and the immune response mounted towards *T. muris* have allowed for the identification of possible novel drug targets (Klementowicz *et al.* 2012; Cruz *et al.* 2021).

The life cycle of *T. muris* is similar to that of *T. trichiura*; following ingestion of embryonated eggs from contaminated environment, eggs hatch in the caecum and proximal colon in response to molecular signals from the host gut microbiota. L1 larvae hatch and burrow into the epithelium of the caecum and proximal colon where they undergo a series of moults. These worms reach patency at approximately 33 days post-infection and, during chronic infection, may survive in their host for more than 100 days (Bancroft and Grensis 2021). Mature, adult females lay eggs which are released into the intestinal lumen and passed in the faeces, which become embryonated in the environment in temperatures between 0-37°C (Else *et al.* 2020).

2.6 The Immune Response to Helminths; Worm Expulsion vs Chronic Infection

In general, immunity to intestinal helminths is dependent on the induction of a type 2 immune response, which is essential for worm expulsion while promoting tissue repair. During *Trichuris* infection, the polarisation of the immune response towards a type 2 phenotype is associated with worm expulsion, whereas a type 1 response facilitates chronic infection (Cliffe *et al.* 2005). Though enteric *T. spiralis* induces a mixed T_h1/2 response, a predominance in polarisation towards a type 2 phenotype during the systemic phase of infection induces expulsion of adult worms from the intestine (Allen & Maizels 2011). This T_h2-dominated response to both helminths drives significant change in intestinal epithelial

physiology, known as the 'weep and sweep' response, to physically expel the helminths from their niche (Darlan *et al.* 2021).

In intestinal helminth infection, physical invasion of the intestinal epithelium by helminth larvae triggers the release of alarmin cytokines, including interleukin (IL)-25, IL-33 and thymic stromal lymphopoietin (TSLP), which are essential to the recruitment of dendritic cells (DCs) and other antigen presenting cells (APCs) to the intestinal mucosa (Owyang *et al.* 2006; Angkasekwinai *et al.* 2013; Kumar *et al.* 2014). Presentation of parasite antigen to adaptive immune cells in the mesenteric lymph node (mLN) coordinates the expansion of a T_H1 or T_H2 response. In resistant animals, release of type 2 cytokines including IL-4, IL-5, IL-9 and IL-13 drives the 'weep and sweep' response to control helminth infection. Conversely, production of type 1 cytokines, including IL-12 and interferon (IFN) γ , facilitates the establishment and persistence of chronic infection (Cliffe *et al.* 2005).

A T_H2-dominated immune response is characterised by IL-4 production; IL-4 signalling through STAT6 promotes and stabilises T_H2 cell differentiation via upregulation of the T_H2-specific transcription factor GATA3, which also inhibits T_H1 cell differentiation (Kanhere *et al.* 2012). In *T. muris* infection, knockout of IL-4 induces a susceptible phenotype in male BALB/c mice. Female littermates, who benefit from compensatory enhancement of T_H2 responses through 17 β oestradiol (Lambert *et al.* 2005; Hamano *et al.* 1998) retain their resistance until IL-13 is also ablated (Bancroft *et al.* 1998). In *T. spiralis* infection, mice lacking functional IL-4 α , a key component of both IL-4 and IL-13 receptors, are incapable of clearing adult worms from the small intestine (Urban *et al.* 2000). IL-13 is central to the 'weep and sweep' response, promoting increased epithelial turnover, goblet cell hyperplasia and changes in mucous composition (Grencis 2001; Hayes *et al.* 2007). IL-9 enhances immunity to helminths through its induction of colonic muscle hypercontractility and intestinal mastocytosis (Khan *et al.* 2003; Faulkner *et al.* 1997). Neutralisation of endogenous IL-9 by vaccination renders C57BL/6 mice susceptible to *T. muris* infection (Richard *et al.* 2000), and transgenic mice overexpressing IL-9 show rapid *T. spiralis* expulsion attributed to increased muscle contractility and mast cell degranulation (Khan *et al.* 2003).

Conversely, a T_H1 response to helminth infection is associated with susceptibility to chronic infection (Else & Grencis 1991; Else *et al.* 1992). Chronic *T. muris* infection is characterised by production of T_H1-associated cytokines; IL-12 is central to the stabilisation of T_H1 polarisation through STAT4 signalling and induces production of IFN γ from natural killer (NK) and undifferentiated CD4⁺ T cells (D'Andrea *et al.* 1992; Zhu *et al.* 2006). Administration of recombinant IL-12 (rIL-12) in resistant mice induces a susceptible phenotype and chronic infection; rIL-12 pretreatment allows for establishment of a chronic high-dose *T. muris* infection, to which most inbred laboratory mouse strains are naturally resistant (Bancroft *et al.* 1997). However, mice in which both IL-12 and IFN γ have been concurrently depleted retain worm expulsion capabilities, suggesting that IL-12 induced chronicity of *T. muris* infection is IFN γ dependent (Bancroft *et al.* 2001). Neutralisation of IFN γ in susceptible AKR mice induces a resistant phenotype and *T. muris* expulsion (Else *et al.* 1994). IL-18 plays a supporting role in maintenance of a chronic *T. muris* infection through direct antagonism of T_H2 cytokines, most notably IL-13 (Helmsby *et al.* 2001). In *T. spiralis* infection, IFN γ -deficient mice expel enteric worms more rapidly than wild-type littermates, and STAT6 deficient mice show increased IFN γ production associated with defective worm

expulsion (Urban *et al.* 2000). Thus, IFN γ is central to the maintenance of chronic infection in both *T. muris* and *T. spiralis* infections.

The T_h2-dominated immune response mounted towards intestinal helminth infection is associated with IL-4 driven B cell expansion, inducing production of parasite-specific IgG, IgE and IgA as early as 14 days post-infection (Blackwell & Else 2002). Parasite-specific IgG1, IgG2 and IgE increase significantly in *T. muris* infection, although this effector mechanism is redundant in the response to this helminth; adoptive transfer of CD4⁺ T cells into SCID mice, who are naturally susceptible to chronic infection, induces a resistant phenotype (Betts & Else 1999), implicating that B cell responses are obsolete in *T. muris* expulsion. Similarly, in *T. spiralis* infection, IgE deficient mice retain their ability to expel enteric worms (Watanabe *et al.* 1988), however there may be a protective role for antibodies in challenge infection with monoclonal antibody transfer reducing larval migration and muscle larvae burden (McVay *et al.* 2000; Gu *et al.* 2013; Hao *et al.* 2014).

IL-5-driven eosinophilia is also characteristic of a T_h2 response to helminth infection (Coffman *et al.*, 1989; Sher *et al.*, 1990). However, there is no alteration in *T. muris* expulsion capability in mice treated with anti-IL-5 antibodies (Betts & Else 1999). Similarly, in primary *T. spiralis* infection IL-5 blockade causes no significant alteration in parasite expulsion or larval survival, however IL-5 deficient mice show impaired worm expulsion following secondary infection, indicating that eosinophilia may play a role in protection against challenge *T. spiralis* infection (Coffman *et al.* 1989; Sher *et al.* 1990; Vallance *et al.* 2000).

T_h2-driven mastocytosis is dispensable to *T. muris* expulsion; naturally mast cell-deficient W/W^v mice show delayed *T. muris* expulsion, and ablation of the stem cell factor receptor *c-kit*, which plays a key role in mast cell differentiation, has no effect on *T. muris* expulsion (Betts & Else 1999). Conversely, *T. spiralis* expulsion from the small intestine is dependent upon mastocytosis, with mice deficient in *c-kit* unable to expel worms (Knight *et al.* 2000; McDermott *et al.* 2003), and depletion of the mouse mast cell protease-1 (MMCP-1), which is expressed by mucosal mast cells, resulting in significantly delayed worm expulsion (Knight *et al.* 2000).

Expulsion of *T. muris* is critically dependent upon the mounting of a 'weep and sweep' response; the release of T_h2 cytokines and amphiregulin from type 2 intraepithelial lymphocytes (ILC2s) (Kumar 2014; Harris 2017), T_h2 cells, basophils and mast cells (Ho *et al.* 2007; Kondo *et al.* 2008) induce this response, characterised by remodelling of the intestinal epithelium, changes to intestinal mucous production and increased intestinal smooth muscle activity, in order to physically remove worms from their niche within the epithelium (Anthony *et al.* 2007).

2.7 The Intestinal Epithelium in Helminth Infection

The intestinal epithelium is composed of a single-cell layer which selectively facilitates the absorption of water, nutrients and electrolytes from the intestinal lumen, while maintaining an effective barrier against intraluminal toxins, pathogens and the resident microbiota. The intestinal epithelial layer is composed of both absorptive cells, such as enterocytes and microfold cells which orchestrate nutrient

absorption, and secretory cell types. Secretory cells, including goblet cells, enteroendocrine cells and tuft cells, are critical to transit of luminal contents, absorption of nutrients and pathogen defence (Okumura & Takeda 2017; Iftekhhar & Sigal 2021).

The gut acts as an ideal niche for soil-transmitted helminths, with an easily penetrated mucosal surface for access to rich microvasculature and continuous transit of nutrients within the intestinal lumen (Hotez *et al.* 2005; Mckay *et al.* 2017). Furthermore, in some cases the gut microbiota facilitates helminth infection; eggs of *Trichuris* species rely upon interactions with host gut microbiota species for hatching (Hayes *et al.* 2010; Goulding *et al.* 2025), and *Heligmosomoides polygyrus* infection in germ-free mice is reduced compared to wild-type controls (Rausch *et al.* 2018). The continuous transit of waste material through the gastrointestinal tract allows for dissemination of helminth eggs into the environment for embryonation and transmission (Else *et al.* 2020).

Physical invasion of the intestinal epithelium by helminths triggers the release of alarmin cytokines from epithelial cells, including IL-25, IL-33 and thymic stromal lymphopoietin (TSLP), which are essential to the coordination of adaptive immune responses and epithelial remodelling to aid in parasite expulsion and epithelial damage repair (Duchesne *et al.* 2022; Xing *et al.* 2024). IL-25 and IL-33 are the most well-characterised alarmins in helminth infection, with an absence of IL-25 and IL-33 impairing *Nippostrongylus brasiliensis* expulsion (Neill *et al.* 2010). IL-25 and IL-33 play a key role in immunity to *T. muris* (Owyang *et al.* 2006; Chen *et al.* 2021) and *T. spiralis* (Angkasekwinai *et al.* 2017), however TSLP is also an essential alarmin in the expulsion of *T. muris* and *T. spiralis*, through suppression of IL-12 secretion and thus supporting the development of a T_H2 response. (Massacand *et al.* 2009; Giacomini *et al.* 2012).

Helminth-mediated changes to the intestinal epithelium, either directly, such as through direct suppression of secretory cell expansion (Drurey *et al.* 2021) or indirectly, such as through T_H2 cytokine-mediated alterations to epithelial turnover (Cliffe *et al.* 2005), are essential to immunity to helminths.

2.7.2 Tuft Cells

Tuft cells (TCs) are a chemosensory epithelial cell type expressed in various areas of the body, including the airways, stomach, pancreas and urethra (Rhodin & Dalhamn 1956; DelGiorno *et al.* 2020; Saqui-Salces *et al.* 2011; Perniss *et al.* 2021). TCs can be found sporadically and solitarily distributed along the intestinal epithelium, accounting for as few as 0.4% of murine intestinal epithelial cells (Gerbe *et al.* 2011). Despite their sparse distribution in the intestine, TC hyperplasia has been observed following helminth infection; significant increases in TC frequency are seen in *N. brasiliensis* and *H. polygyrus* infection (Gerbe *et al.* 2016, Howitt *et al.* 2016). Following trickle *T. muris* infection, characterised by repeated, low-dose infections, a small but significant increase in TC frequency is seen in the caecum, and probiotic ingestion of *T. suis* eggs results in TC hyperplasia in mice (Glover *et al.* 2019). *T. spiralis* infection significantly increases TC frequency, with a 10-fold increase in intestinal TC abundance (Luo *et al.* 2019).

In recent years, TCs have been identified as key orchestrators of the type 2 response to helminths (Gerbe *et al.* 2016); the precise ligand-receptor interactions by which intestinal TCs sense helminths is yet to be elucidated, however there is evidence to suggest that the bitter taste receptors (*Tas2rs*) expressed by tuft cells play a critical role in intestinal helminth sensing and thus the initiation of a type 2 immune response (Luo *et al.* 2019). Stimulation of murine intestinal organoids using *T. spiralis* antigen results in tuft cell depolarisation and upregulation of genes of the *Tas2r* family, and inhibition of *Tas2rs* using allyl isothiocyanate (AITC) abrogates *T. spiralis*-induced release of IL-25 from tuft-cells, whereas treatment using the *Tas2r* agonist salicin increases tuft cell-derived IL-25 (Luo *et al.* 2019).

Tuft cells constitutively express the alarmin cytokine IL-25; activation of intestinal tuft cells following helminth infection leads to release of IL-25 and cysteinyl leukotrienes (cysLTs) which activate group 2 innate lymphoid cells (ILC2s) as soon as 16 hours post-infection (Von Moltke *et al.* 2016, McGinty *et al.* 2000), highlighting the critical role of tuft cells in early immunity to helminths. ILC2-derived IL-13 then acts directly on the intestinal epithelium to drive tuft cell expansion thus increasing IL-25 production, thereby driving a positive feedforward loop to regulate tuft cell frequency in the epithelium (von Moltke *et al.* 2016). Given the role of ILC2-derived IL-13 in intestinal epithelial remodelling, it is possible that this feedforward loop may also regulate other secretory cell lineages; although Paneth and enteroendocrine cells appear unaffected, goblet cell hyperplasia is inhibited in *N. brasiliensis*-infected mice lacking IL-25, abrogating worm clearance (von Moltke *et al.* 2016), thus highlighting the critical role of TCs in regulation of the type 2 response.

Although it is well known that intestinal helminths act to remodel their niche, it is interesting to note that *H. polygyrus* excretory/secretory products (ESPs) can directly suppress tuft cell expansion (Drurey *et al.* 2022), thereby preventing IL-25-induced type 2 expulsion mechanisms. Furthermore, the sweet taste receptor *Tas1r3* on tuft cells responds to *Tritrichomonas muris* but not to *H. polygyrus* (Howitt *et al.* 2016), indicating a selective tuft cell response to different helminth infections.

2.7.3 Goblet Cells and Mucins

The continuous mucus barrier, composed of the secretory products of goblet cells, lining the intestinal epithelium provides a physical barrier between the epithelium and the luminal contents including intestinal pathogens (Thornton *et al.* 2008; Hurst & Else 2013). Changes to the composition of this mucosal barrier are implicated in aberrant pathologies and are also observed during *T. muris* infection; in resistant animals, upregulation of the transcription factors atonal homolog 1 (*Math-1*) and SAM pointed domain containing ETS transcription factor (*Spdef*) drives the differentiation of caecal progenitor stem cells towards secretory cell types and terminal differentiation into goblet cells, respectively (Noah *et al.* 2009; Shroyer *et al.* 2005). During acute infection, IL-13 also drives upregulation of the GABA- α 3 receptor expression in the caecum, mediating secretion of glycoproteins into the mucus barrier (Hasnain *et al.* 2011b). Conversely, during chronic infection, enterocyte proliferation is promoted by IFN γ -driven upregulation of the transcription factor hairy and enhancer of split 1 (*Hes-1*) (Shroyer *et al.* 2005).

Mucins are heavily glycosylated proteins produced and secreted mainly by epithelial goblet cells and provide viscoelastic and protective characteristics to secreted mucus (Lamont 1992, Kim & Khan 2013).

In the intestine, mucin (MUC)2 is the major gel-forming mucin stored within goblet cell granules and plays a significant role in protection against helminth infection; increased MUC2 production in the caecum of mice infected with *T. muris* correlates with worm expulsion, and susceptible AKR mice show no increase in MUC2 production during infection (Hasnain *et al.* 2010). Cell surface mucins MUC4, MUC13 and MUC17 have also been seen to increase in response to *T. muris* infection, with MUC4 and MUC13 elevated during acute infection and MUC17 raised during chronic infection (Hasnain *et al.* 2011b). This is associated with changes in glycocalyx thickness, and increased MUC4 and MUC13 likely contribute to the resistant phenotype although impairment of worm invasion, motility and feeding capacity (Kim & Khan 2013). Although MUC5AC is predominantly expressed in the airway and gastric mucus, there appears to be a critical role for MUC5AC in intestinal immunity and pathology, with MUC5AC expression in the intestine of patients with ulcerative colitis and diverticulitis (Forgue-Lafitte *et al.* 2007), and in enteric nematode infection. MUC5AC-deficient mice show significant delays in expulsion of *T. spiralis* and *N. brasiliensis* (Campbell *et al.* 2019). In *T. muris* infection, MUC2-deficient mice maintain their resistant phenotype in the presence of MUC5AC expression, and a lack of MUC5AC induces a highly susceptible phenotype (Hasnain *et al.* 2010). MUC5AC is expression driven by IL-13 and detectable in the caecum a short time before worm expulsion (Hasnain *et al.* 2010; Hasnain *et al.* 2011a). It is unknown whether MUC5AC has any direct effect on nematode vitality; dose-dependent decrease in ATP levels (used as a measure of worm viability) of worms placed on human colonic cell lines producing MUC5AC (HT-29) can be observed when treated with increasing levels of MUC5AC, and MUC5AC monomerised by trypsin did not affect worm viability (Hasnain *et al.* 2011b), implicating a direct deleterious effect of MUC5AC on *Trichuris*, and a role of MUC5AC as an effector molecule.

In general, during acute *T. muris* infection we see goblet cell hyperplasia and subsequent expression of MUC5AC. Conversely during chronic infection, IFN γ -driven goblet cell depletion and crypt hyperplasia, and a lack of IL-13-driven MUC5AC production drives the maintenance of a favourable niche for chronic infection (Hasnain *et al.* 2010; Hasnain *et al.* 2011b). Understanding the factors which alter goblet cell productivity, and mucous composition, charge density and viscosity, as well as the anti-parasitic effects of mucous components, is essential to the identification of novel therapies against *Trichuris*.

2.7.4 Enteroendocrine cells

Enteroendocrine cells (EECs) are dispersed along the gastrointestinal mucosa as single secretory cells which, together, comprise the largest endocrine organ system in the human body (Sternini *et al.* 2008). EECs are categorised based on their major secretory hormone; initial findings spurred the dogma that terminally differentiated EECs produced a single peptide hormone (Figure 2.4), although this has more recently been superseded by increased understanding of EEC plasticity which allows for secretion of different hormones and peptides based on luminal changes (Beumer *et al.* 2020). Studies using transgenic reporter mice and cell ablation studies have revealed significant overlap of peptide hormones released by EECs (Egerod 2012; Habib 2012), however it is likely that these peptide hormones are rarely co-expressed (Svendsen 2015; Svendsen 2016).

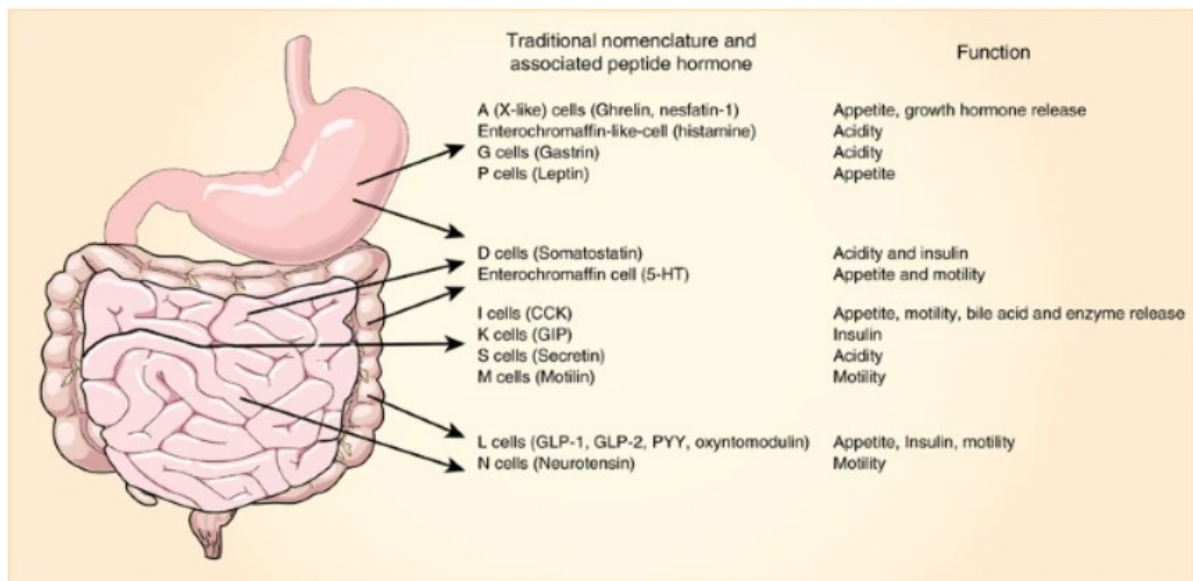


Figure 2.4: Spatiotemporal expression of human enteroendocrine peptide hormones and their functions, based on traditional nomenclature and associated peptide hormones. Figure illustrates the distribution of cells which produce the key peptide hormones ghrelin, gastrin, leptin, somatostatin, serotonin (5-HT), cholecystokinin (CCK), gastric inhibitory peptide (GIP), secretin, motilin, glucagon-like peptide (GLP)-1 and GLP-2, protein YY (PYY) and neurotensin, with their associated functions. Figure adapted from Worthington *et al.* 2018.

Changes in EEC function are implicated in inflammatory gut disorders; the density of EECs producing serotonin (5-HT) is reduced in trinitrobenzene sulfonic acid (TNBS)-induced colitis models (El-Salhy & Hatlebakk 2016). Ghrelin is increased and leptin is decreased in inflammatory bowel disease (IBD) patients (Karmiris *et al.* 2006). EEC function is also altered in helminth infection, likely due to the close association of helminths with the intestinal epithelium; pigs infected with *Ascaris suum* exhibit weight loss associated with increased cholecystokinin (CCK) production (Dynes *et al.* 1998). Further studies in rodent models have demonstrated that CCK⁺ cell hyperplasia and increased CCK synthesis modulates hypophagia during *T. spiralis* infection (McDermott *et al.* 2006; Worthington *et al.* 2013) In humans, CCK⁺ cell hyperplasia and hypersecretion is seen in *Giardia lamblia* infection (Lesie *et al.* 2003). During *T. muris* infection, resistant BALB/c mice possess significantly higher numbers of enterochromaffin cells, which produce 5-HT, than susceptible AKR mice, with significant correlation between worm burden and the number of enterochromaffin cells and 5-HT levels (Motomura *et al.*, 2008).

Receptors for EEC-derived peptide hormones are expressed across a variety of cell and tissue types throughout the body (Zietek & Rath 2016; Nery Neto *et al.* 2023). Interestingly, immune cells express a range of receptors for EEC-secreted peptide hormones (Genton & Kudsk 2003). For example, ghrelin receptor expression has been demonstrated in T cells and monocytes (Dixit *et al.* 2004). The CCK receptor CCK2r is expressed in T cells, dendritic cells and macrophages in mice (Li *et al.* 2007; Jia *et*

al. 2014; Zhang *et al.* 2011). Furthermore, glucagon-like peptide (GLP-1) receptor expression has been associated primarily with intraepithelial lymphocytes (Yusta *et al.* 2015; He *et al.* 2019; Wong *et al.* 2022) but other studies have observed GLP-1r expression on induced regulatory T cells (Rode *et al.* 2022) and terminally differentiated CD4⁺ and CD8⁺ effector memory T cells (Nasr *et al.* 2024).

Taken together, these observations indicate a role for EECs and peptide hormones in intestinal helminth infection.

2.7.5 Intestinal Muscle Contractility

A key mechanism associated with intestinal helminth expulsion is immune-associated hypercontractility of smooth muscle cells lining the intestine (Motomura *et al.* 2010). Jejunal muscle contractility is significantly increased in C57BL/6 mice following IL-9 administration and during *T. spiralis* infection. IL-9 administration accelerates worm expulsion, although IL-9 neutralisation has no significant effect on *T. spiralis* expulsion (Khan *et al.* 2003). During *T. muris* infection, T_H2-associated IL-9 drives colonic muscle hypercontractility; IL-9 neutralisation induces hypocontractility and ultimately inhibits worm expulsion in normally resistant mouse strains even following high-dose infection (Richard *et al.* 2000, Khan *et al.* 2003). Given the differences in infection outcome, it appears that this IL-9-driven contractility and its subsequent effects on worm expulsion are parasite-dependent.

In mouse strains susceptible to *T. muris* infection, IFN γ acts directly on smooth muscle to decrease cell contractility, reportedly through decreased expression of structural protein α -smooth muscle actin (α SMA), which supports smooth muscle cell contraction, proliferation and migration, with hypocontractility reduced by immunosuppressive treatment using dexamethasone (Motomura *et al.* 2010, Ford *et al.* 2019).

This understanding of IL-9-driven smooth muscle contractility and its role in *T. muris* expulsion may highlight an alternative route for treatment of this intestinal helminth infection.

2.7.6 Epithelial Turnover

Intestinal enterocytes undergo proliferation, differentiation and maturation while migrating from the proliferation zone to the shedding zone of intestinal crypts, before apoptotic cell death and extrusion into the intestinal lumen (Potten 1998). Alterations in this epithelial turnover process play a key role in helminth infection; increased rate of epithelial cell movement up the 'epithelial escalator' leads to physical displacement of worms from their niche and ultimately extrusion of worms from the epithelium into the intestinal lumen while concurrently removing damaged and potentially microbially infected enterocytes (Cliffe *et al.* 2005, Oudhoff *et al.* 2016). This has been observed in a variety of helminth infections; *Echinostoma caproni* infection in rats is associated with early IL-13-driven acceleration in epithelial turnover, concurrent with worm expulsion (Cortes *et al.* 2015). Furthermore, a rapid increase in epithelial turnover can be seen early in *Gymnophalloides seoi* infection in C57BL/6 mice, coinciding with worm expulsion (Lee *et al.* 2014). Conversely, helminth infection can result in crypt hyperplasia, as is seen in enteral *T. spiralis* infection (Garside *et al.* 1992) and *E. caproni* infection in rats (Cortes *et al.* 2005).

In *T. muris* infection, an increase in intestinal epithelial cell turnover can be observed in both susceptible and resistant mice following infection, however in resistant (C57BL/6) mice a significant increase by day 14 post-infection is sufficient to expel worms from the epithelium. A comparable rate of epithelial turnover can be seen in susceptible AKR mice at day 21 post-infection, however the worms are significantly larger by this time point and reside higher in the crypt than at day 14 and are therefore no longer within the compartment of the crypt where movement of cells is most rapid. Thus, by day 21 post-infection, this increased epithelial turnover is not sufficient to remove these worms. Interestingly, by day 35 post-infection the rate of epithelial turnover returns to naïve levels in both resistant and susceptible mouse strains, despite the relative absence and persistence of worms by this time point (Cliffe *et al.* 2005). The rapid increase in rate of epithelial turnover in resistant mouse strains is associated with a T_H2 -driven immune response, in particular IL-13, with IL-4 dispensable in this expulsion mechanism (Cliffe *et al.* 2005).

During chronic *T. muris* infection, IFN γ locally induces IFN γ -induced protein 10 (CXCL10) which acts to directly downregulate epithelial cell turnover (Else *et al.* 1994; Sasaki *et al.* 2002). Both IFN γ and CXCL10 are present in the intestinal epithelium of susceptible mice 21 days post-infection but absent in resistant mice at the same time point (Cliffe *et al.* 2005). Furthermore, during chronic infection, the transcription factor Hes-1, which drives differentiation of progenitor cells to an enterocyte fate, is upregulated thereby increasing enterocyte proliferation while limiting differentiation to secretory cell types such as goblet cells (Hasnain *et al.* 2011b). Crypt hyperplasia is essential to maintenance of a chronic infection; susceptible AKR and SCID mice treated with anti-CXCL10 show an increase in epithelial cell turnover compared with untreated mice. This leads to reduced worm burden in SCID mice, and total worm expulsion in AKR mice, suggesting that this mechanism alone is sufficient to induce worm expulsion (Cliffe *et al.* 2005).

The increased apoptosis associated with crypt hyperplasia chronic *T. muris* infection is not a direct consequence of epithelial damage elicited by the helminths; there is spatial separation between the invading helminths and apoptotic areas, with no apoptosis visible in the epithelial tunnels surrounding the worms and instead apoptosis occurring in the stem cell compartment of crypts (Cliffe *et al.* 2007). Apoptosis of crypt stem cells would have a more profound effect on crypt elongation than it would on differentiated enterocytes, indicating that this is a host-induced mechanism to control deleterious cell elongation. This is consistent with Li *et al.* (1998) who showed that *T. spiralis* induced-epithelial damage did not induce epithelial cell apoptosis *in vitro*. Ultimately, this response is beneficial to both host and helminth (Cliffe *et al.* 2007).

Furthermore indoleamine 2,3-dioxygenase (IDO), an enzyme involved in tryptophan metabolism (Sugimoto *et al.* 2006) has been implicated in regulation of epithelial turnover during chronic *T. muris* infection; inhibition of IDO in SCID mice using 1-methyl tryptophan resulted in increased epithelial turnover and thus worm expulsion (Bell & Else 2011). This response does not appear common to all helminth infections; interestingly, *T. spiralis* ESPs have been shown to induce expression of IDO by dendritic cells promoting the development of tolerogenic regulatory T cells further facilitating parasite survival (Ilic *et al.* 2018).

Selective modulation of the Hippo signalling pathway, which regulates cell proliferation, differentiation and survival, significantly accelerates epithelial turnover and *T. muris* expulsion. Selective deletion of the lysine methyltransferase SETD7 from intestinal epithelial cells accelerates expulsion of a high-dose *T. muris* infection through increased epithelial turnover, independently of changes to IL-13 or IFN γ production; SETD7 is required for cytoplasmic localisation and retention of the Hippo signalling pathway transducer YAP, which acts as a transcriptional coactivator of genes associated with proliferation and inhibition of apoptosis. Therefore, deletion of this protein induces dysregulation to the Hippo signalling pathway and thus control of epithelial proliferation and apoptosis. This allows for more rapid expulsion of worms, with significantly lower worm burden in *Setd7*^{-/-} mice at day 14 post infection and all worms expelled from both groups by day 21 (Oudhoff *et al.* 2016). This group also showed that inhibition of YAP interactions with TEAD transcription factors using verteporfin (VP) induces a susceptible phenotype in wild-type mice. However, this inability to clear infection following VP treatment was also associated with increased IFN γ production and reduced TSLP and MUC5AC markers, implicating a wider role for Hippo pathway signalling in immunity to *T. muris* than through its control of epithelial turnover alone (Oudhoff *et al.* 2013; Oudhoff *et al.* 2016)

Understanding the factors which modulate intestinal epithelial turnover during *Trichuris* infection may be important in identifying novel therapeutic targets and therapies. The role of IL-13 in acceleration epithelial turnover and *T. muris* expulsion is well-characterised (Else *et al.* 1994). However, the observation that intrinsic intestinal epithelial cell expression of SETD7 negatively regulates resistance to infection may offer a novel therapeutic target (Oudhoff *et al.* 2016).

2.7.7 Intraepithelial Lymphocytes

Given the close physical association of *Trichuris* species and the intestinal epithelium, the roles of the immune cells in close proximity to this niche have been of significant interest. At the basolateral side of epithelial enterocytes are intraepithelial lymphocytes (IELs), a specialised heterogeneous population of intestinal immune cells providing a front line of defence against the antigen-rich environment in the intestinal lumen, while maintaining the integrity of the epithelial barrier (Cheroutre *et al.* 2011).

The ability of some IELs to produce type 2 cytokines suggests a role for these immune cells in the immune response to *Trichuris* species (Ferrick *et al.* 1995; Inagaki-Ohara *et al.* 2004). IELs can be classified as belonging to one of two groups based on phenotypic characteristics; induced IELs are CD8 $\alpha\beta$ TCR $\alpha\beta$ ⁺ or CD4⁺TCR $\alpha\beta$ ⁺ cells which are activated in the gut-associated lymphoid tissues (GALT) or intestinal draining lymph nodes prior to relocation to the intestinal epithelium. Natural IELs are CD8 $\alpha\alpha$ ⁺ or CD8 $\alpha\alpha$ ⁻ T cells expressing either TCR $\alpha\beta$ ⁺ or TCR $\gamma\delta$ ⁺ cells, and do not express CD4 or CD8 $\alpha\beta$. Induced IELs are the progeny of conventional CD4⁺ or CD8 $\alpha\beta$ ⁺TCR $\alpha\beta$ ⁺ T cells which are MHC class-II and -I restricted, respectively. Induced IEL activation arises post-thymically in response to peripheral antigens, whereas natural IELs acquire activation during thymic development (Qiu & Yang 2013; Cheroutre *et al.* 2011)

Cytokines produced by IELs play a key role in the modulation of the intestinal mucosa, with essential roles in regulation of epithelial barrier function, epithelial cell turnover and the response to pathogens

(Shires *et al.* 2001; Inagaki-Ohara *et al.* 2004; Inagaki-Ohara *et al.* 2011). Given the close proximity of intestinal IELs to invading *Trichuris* species, and the ability of TCR $\gamma\delta$ T-cells to produce type 2 cytokines (Ferrick *et al.* 1995; Inagaki-Ohara *et al.* 2011), it is likely that these IELs play a role in the immune response to *Trichuris* infection. The use of TCR δ $-/-$ mice to investigate the role of these cells in helminth infections has shown increased mortality and retention of intestinal worm burden in *N. brasiliensis* infection, attributed to decreased production of type 2 cytokines and thus delayed goblet cell hyperplasia (Inagaki-Ohara *et al.* 2011).

Intestinal IELs are one of the immune cell populations known to express a functional receptor for the enteroendocrine-secreted peptide hormone GLP-1; interestingly TCR $\gamma\delta$ and TCR $\alpha\beta$ IELs display comparable GLP-1r expression (Yusta *et al.* 2015; He *et al.* 2019). Studies employing integrin $\beta 7^{-/-}$ mice, which lack gut IELs, demonstrated a key role for these IELs in glucose regulation attributed to control of local bioavailability of GLP-1, produced by nearby GLP-1 $^{+}$ EECs (He *et al.* 2019). However, this also suggests a role for GLP-1 in orchestrating the immune response to helminth infection. Both *in vitro* and *in vivo* studies have shown that use of GLP-1r agonists (GLP-1rAs) suppresses T $_H$ 1 proliferation and production of proinflammatory cytokines such as IFN γ and TNF α (Marx *et al.* 2010; Yusta *et al.* 2015; Moschovaki Filippidou *et al.* 2020) and increases production of type 2 cytokines such as IL-13 (Yusta *et al.* 2015). Therefore, GLP-1 may play a role in the orchestration of a type 2 immune response at the parasite niche.

2.8 GLP-1

Glucagon-like peptide (GLP)-1 is a peptide hormone synthesised in small intestinal and colonic EECs by post-translational proteolytic cleavage of its precursor, proglucagon, by prohormone convertase 1/3 (PC1/3), (Campbell & Drucker 2013). The distribution of these GLP-1 $^{+}$ cells increases distally, with a sparse distribution in the duodenum, increased number in the jejunum and the greatest density within the ileum and colon (Baggio *et al.* 2007). GLP-1 is stored in EECs within vesicles, which are exocytosed in response to dietary carbohydrates, proteins and fats (Baggio & Drucker 2007; Belza *et al.* 2013; Hirasawa *et al.* 2005). GLP-1 exists in the circulation briefly as two major active forms: GLP-1 (7-37) and GLP-1 (7-36) with the latter form circulating in higher proportions (Campbell & Drucker 2013; Lafferty *et al.* 2021). Endogenous GLP-1 has a half-life of less than two minutes in humans due to rapid clearance of GLP-1 by the kidneys, breakdown of GLP-1 by primarily dipeptidyl-peptidase (DDP)-4 and, to a lesser extent by the membrane-bound zinc metallopeptidase, neutral endopeptidase 24.11 (NEP 24.11) (Deacon & Holst 2009; Plamboeck *et al.* 2005).

Previous research has primarily focused on the roles of GLP-1 in satiety, insulin control, gut motility and alterations in gastrointestinal secretions, although the widespread expression of GLP-1 receptors (GLP-1rs), including expression in the heart, lung, skin, kidney, nervous system and some immune cells (Abu-Hamdah *et al.* 2009) mirrors the diversity of the biological function functions of GLP-1 throughout the body (Figure 2.5).

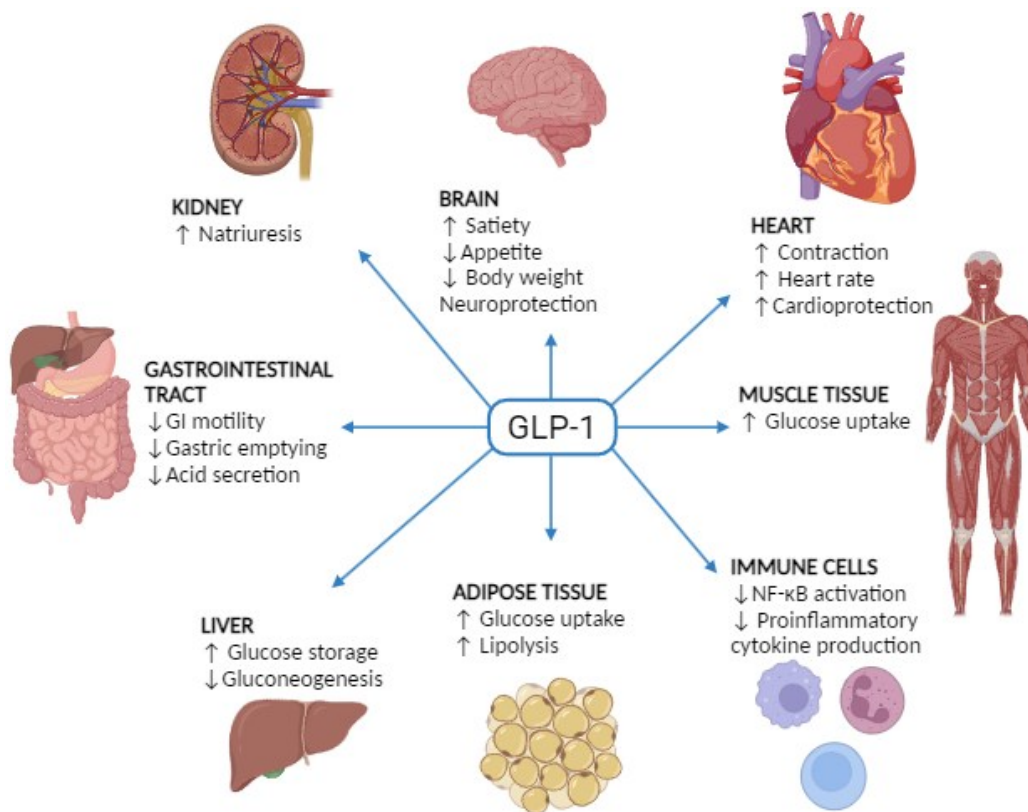


Figure 2.5: Biological functions of glucagon-like peptide-1 (GLP-1). The widespread expression of the GLP-1 receptor allows for a range of biological functions; the primary functions of GLP-1 are in glucose regulation via increased glucose-dependent insulin secretion and inhibition of glucagon secretion in the pancreas, increased glucose uptake by muscle, fat and hepatic tissues. Figure created using BioRender; adapted from Cheang & Moyle 2018, using information from Lee *et al.* 2012, Kodera *et al.* 2011 and Alharbi 2024.

GLP-1 functions primarily as an incretin hormone, acting to reduce postprandial glycaemic excursions through increased glucose-dependent insulin secretion and inhibition of glucagon from the pancreas (Drucker *et al.* 2017). Sensing of dietary glucose to allow for glucose-dependent GLP-1 secretion is facilitated by sodium-coupled glucose transporters (SGLTs); dietary glucose is co-transported with sodium into EECs via SGLTs, and the resultant Na⁺ uptake triggers membrane depolarisation, opening voltage-gated Ca²⁺ channels, initiating the exocytosis of vesicles containing GLP-1. (Ritzel *et al.* 1997; Reimann & Gribble 2002; Gribble *et al.* 2003). Other luminal dietary nutrients, such as oligopeptides and fatty acids, are taken up via interactions at G protein-coupled receptors (GPCRs) such as GPR142 and GPR120, respectively (Lin *et al.* 2016; Gribble & Reimann 2016). More recently, the discovery of the expression of a wide repertoire of receptors at their cell surface has increased interest in the luminal sensing abilities of GLP-1⁺ EECs; an alternative mechanism by which luminal glucose stimulates GLP-1 secretion is through sweet taste receptors (TAS1rs); glucose activation of gustducin-coupled receptors TAS1r2 and TAS1r3 expressed by GLP-1⁺ EECs stimulates GLP-1 secretion (Jang *et al.* 2007). Similarly, functional bitter taste receptor (TAS2r) expression has been shown on these cells (Kim

et al. 2014; Wang *et al.* 2024). A role for bitter taste receptors in sensing of *T. spiralis* infection has been uncovered (Luo *et al.* 2019), however the relationship between helminth infection and EEC-dependent GLP-1 secretion via TAS2rs has not yet been elucidated.

In recent years the immunomodulatory effects of GLP-1r activation have gained interest; activation of GLP-1r by exogenous agonists such as exendin-4 suppresses production of proinflammatory cytokines such as tumour necrosis factor (TNF) α , IL-6 and IL-1 β are suppressed (Hogan *et al.* 2014; Chaudhuri *et al.* 2012) via suppression of NF- κ B activation (Kodera *et al.* 2011; Lee *et al.* 2012). GLP-1 has also been suggested to carry out cytoprotective functions in the murine intestine; GLP-1 acts through GLP-1rs expressed on intestinal IELs in both the small and large intestine to modulate local inflammatory responses (Yusta *et al.* 2015). Furthermore, GLP-1 has been associated with macrophage polarisation to the M2 phenotype, and therefore associated with anti-inflammatory, tissue-repair and angiogenic actions through STAT3 activation (Shiraishi *et al.* 2012). Human neutrophils and eosinophils have also been shown to express GLP-1r, with activation resulting in significant decrease in the expression of eosinophil surface activation markers and in IL-4, IL-8 and IL-13 (Mitchell *et al.* 2016).

Loss of GLP-1r signalling is associated with increased susceptibility to gut injury, with central blockade of GLP-1r signalling resulting in enhanced pyrogenicity of lipopolysaccharide (LPS) (Rinaman 2000); both *in vivo* and *in vitro* studies have demonstrated expression of functional toll-like receptors (TLRs) by GLP-1⁺ EECs, with GLP-1 secretion triggered via LPS interaction with TLR4 (Bogunovic *et al.* 2007; Lebrun *et al.* 2023). Central blockade of GLP-1r signalling also enhances sensitivity to intestinal injury and epithelial damage in dextran sodium sulphate (DSS)-induced colitis models (Yusta *et al.* 2015), with exogenous GLP-1r agonist treatment ameliorating colitis-associated injury in mice (Bang-Berthelsen *et al.* 2016).

GLP-1 contributes to intestinal recovery of mucositis following chemotherapy (Kissow *et al.* 2013). Furthermore, endogenous GLP-1 improves gut permeability, growth, and barrier function, although this response is modest, the effects can be boosted using exogenous GLP-1rA treatment (Nozu *et al.* 2017; Kissow *et al.* 2013; Bang-Berthelsen *et al.* 2016).

Interestingly, there is a postulated link between the gut microbiome and its metabolic by-products and the level of GLP-1 production; studies have shown that gut microbiota depletion alters fasting and postprandial GLP-1 production (Zarrinpar *et al.* 2018; Wang *et al.* 2024). Given the alterations to the gut microbiota induced by *T. muris* infection, one may postulate that gastrointestinal helminth infection may influence fasting and postprandial GLP-1 production. Furthermore, helminths produce a variety of dipeptidyl peptidases secreted in their ESPs (Yan *et al.* 2024) although these are yet to be fully characterised; it may be possible that helminths may produce a homolog of DDP-4, thus allowing them to modulate local GLP-1 availability.

Given the expression of TAS2rs by GLP-1⁺ EECs, it is possible that helminth infection increases GLP-1 secretion to aid in the repair of helminth-induced epithelial damage, with potential further functions in immunity to helminths. If this is the case, GLP-1rA treatment may aid in immunity to, or recovery from pathophysiology induced by helminth infection.

2.9 GLP-1 Receptor Agonists

Given the roles of GLP-1 in glucose homeostasis, the GLP-1r acts as a significant drug target in the treatment of type 2 diabetes mellitus (T2DM). The efficacy of endogenous GLP-1 as a therapeutic agent is significantly limited by its rapid degradation by DPP-4; the breakdown of GLP-1 by DPP-4 produces an inactive peptide of 2 amino acids less (de Graaf *et al.* 2016). However, the limitation of endogenous GLP-1 as a therapeutic agent have been superseded by the development of GLP-1 receptor agonists (GLP-1rAs) resistant to endogenous DPP-4 (Gilbert & Pratley 2020). Exendin-4 (Ex-4) is a 39 amino acid peptide and potent GLP-1rA present in the saliva of the Gila monster, *Heloderma suspectum*. Despite sharing only 50% sequence similarity with human GLP-1, Ex-4 acts as a full GLP-1r agonist, causing dose-dependent, glucose-dependent insulin secretion (Goke *et al.* 1993). Since its discovery, synthetic Ex-4, exenatide, has been approved in the UK for the treatment of T2DM (Kyriacou & Ahmed 2010).

GLP-1rAs can be short- or -long acting based on pharmacokinetic and pharmacodynamic properties (Drucker 2018; Gilbert & Pratley 2020). Currently, there are seven approved GLP-1rAs which are often prescribed as add-on therapies for patients with T2DM; GLP-1rA treatment reduces exogenous insulin dose requirements and boosts therapeutic effects. They are preferable over sulfonylureas and meglitinides; these drug classes act to increase insulin secretion from pancreatic β cells albeit in a glucose-independent manner thereby increasing risk of hypoglycaemia. GLP-1rAs, on the other hand increase glucose-dependent insulin secretion and so risk of hypoglycaemia is low (Gilbert & Pratley 2020; Elkinson & Keating 2013).

Given the role of GLP-1 in increased satiety and decreased appetite, a commonly observed side effect of GLP-1rA treatment in T2DM patients was weight loss (Beggs & Woods 2013; Iqbal *et al.* 2022). Obesity poses a significant global health burden, with 64.3% of adults in England being overweight or obese (NHS, 2024) with 1 in 8 individuals living with obesity worldwide (WHO 2024). Therefore, the anorexigenic properties of GLP-1 and its analogues gained considerable attention. In 2021, the FDA approved semaglutide for the treatment of obesity, at a dose of 2.4mg to be administered subcutaneously once per week. This drug is indicated in patients with a body mass index of $27\text{kg}/\text{m}^2$ who also suffer from at least one weight-related condition, such as type 2 diabetes mellitus, or patients with a BMI of $30\text{kg}/\text{m}^2$ or above (FDA, 2021). In 2023, semaglutide was approved by the Medicines and Healthcare products Regulatory Agency (MHRA) for the treatment of obesity in the UK (MHRA 2024)

Lixisenatide is also a synthetic analogue of Ex-4, which is approved for the treatment of T2DM (Elkinson & Keating 2013). Excitingly, Dooley (2022) recently showed that lixisenatide drives expulsion of chronic *T. muris* infection via an immune dependent increase in epithelial turnover.

2.10 Aims

Trichuriasis is a neglected tropical disease afflicting over one billion people worldwide, with widespread implications for the agricultural industry. Increasing prevalence of drug-resistant strains of the parasites of the *Trichuris* genus highlights the necessity for alternative treatment strategies. The aims of this study were to 1) utilise a small intestinal organoid model to investigate the effect of intestinal helminths on GLP-1⁺ EEC development and function, and 2) to investigate the efficacy of the GLP-1 receptor agonist, lixisenatide, against *T. muris* infection.

The mechanism underpinning host sensing of intestinal helminth infections is currently unknown. Furthermore, the effects of intestinal helminths on local GLP-1⁺ EEC development and GLP-1 secretion are yet to be elucidated. Therefore, a small intestinal organoid platform will be used to determine the effects of *Trichuris muris* and *Trichinella spiralis* antigen on GLP-1⁺ cell development, using immunofluorescent staining of GLP-1 to investigate changes in GLP-1⁺ EEC frequency in small intestinal organoids. This organoid model will also be used to determine the effect of *T. muris* and *T. spiralis* antigen on GLP-1 secretion; a GLP-1 secretion assay will be utilised to identify changes in GLP-1 secretion following organoid co-culture with helminth antigen, and use of the bitter taste receptor inhibitor AITC will allow for the determination of the role of these receptors in host sensing of intestinal helminths.

Based on the reviewed literature, GLP-1⁺ IELs appear to be a potential drug target in the treatment of *Trichuris* infection. This project will use the mouse model of trichuriasis, *T. muris*, to further investigate the efficacy of GLP-1rA treatment against *T. muris* infection. A trickle infection model will be used to determine the potential for the GLP-1rA, lixisenatide, to induce protective immunity against challenge *T. muris* infection. Recombinant IL-12 pretreatment will also be used to induce a chronic, high-dose *T. muris* infection, allowing for the investigation of the efficacy of lixisenatide on a chronic, high-dose infection. Serum IgG1 and IgG2a will be used to determine the nature of the immune response in these mice. Histological analysis of caecal crypt and goblet cell structure, and epithelial turnover will be essential to determine the expulsion mechanisms underpinning lixisenatide-driven worm expulsion. Flow cytometric analysis of immune cell populations of the mLN will allow for further characterisation of the immune response, and cytokines underpinning lixisenatide-driven *T. muris* expulsion.

Given that GLP-1rAs are already licensed for use in patients with diabetes and obesity, it may be possible to repurpose these drugs, with already well-characterised safety profiles and mechanisms of action, to treat trichuriasis in both humans and in livestock, providing higher quality of life to those, many of whom are children, afflicted by trichuriasis.

3. Methods

3.1 Animals

C57BL/6 mice, C5BL/6 RAG^{-/-} mice (A kind gift from Dr K Okkenhaug; Babraham Institute, Cambridge, England, Hao *et al.* 2001) and QuCCi mice (a kind gift of Dr Richard Mort; Lancaster University, Briggs

2024) mice were housed at Lancaster University in individually ventilated cages on a 12-hour light/dark cycle at $22 \pm 1^\circ\text{C}$ and 65% humidity. All procedures were carried out at Lancaster University on 6–12-week-old littermates after 1 week of acclimatisation in accordance with the Home Office Science Act 1986, under the project licence PP4157153. All procedures conformed to the Lancaster University Animal Welfare and Ethical Review Body (AWERB) and ARRIVE guidelines. All animals were humanely terminated by cervical dislocation followed by terminal exsanguination.

3.1.1 Small Intestinal Epithelial Organoid Culture.

Mice were sacrificed and small intestine was removed, opened longitudinally, cut into 2mm pieces and washed in cold ($2-4^\circ\text{C}$) PBS and agitated in room temperature ($15-25^\circ\text{C}$) Gentle Cell Dissociation Reagent for 15 minutes on a rocking platform at 20 rpm. Intestinal pieces were resuspended in 0.1% BSA-PBS and filtered through a $100\mu\text{m}$ sieve to generate 6 fractions. Fractions were assessed by light microscopy to determine those with least cellular debris. Approximately 500 crypts were embedded in $150\mu\text{L}$ undiluted Matrigel matrix (Corning) and $150\mu\text{L}$ room temperature complete Organoid Growth Medium (Mouse, Intesticult) for 10 minutes at 37°C , in 24-well plates. After Matrigel polymerization, $750\mu\text{L}$ Organoid Growth Medium containing penicillin/streptomycin (Gibco) was added. Some organoids were cultured in Matrigel containing *T. muris* antigen at a concentration of $10\mu\text{g/ml}$, and *T. spiralis* antigen at a concentration of $10\mu\text{g/ml}$ cultured in media containing the rock inhibitor Y27632 (Sigma) at a final concentration of 0.5mg/ml in culture media as indicated. Organoids were cultured at 37°C in 5% CO_2 in an incubator, and the cell culture medium was changed three times per week, and organoids were allowed to grow for 10 days.

3.1.2 Immunofluorescent Staining of Small Intestinal Epithelial Organoids

Organoids were fixed with 4% paraformaldehyde (PFA, Sigma) for 60 minutes at room temperature, then washed with PBS (Gibco) and incubated with rabbit anti-mouse GLP-1 antibodies (1 in 200, Abcam ab22625) overnight at 4°C . Organoids were washed with PBS and incubated with goat anti-rabbit IgG antibodies (1 in 50, Alexa Fluor) overnight at 4°C , in the dark. Organoids were washed once again and mounted using fluoroshield with 4',6-diamidino-2-phenylindole (DAPI) (Sigma). Images were obtained by confocal microscopy (Zeiss LSM80).

3.1.3 GLP-1 Secretion Assay

Mouse small intestinal organoids were cultured as above. Following 10 days of growth, culture media was removed and washed three times with 0.5mls of 138 buffer (4.5mM KCl, 138mM NaCl, 4.2mM NaHCO_3 , 1.2mM NaH_2PO_4 , 2.6mM CaCl_2 , 1.2mM MgCl_2 , 10mM HEPES). Organoids were then incubated with $250\mu\text{L}$ substrate solution and incubated at 37°C and 5% CO_2 for 4 hours. Some organoids were cultured with 10pM forskolin (Sigma), $10\mu\text{M}$ 3-Isobutyl-1-methylxanthine (IBMX, Sigma) and 10mM glucose as a positive control. During incubation, lysis solution was made by adding 0.25g deoxycholic acid, 0.5ml Igepal CA-630, 2.5ml 1M Tris-HCL, 1.5M NaCl and 1 tablet of complete EDTA-free protease inhibitor cocktail, made up to 50ml with dH_2O , and kept on ice. Following incubation, the substrate solution was removed from each well of the 24-well plate and transferred to a corresponding

eppendorf. The 24-well plate was placed on ice and to each well 0.5ml lysis solution was added, after 5 minutes each well was scraped with a cell scraper and lysate from each well was transferred into eppendorfs. Substrate solution was centrifuged at 400rcf for 5 minutes, and the lysate was centrifuged at 4°C at 10 000rpm for 10 minutes. Supernatants were transferred into fresh eppendorfs and stored at -80°C.

3.1.4 GLP-1 ELISA

Lysate samples were diluted 1:10, and secretion samples 1:2 in buffer and GLP-1 secretion was quantified by an active GLP-1 ELISA kit (cat. EGLP-35K; Millipore, Watford, UK). All steps were performed according to manufacturer's instructions, and plate was read on Tecan Infinite Pro plate reader with an excitation/emission wavelength of 355nm/460nm

3.1.5 *T. muris* Infection, Faecal Egg Counts and Determination of Worm Burden

Mice were infected with a low dose (approximately 30 embryonated eggs, in 200µL PBS), or high dose (approximately 200 embryonated eggs in 200µl PBS) by oral gavage using a blunt needle. To monitor infection status, faecal egg counts were completed using a modified McMaster technique; faecal pellets were collected and weighed. 1ml dH₂O saturated with MgSO₄ (to a specific gravity of 1.2) was added to each tube and the pellet solubilised. This solution was then filtered through a 100µm filter and the filtrate added to one of two chambers on the McMaster counting slide and observed under a light microscope. The egg load in faeces was calculated as eggs per gram of faeces. Worm burden post-termination was determined by counting worms present in caecum and proximal colon samples.

3.1.6 High dose chronic infection

Naïve C57BL/6 mice were treated with rIL-12 (1µg in 200µL PBS) by intraperitoneal injection for 3 days and infected with a high-dose (approx. 200 eggs) *T. muris* infection by oral gavage, and infection was allowed to establish for 34 days.

3.1.7 GLP-1 Receptor Agonist Treatment

10µg lixisenatide in 200µl PBS, or 200µl PBS alone, was administered by intraperitoneal injection using a 25G 5/8" needle.

3.1.8 T cell transfer

Mesenteric lymph node (mLN) cells were prepared from day 21 post-infection C57BL/6 mice, in RPMI-1640, supplemental with 10% foetal calf serum, 100µg/ml penicillin/streptomycin and 1mM L-glutamine (complete media). CD4⁺ T cells were isolated via negative selection using an isolation kit (Miltenyi Biotec) Evaluation of CD4⁺ purity was by flow cytometry. SCID mice received 4x10⁶ cells in PBS via intraperitoneal injection, 10 days before low-dose *T. muris* infection.

3.2 Parasite-Specific Enzyme-Linked Immunosorbent Assay (ELISA)

Blood collected from sacrificed animals by terminal exsanguination was left at room temperature to clot. Serum was collected from each sample, aliquoted and stored at 0°C until required for analysis.

96-well plates were coated with 50µl of 10µg/ml *T. muris* E/S at 5µg/ml in carbonate bicarbonate buffer, then plates were washed 5 times in PBS-Tween 20 (PBS-T) (Sigma Aldrich). After blocking with phosphate-buffered saline (PBS) containing 3% bovine serum albumin (BSA), plates were washed once again and incubated with 50µl sera serially diluted in PBS-Tween 20 from 1:20 to 1:2560. Bound parasite-specific antibody was detected using 50µl biotinylated rat anti- mouse IgG1 (BD PharMingen, Cat. 553441) at 0.25µg/ml in PBS-T, or 50µl biotinylated rat anti-mouse IgG2a (BD PharMingen, Cat. 550332) at 1µg/ml in PBS-T, incubating for 60 minutes at room temperature. Bound biotinylated antibody was detected by 50µl streptavidin peroxidase (Roche, 1:40 in PBS-T), incubated for 1 hour at room temperature. Plates were developed using 50µl 3, 3', 5,5' Tetramethylbenzidine liquid substrate (Sigma-Aldrich) and the reaction stopped after approximately 2 minutes using H₂SO₄. Plates were read at 450nm with 490nm reference on a Tecan Infinite Pro plate reader.

3.3 Histology

Caecal tips were obtained at the time of sacrificed and fixed in Carnoys (60% absolute ethanol, 30% chloroform, 10% glacial acetic acid) solution for 24 hours before being stored in 70% ethanol. Samples were dehydrated through an ethanol-xylene gradient; 90% ethanol for 1 hour, 100% ethanol for 1 hour, xylene for 45 minutes and then fresh xylene for an additional 45 minutes, before storing in paraffin wax overnight. Samples were then embedded in paraffin wax and ribbons of 5µM were taken using a microtome, before being transferred to a water bath and ultimately to slides.

3.3.1 Alcian Blue-PAS for Goblet Cells

Slides were dewaxed in xylene and moved through an alcohol gradient (100%, 90%, 70%, 50%) before staining in 1% alcian blue (in 3% periodic acid, Sigma). Sections were washed in dH₂O and incubated in periodic acid (Thermo Scientific) for 5 minutes, and then in Schiff's reagent (Thermo Scientific) for 15 minutes. Counterstaining was completed using Mayers haematoxylin (Thermo Scientific), before dehydrating using 70% and 100% ethanol, and xylene. Sections were mounted for imaging using DPX mounting medium.

3.3.2 BrdU Pulse-Chase Experiment for Epithelial Turnover

BrdU (Sigma) was administered by intraperitoneal injection at a dose of 10mg per mouse with a 25G needle at 23:00hrs and mice were terminated after a 12-hour period. Caecal tip samples collected and fixed in Carnoys (60% absolute ethanol, 30% chloroform, 10% glacial acetic acid) solution for 24 hours before being stored in 70% ethanol until slide preparation. Slides were prepared as previously described.

Slides were dewaxed in xylene for 1 hour and washed in 100% ethanol. Peroxidase activity was then blocked using peroxidase block (180ml methanol + 3ml H₂O₂) for 20 minutes at room temperature.

Slides were hydrolysed in 1M hydrochloric acid for 8 minutes at 60°C, then washed in PBS, and after each subsequent step. Slides were then blocked using 5% rabbit serum in PBS for 30 minutes at room temperature. Slides were washed once again before incubating in anti-BrdU (1:20 in PBS, Abcam) for 1 hour at room temperature. Slides were incubated in polyclonal rabbit anti-rat immunoglobulins/HRP (Dako, 1:100 in 10% mouse serum-PBS) for 1 hour at room temperature. Sections were developed in DAB for 2-3 minutes, washed, and then counterstained in haematoxylin (1:5 in dH₂O) for 1 minute before being washed through an alcohol gradient into xylene and mounted using DPX mounting medium.

3.4 Mesenteric Lymph Node Cell Isolation and Restimulation

Mesenteric lymph nodes (mLNs) were gently disaggregated through a 100µm sieve and counted using Countess automated cell counter (Invitrogen). and plated out at 4.3×10^5 cells per well in 1ml full media (RMPI with 10% FCS (Sigma), 1% 1M HEPES, 1% L-glutamine (Sigma), 1% pen-strep (Sigma), 1% MEM non-essential amino acids 100x (Sigma), and 50µM β-mercaptoethanol). Cells were stimulated with cell stimulation cocktail with protein transport inhibitors (1X, Invitrogen) overnight at 37°C and 5% CO₂. Cells were then prepared and stained for flow cytometry.

3.5 Flow Cytometry

All samples were centrifuged at 400rcf and supernatant discarded. Pellets were resuspended in 50µl fix-perm solution (Invitrogen) and placed on ice for 30 minutes. Samples were then centrifuged at 400xg for 5 minutes at room temperature, and pellet resuspended in 50µl FC block (1:200 in 1x perm buffer (Invitrogen)) and incubated on ice for 15 minutes. Antibody mix was prepared using 1x perm buffer and antibodies as listed in table 3.1, and was added to each sample to a final surface stain cover concentration of 1.5µg/ml. After staining was complete, samples were centrifuged at 400g for 5 minutes and pellets were resuspended in 200µl 1% PBS-BSA. Suspended samples were run using Beckman Coulter Cytoflex flow cytometer and analysed using FlowJo (Version 10.10.0) using the gating strategy shown in Fig 3.1.

Table 3.1: Mesenteric Lymph node flow cytometry antibody panel

Antibody	Manufacturer	Fluorophore	Clone
CD45	eBioscience	e506	30-F11
CD3	eBioscience	AF700	17A2
CD4	Biolegend	APC-Cy7	GK1.5
CD8	BD Biosciences	PE-CF594	53-6.7
CD45RB	eBioscience	PE	C363.16A
CD69	eBioscience	PerCP-Cy5.5	H1.2F3
IFNγ	eBioscience	AF488	XMG1.2
IL-13	eBioscience	e450	13A
IL-17	eBioscience	APC	17B7

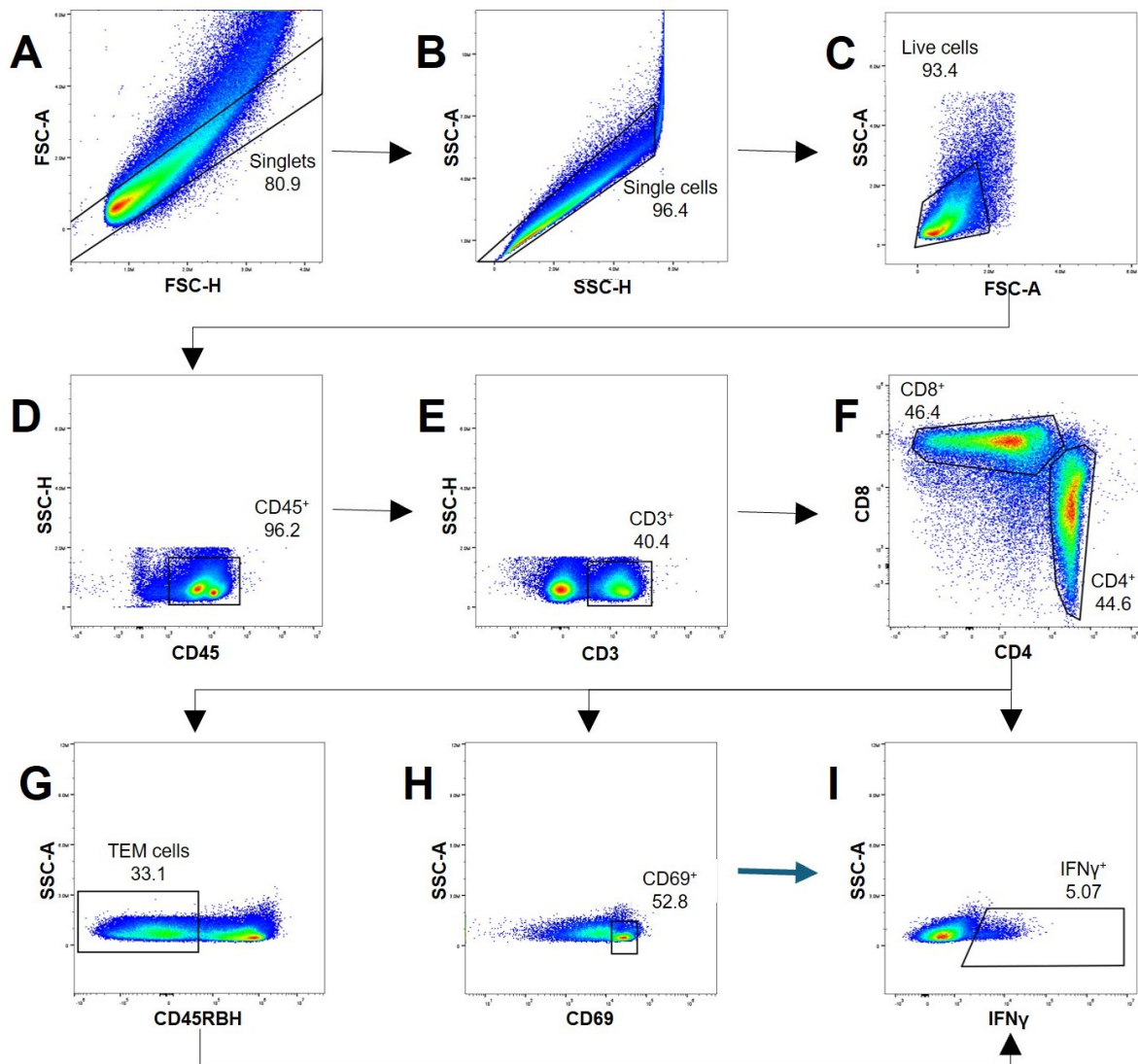


Figure 3.1: Gating strategy of mesenteric lymph node data. A) Singlets were gated using FSC-H against FCS-A. B) Single cells were then gated using SSC-H against SSC-A. C) Live cells were then gated using FSC-A against SSC-A. D) From live cells, CD45⁺ cells were gated using e506 (KO525-A) against SSH-H. E) Then, CD3⁺ cells were gated using AF700 (APC-A700-A) against SSC-H. F) CD4⁺ and CD8⁺ cells were then gated using APC-A750-A against ECD-A. G) Effector/memory T (TEM) cells were then gated from each of the CD4⁺ and CD8⁺ populations using PE (PE-A) against SSC-A. H) Recently activated (CD69⁺) T cells were gated from the populations in (F) and (G) using PerCP-Cy5.5 (PC5.5A) against SSC-A. I) Cytokines produced by the populations shown in (F), (G) and (H) were analysed using the antibodies shown in table 3.1 against SSC-A.

Statistical analysis.

Statistical analyses were performed and figures were created using GraphPad Prism, and results presented as mean \pm SEM. Data normality was determined using Shapiro Wilks test, and where two experimental groups were compared, Student's T test and Mann Whitney U tests were used where data were parametric and non-parametric, respectively. Where data were parametric, three or more groups

were compared using ANOVA with Dunnett's or Tukey's multiple comparisons test. Where data were non-parametric, three or more groups were compared using Kruskal-Wallis test with Dunn's multiple comparisons test, as indicated. Values were considered statistically significant at $P < 0.05$. $P < 0.05 = *$, $P < 0.01 = **$, $P < 0.001 = ***$, $P < 0.0001 = ****$ for indicated comparisons. Error bars represent SD of mean.

4. Results

GLP-1 is a proglucagon-derived peptide hormone secreted by enteroendocrine cells (EECs) throughout the small intestine and colon. Though the primary role of GLP-1 is in glucose regulation, EECs have been shown to play a key role in intestinal disease progression; EEC toll-like receptor activation allows for modulation of their secretome in response to pathogenic detection (Selleri 2008). Here, a murine small intestinal organoid platform was used to elucidate whether helminths directly influence GLP-1⁺ EEC activity.

4.1 Organoid culture represents expected GLP-1⁺ EEC spatiotemporal ratio and development pathways

Previous studies observe an increase in GLP-1⁺ cell density across a proximal to distal axis in the small intestine (Baggio *et al.* 2007). Organoids cultured from crypts isolated from duodenal, jejunal and ileal sections of small intestine of naïve mice demonstrated that this distal increase in GLP-1⁺ EECs translates *ex vivo* to the organoid system (Figure 4.1); there was a small increase in GLP-1⁺ EECs between the duodenum and jejunum, although not statistically significant here. The number of GLP-1⁺ EECs in organoids grown from ileal crypts was significantly higher than in the duodenum ($P < 0.0001$) and jejunum ($P < 0.0001$).

crypts with the Rho-associated protein kinase inhibitor Y27632 as described by Petersen *et al.* (2018), which has previously been shown to drive EEC differentiation. The optimal concentration of Y27632 for optimisation of GLP-1+ EEC frequency was determined, as shown in Figure 4.2; 10 μ M Y27632 was sufficient to significantly increase GLP-1+ cell frequency as compared to controls (P=0.0001) without inducing organoid death.

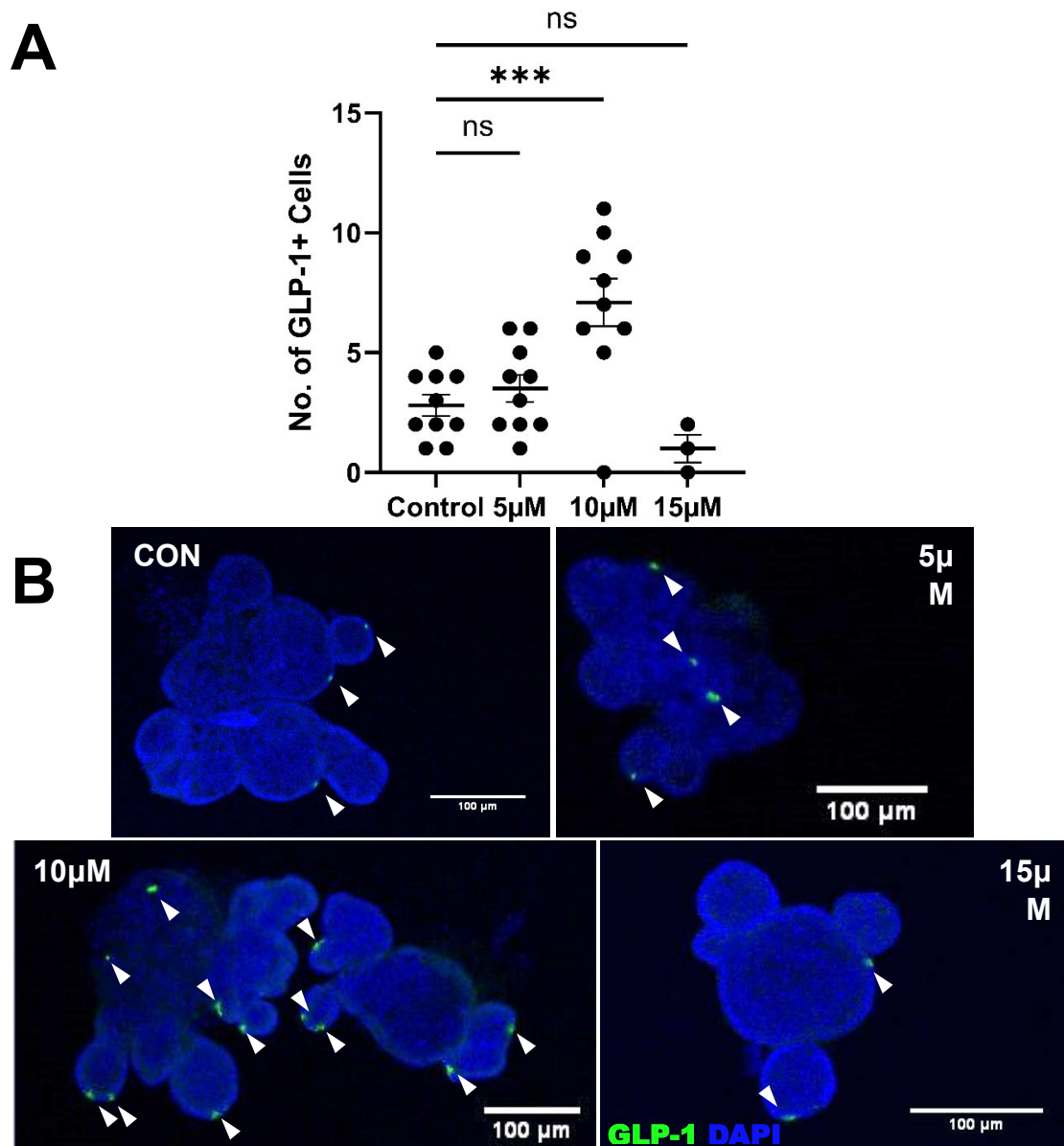


Figure 4.2: Optimal concentration of ROCK inhibitor Y27632 for culture with murine small intestinal organoids is 10 μ M in culture medium for the first 48 hours of culture to optimise GLP-1+ cell frequency. Ileal crypts were isolated from naïve C57BL/6 mice and cultured with 5 μ M, 10 μ M and 15 μ M Y27632 in culture medium for the first 48 hours of culture. A) Plotted data shows the number of GLP-1+ cells per organoid, B) representative imaged of stained organoids, where bars represent 100 μ m. Data (experimental n=3, where 3-4 organoids were randomly selected in each experiment) are presented as mean \pm SEM, where each plotted point represents one organoid. Statistical analyses were performed using one-way ANOVA with Dunnett's multiple comparisons test where ***=p<0.001.

These data demonstrate that this organoid culture technique supports GLP-1⁺ EEC development and represents the expected small intestinal GLP-1 ratio, allowing a platform for the successful examination of the effects of helminths on GLP-1⁺ EEC differentiation and GLP-1 secretion.

4.2 Helminth antigen increases secretion of GLP-1 without direct influence on GLP-1⁺ EEC development

To investigate the effects of helminth antigen on GLP-1⁺ cell density in the small intestine, ileal crypts were isolated from naïve C57BL/6 mice which were cultured with *T. muris* or *T. spiralis* antigen (Fig. 4.3). There was no significant difference in GLP-1⁺ cell frequency in organoids co-cultured with *T. muris* or *T. spiralis* antigen ($P>0.05$) compared to controls.

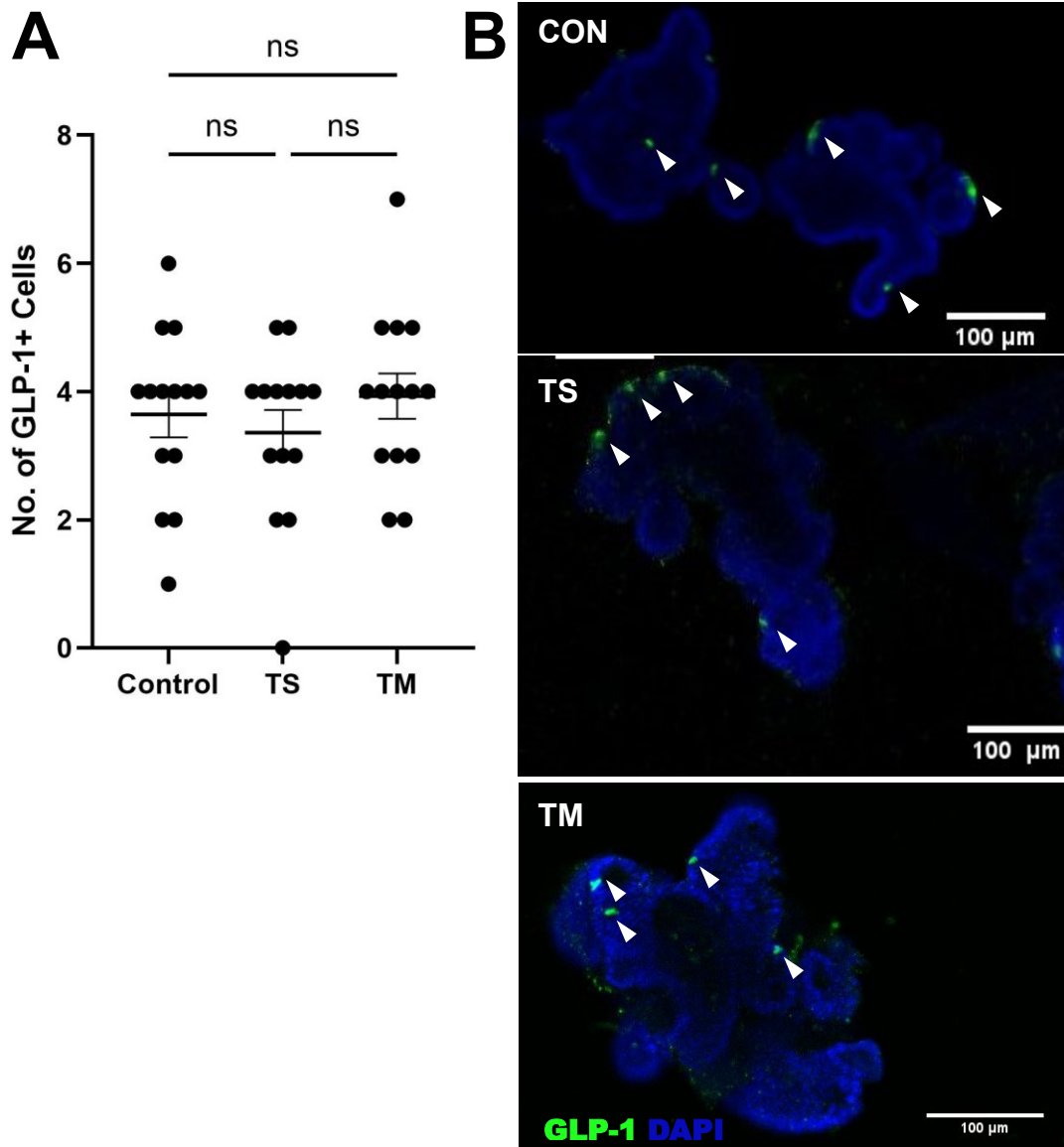


Figure 4.3: Helminth antigen has no significant effect on GLP-1⁺ cell frequency in murine small intestinal organoids. Ileal crypts were isolated from C57BL/6 mice and cultured with 10μg/ml *Trichinella spiralis* (TS) or *Trichuris muris* (TM) antigen, or in organoid growth medium only (control). After 10 days of culture, organoids were fixed and stained using GLP-1 antibodies, before imaging using confocal microscopy. A) Plotted data shows the number of GLP-1⁺ cells per organoid, B) representative imaged of stained organoids, where bars represent 100μm. Data (experimental n=4, were 3-4 organoids were randomly selected in each experiment) are presented as mean ± SEM. Each plotted point represents one organoid. Statistical analyses were performed using Kruskal-Wallis test with Dunn's multiple comparisons test. Results were statistically significant where p<0.05

To determine the effect of helminth antigen on GLP-1 secretion, a small intestinal organoid platform was used, boosting the frequency of GLP-1⁺ cells using Y27632 to allow maximal potential for GLP-1 secretion and detection. Organoids were incubated with *T. muris* or *T. spiralis* antigen, and the fold change in percentage GLP-1 secreted from EECs, compared to vehicle-only controls, was determined (Fig 4.4). Some organoids were cultured with forskolin and There was no significant increase in GLP-1 secretion following incubation with *T. muris* antigen as compared to vehicles, however incubation with *T. spiralis* antigen caused a significant increase (P=0.0259) as compared to vehicles (Fig 4.4A). Positive control shows the cells are capable of secreting GLP-1 to the maximum level, and therefore the helminth-dependent changes are biologically relevant. To determine the potential pathway, organoids were cultured with helminth antigen in the presence and absence of the bitter taste receptor inhibitor allyl isothiocyanate (AITC). Culturing with inhibitor only demonstrated that GLP-1 secretion does not decrease in response to inhibitor only; there was no inhibitor-directed toxicity, therefore the readings from those cultured with inhibitor and antigen were biologically relevant. No alteration was seen in the previous stable negative response to *T. muris*, but the inhibitor prevented the previous significant increase in secretion following *T. spiralis* incubation.

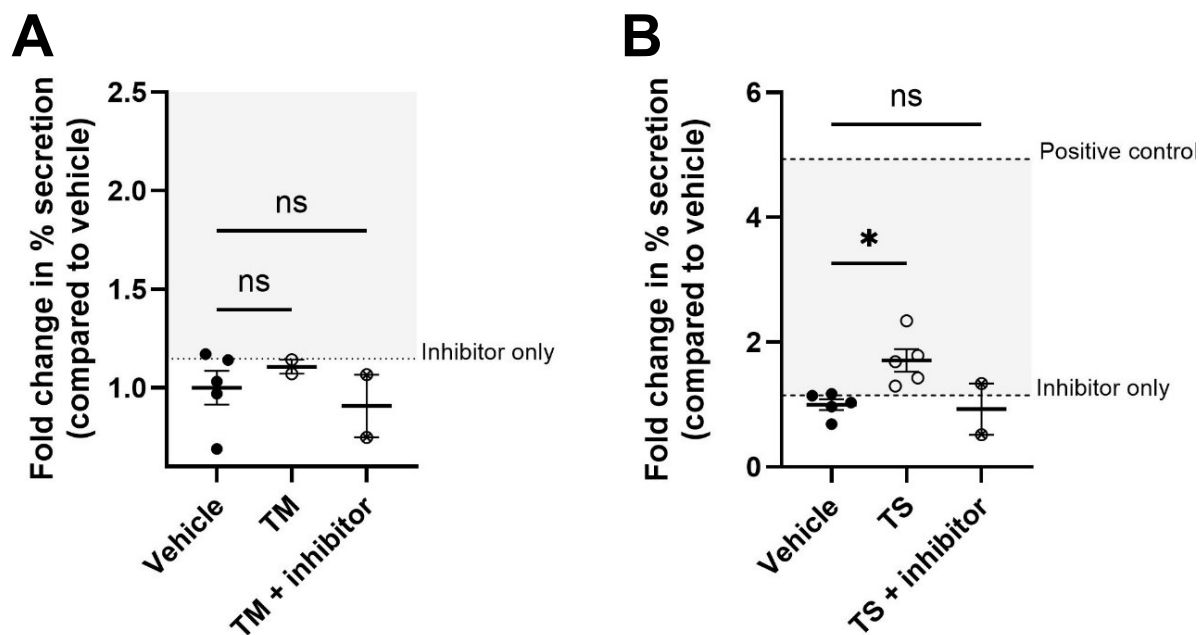


Figure 4.4. GLP-1 secretion increases in response to *T. spiralis* antigen in a taste receptor-dependent mechanism. Ileal crypts were isolated from naïve C57BL/6 mice and co-cultured with 10 μ M Y27632 in culture medium for 10 days. Ileal organoids were then incubated with substrate solution containing vehicle only, A) *T. spiralis* (TS) antigen or B) *T. muris* (TM) antigen, with and without AITC (inhibitor). Some organoids were cultured with inhibitor only, and some were cultured with forskolin, IBMX and glucose (positive control). After 4 hours, substrate containing secreted GLP-1 was removed, and lysis solution was added to organoids to release remaining GLP-1. The quantity of GLP-1 in lysate and substrate were determined by ELISA, and fold change in percentage of GLP-1 secretion compared to vehicle-only controls was calculated. Data (experimental n=2-5 per group), presented as mean \pm SEM. Statistical analyses were completed using one-way ANOVA with Dunnett's multiple comparisons test, where *=p<0.05.

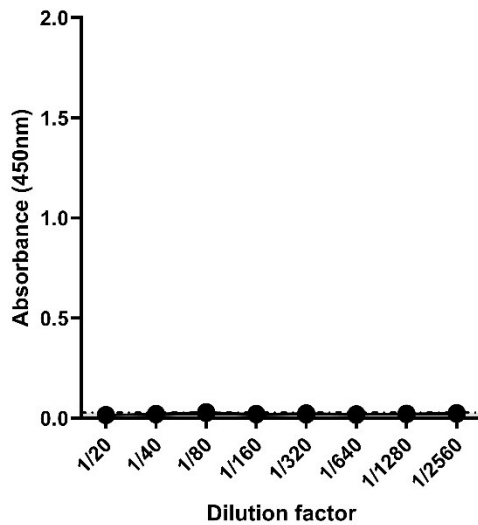
Collectively this indicates that helminth antigen does not influence GLP-1 development, but *T. spiralis* antigen does increase GLP-1 secretion via a taste receptor dependent mechanism.

4.3 The influence of GLP-1rA treatment on a trickle *T. muris* reinfection

Trichuriasis is a neglected tropical disease afflicting more than 600 million people worldwide. Anthelmintic treatments are effective in clearing chronic infection, however in areas where trichuriasis is prevalent there are high rates of reinfection (Speich *et al.* 2014); currently used anthelmintic drugs do not convey protection from subsequent infection. Dooley (2022) showed that acute lixisenatide treatment clears low dose *T. muris* infection in C57BL/6 mice via increased epithelial turnover. Therefore, a trickle infection model of *T. muris* infection was used to investigate whether lixisenatide treatment is protective against subsequent reinfection.

Serum IgG1 and IgG2c indicate the type of immune response occurring, with increased IgG1 and IgG2c being indicative of T_H2 and T_H1 responses, respectively (Else *et al.*, 1993). Parasite-specific IgG1 and IgG2a (which cross-reacts to IgG2c) ELISAs were used to assess the immune response to infection (Fig. 4.5) Here, parasite specific IgG1 and IgG2a antibody ELISAs showed no significant differences between control and lixisenatide-treated mice ($P > 0.05$), with both treatment groups showing little IgG1 response and comparable IgG2a responses.

IgG1



IgG2a

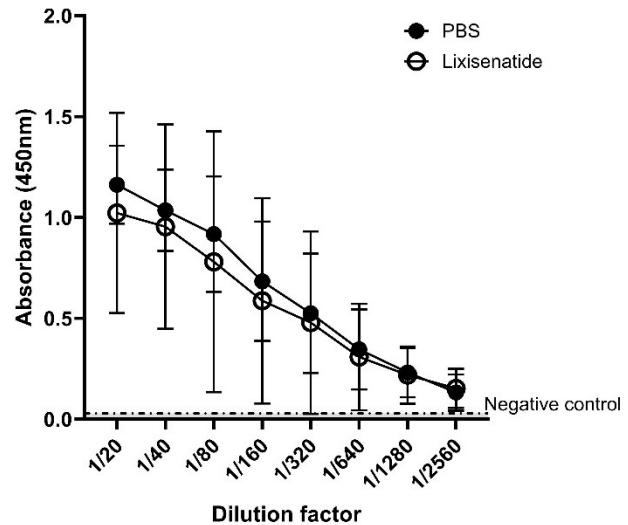


Figure 4.5: Parasite specific IgG1 and IgG2a antibody responses of C57BL/6 mice are not altered following lixisenatide treatment and *T. muris* reinfection. Mice were infected with low dose (approx. 30 eggs) *T. muris* and infection was allowed to establish for 34 days. Mice were treated with either PBS (control) or lixisenatide by intraperitoneal injection. 3 days after treatment, mice were reinfected low dose (approx. 30 eggs) *T. muris* infection. Mice were then sacrificed, and serum obtained. Serial dilutions of sera were incubated with biotinylated rat anti-mouse A) IgG1 and B) IgG2a antibodies in antigen coated ELISA plates. Bound antibody was detected using streptavidin peroxidase and TMB substrate, and reaction stopped using sulphuric acid. Absorbance was measured using a Tecan Infinite pro plate reader at 450nm with 540nm reference. Negative control data was obtained from plate wells processed without serum. Data are presented as mean \pm SEM (experimental n = 6). Statistical analyses were performed using unpaired T tests at each dilution factor and considered statistically significant where $P < 0.05$.

Goblet cell hyperplasia and mucin hypersecretion are key mechanisms in the expulsion of *T. muris* (Hasnain *et al.* 2010; Hasnain *et al.* 2011a; Hasnain *et al.* 2011b). Dooley (2022) saw no changes in caecal crypt or goblet structure or goblet cell morphology following lixisenatide treatment. To determine whether changes in goblet cell and caecal crypt structure occur following post-treatment reinfection, caecal tip sections were stained using alcian-blue-PAS staining for goblet cells. Caecal crypt length, goblet cell frequency and goblet cell size of 20 randomly selected caecal crypt units (CCUs) were measured. Here, there was no significant difference in crypt length (Fig. 4.6A), goblet cell number (Fig. 4.6B) or goblet cell size (Fig. 4.6C) between PBS- and lixisenatide- treated mice following post-treatment reinfection with *T. muris*.

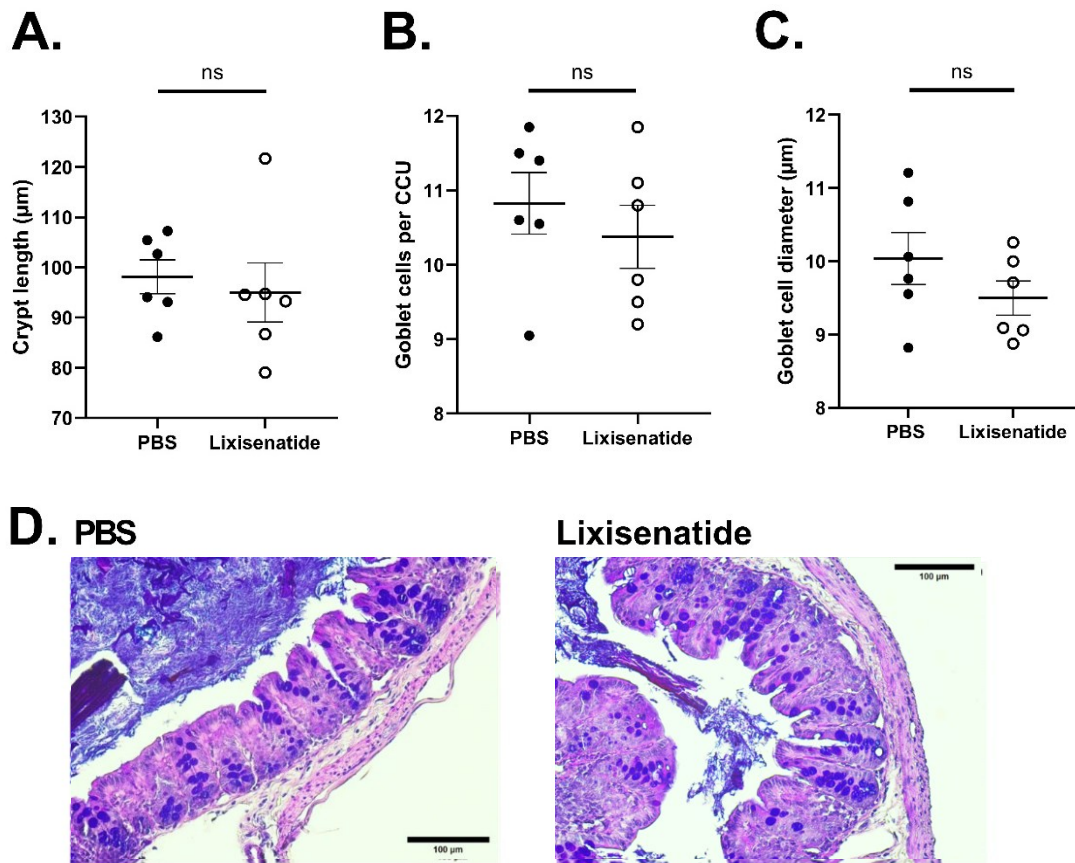


Figure 4.6: Caecal crypt structure or goblet cells are not altered following lixisenatide treatment and *T. muris* reinfection. Mice were infected with low dose (approx. 30 eggs) *T. muris* and infection was allowed to establish for 34 days. Mice were treated with either PBS (control) or lixisenatide by intraperitoneal injection. 3 days after treatment, mice were reinfected with low dose (approx. 30 eggs) *T. muris* infection. Mice were sacrificed 18 days post-reinfection and caecum samples obtained. Caecal tip samples were stained using alcian blue-PAS. Crypt length and goblet cell number per caecal crypt unit (CCU) and goblet cell diameter were analysed using ImageJ (A-C) Quantification for each mouse was performed by measuring 20 CCUs and determining the mean (A) crypt length, (B) number of goblet cells and C) diameter of goblet cells per CCU. (D) Representative images of alcian blue-PAS-stained caecal tip sections in PBS control and lixisenatide treated mice, where bars represent 100 μm . Data are presented as mean \pm SEM where experimental n=6 per group, and each plotted point represents one mouse. Data were analysed using unpaired T tests and considered statistically significant where $P < 0.05$.

Increased epithelial turnover is a key mechanism in the expulsion of *T. muris* (Cliffe *et al.* 2005) therefore, to observe any change in epithelial turnover, The suitability of using a QuCCi mouse system (a cell-cycle reporter mouse system in which fluorescence changes during G1, S, G2/M and G0 stages of the cell cycle, Briggs 2024; Mort *et al.* 2014) to investigate epithelial turnover was explored, however observation of preliminary experiments showed little staining and therefore this method was unsuitable

for subsequent experiments (Appendix 1). Therefore, a bromodeoxyuridine (BrdU) pulse-chase experiment was used over a 12-hour period to determine the number of proliferating cells and rate of epithelial turnover. There was no significant difference in the number of proliferating cells within the caecal crypts of PBS- and lixisenatide-treated mice, as determined by positively stained cells (Fig. 4.7A). Similarly, there was no significant difference in the rate of epithelial turnover between these treatment groups (Fig. 4.7 B).

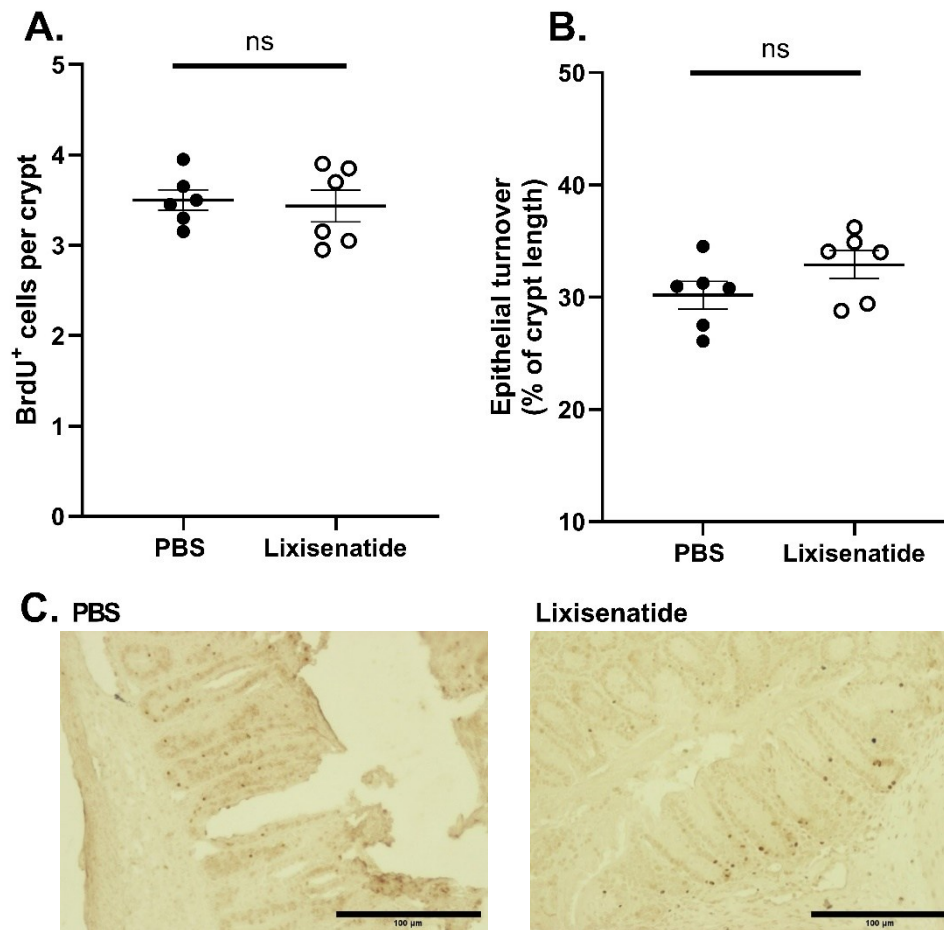


Figure 4.7: Epithelial cell proliferation and turnover are not altered following lixisenatide treatment and *T. muris* reinfection. Mice were infected with low dose (approximately 30 eggs) *T. muris* and infection was allowed to establish for 34 days. Mice were then treated with either PBS (control) or lixisenatide by intraperitoneal injection. 3 days after treatment, mice were infected once again with low dose (approximately 30 eggs) *T. muris* infection. Mice were then sacrificed 18 days post-reinfection and caecum samples obtained. Caecal tip samples were stained using anti-BrdU and A) the number of proliferating cells and B) migration distance assessed by movement of BrdU⁺ cells up the crypt was determined by light microscopy. C) Representative images of BrdU stained caecal tissue of PBS control and lixisenatide-treated mice. Data (experimental n=6 per group) are presented as mean ± SEM, where each plotted point represents one mouse. Data were analysed using unpaired T tests and considered statistically significant where P<0.05.

T cell response in the mesenteric lymph node was next scrutinised; given that T cells and the production of IL-13 and IFN γ are central to helminth expulsion or establishment of chronic infection, respectively, The immune cell populations present in the mLN at the time of sacrifice was assessed by flow cytometry. Analysis of the cellularity of the mLN following *T. muris* reinfection shows no significant difference between those of PBS- and lixisenatide-treated mice (Fig. 4.8A). Subsequent analysis of the percentage of CD45⁺ cells in the mLN following reinfection shows no significant difference in the number of leukocytes present in the mLN (Fig. 4.8B-C)

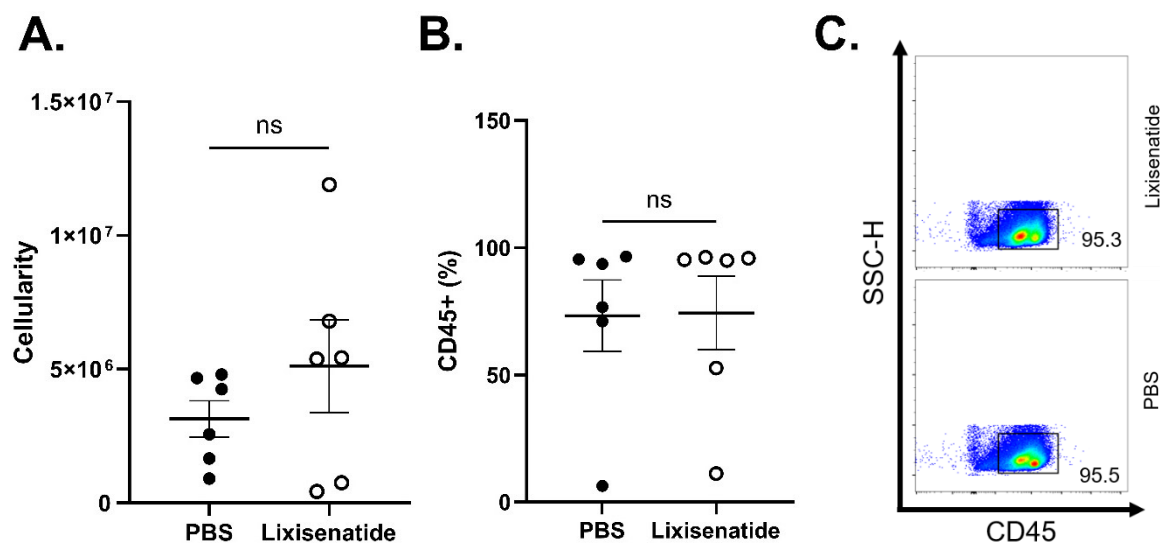


Figure 4.8: Cellularity of the mesenteric lymph node is not altered following lixisenatide treatment and *T. muris* reinfection. C57BL/6 mice were infected with low dose (approx. 30 eggs) *T. muris* and infection was allowed to establish for 34 days. Mice were treated with either PBS (control) or lixisenatide by intraperitoneal injection. 3 days after treatment, mice were infected once again with low dose (approx. 30 eggs) *T. muris* infection. Mice were then sacrificed 18 days post-infection and mLN obtained. mLN were stimulated with Cell Stimulation Cocktail (with protein transport inhibitors) overnight, before cells were collected and analysed by flow cytometry. A) mLN cellularity was determined using a Countess automated cell counter. B) Percentage of CD45⁺ cells in the mLN at the time of sacrifice. C) Representative flow cytometry plots from (B). Data are presented as mean \pm SEM where experimental n=6 per group. Each plotted point represents 1 mouse. Data were analysed using A) unpaired T tests and B) Mann Whitney U test, and considered statistically significant where $P < 0.05$.

The number of T cells and the T cell subsets in the mLN was next assessed; here there was no significant difference in the number of CD3⁺ (Fig.4.9A), CD4⁺ (Fig.4.9C) and CD8⁺ (Fig.4.9D) T cells between PBS- and lixisenatide-treated mice.

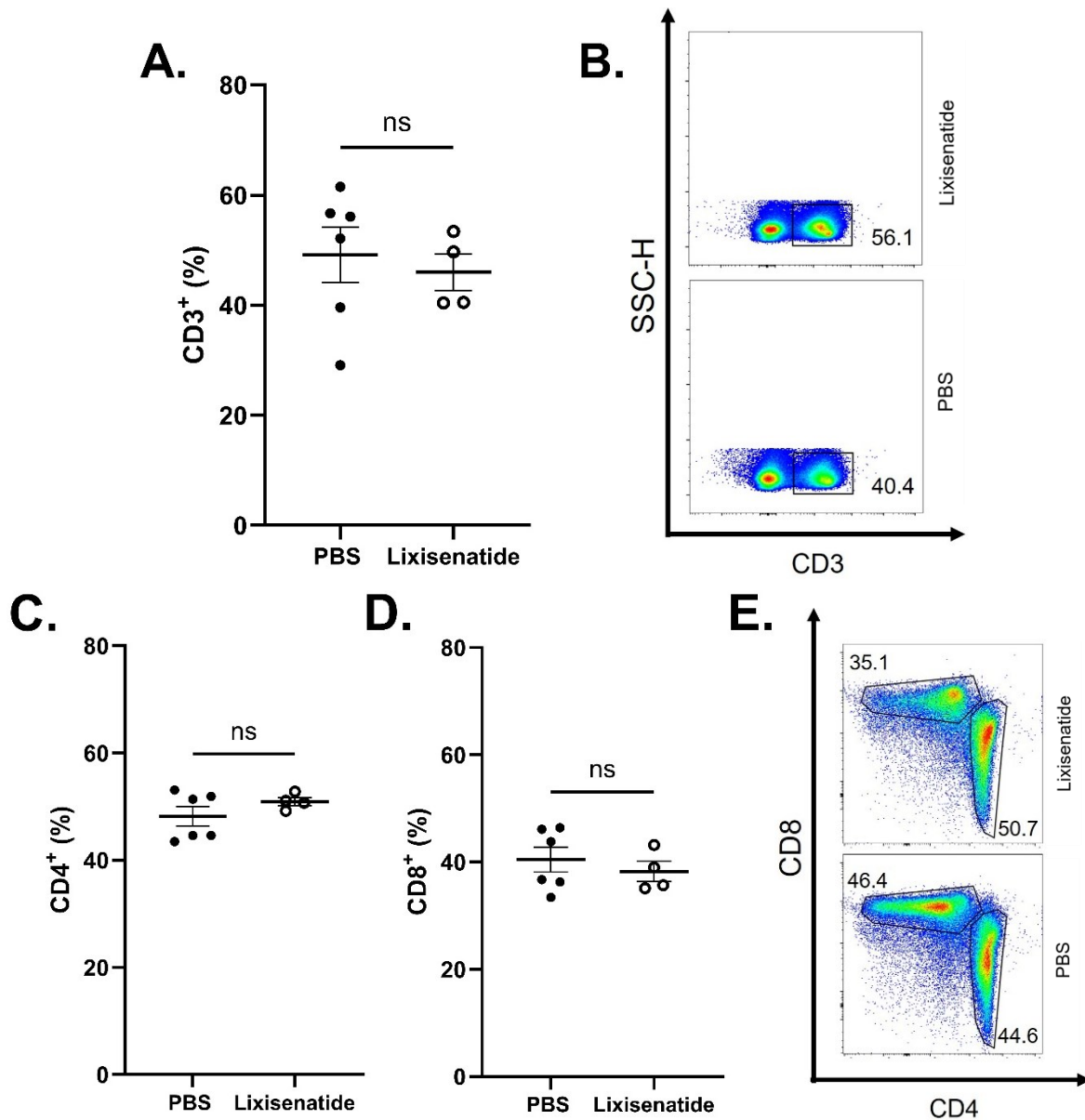


Figure 4.9: The percentage of CD4⁺ and CD8⁺ T cells in the mesenteric lymph node are not altered following lixisenatide treatment and *T. muris* reinfection. C57BL/6 mice were infected with low dose (approx. 30 eggs) *T. muris* and infection was allowed to establish for 34 days. Mice were treated with either PBS (control) or lixisenatide by intraperitoneal injection. 3 days after treatment, mice were infected once again with low dose (approx. 30 eggs) *T. muris* infection. Mice were then sacrificed 18 days post-infection and mLN obtained. mLN were stimulated with Cell Stimulation Cocktail (with protein transport inhibitors) overnight, before cells were collected and analysed by flow cytometry. Plotted data shows the percentage of A) CD3⁺ leukocytes in the mLN with B) representative flow cytometry plots from (A), the percentage of C) CD4⁺ and D) CD8⁺ T cells in the mLN, with E) representative flow cytometry plots from (C) and (D). Data (experimental n=4-6 per group) are presented as mean ± SEM. Each plotted point represents 1 mouse. Data were analysed using unpaired T tests and considered statistically significant where P<0.05.

The cytokine profile of the CD4⁺ and CD8⁺ T cells in the mLN was assessed to observe any difference in IFN γ , IL-13 and IL-17 production (Fig. 4.10). Both CD4⁺ and CD8⁺ T cells showed minimal production of IL-13 (<0.2%) which was comparable between treatment groups in CD4⁺ T cells. Interestingly, IL-13 production in CD8⁺ T cells of lixisenatide-treated mice was lower than that of PBS-treated mice, although this difference was not significant. IFN γ production by both CD4⁺ and CD8⁺ T cells was slightly increased in lixisenatide-treated mice, although not significantly so. Furthermore, IL-17 production in CD4⁺ T cell appears to be raised in lixisenatide-treated mice compared to those treated with PBS, although this difference was not significant, and IL-17 production by CD8⁺ T cells was comparable between treatment groups.

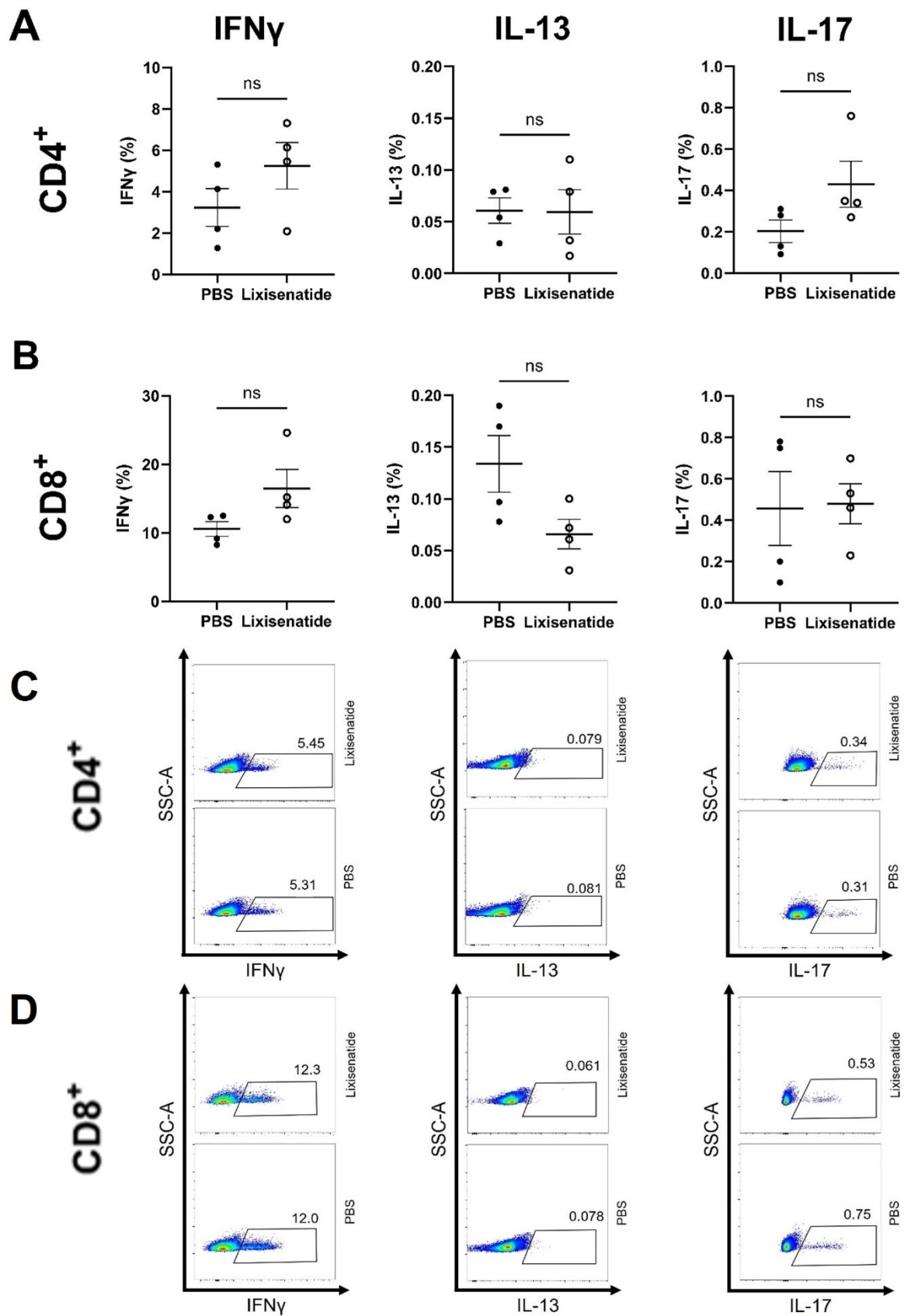


Figure 4.10: Cytokines produced by CD4⁺ and CD8⁺ T cells are unaffected following lixisenatide treatment and *T. muris* reinfection. C57BL/6 mice were infected with low dose (approx. 30 eggs) *T. muris* and infection was allowed to establish for 34 days. Mice were treated with either PBS (control) or

lixisenatide by intraperitoneal injection. 3 days after treatment, mice were infected once again with low dose (approx. 30 eggs) *T. muris* infection. Mice were then sacrificed 18 days post-infection and mLN obtained. mLN were stimulated with Cell Stimulation Cocktail (with protein transport inhibitors) overnight, before cells were collected and analysed by flow cytometry. Plotted data shows levels of IFN γ , IL-13 and IL-17 produced by A) CD4 $^+$ and B) CD8 $^+$ T cells. C) and D) show representative plots from A) and B). Data (experimental n=4 per group) are presented as mean \pm SEM. Each plotted point represents 1 mouse. Data were analysed using unpaired T tests and considered statistically significant where $P < 0.05$.

Staining for the cell surface marker CD45RB allowed for the assessment of the number of effector-memory T (TEM) cells in the mLN at the time of sacrifice via CD4⁺ and CD8⁺ staining. There were no significant differences between PBS- and lixisenatide-treated mice (Fig. 4.11) in terms of either TEM population. IFN γ , IL-13 and IL-17 production by CD4⁺ and CD8⁺ TEM cells was also assessed, although no significant differences were seen between the treatment groups (data not shown).

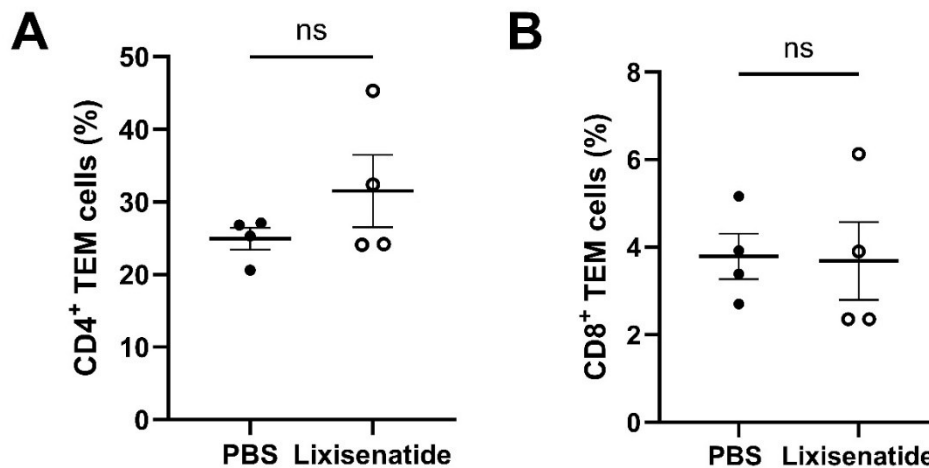
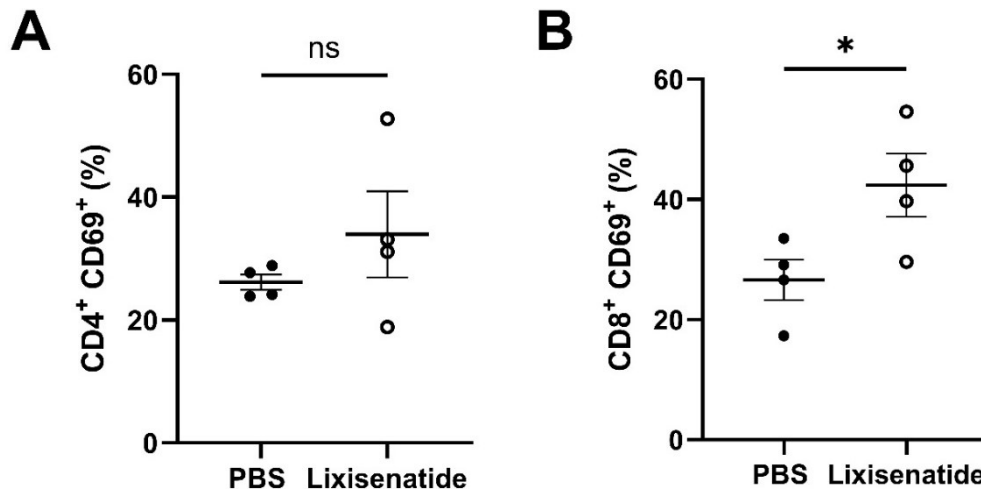


Figure 4.11 CD4⁺ and CD8⁺ effector memory T (TEM) cell frequency is not altered following lixisenatide treatment and *T. muris* reinfection. C57BL/6 mice were infected with low dose (approx. 30 eggs) *T. muris* and infection was allowed to establish for 34 days. Mice were treated with either PBS (control) or lixisenatide by intraperitoneal injection. 3 days after treatment, mice were infected once again low dose (approx. 30 eggs) *T. muris* infection. Mice were then sacrificed 18 days post-infection and mLN obtained. mLN were stimulated with Cell Stimulation Cocktail (with protein transport inhibitors) overnight, before cells were collected and analysed by flow cytometry. Plotted data shows the percentage of A) CD4⁺ and B) CD8⁺ TEM cells in the mLN. Data (experimental n=4 per group) are presented as mean \pm SEM. Each plotted point represents 1 mouse. Data were analysed using unpaired T tests and considered statistically significant where $P < 0.05$.

The number of recently activated T cells in the mLN at the time of sacrifice was assessed through staining of the cell-surface marker CD69 to determine the number of recently activated CD4⁺ and CD8⁺ T cells. Though there was an increased percentage of recently activated CD4⁺ T cells in lixisenatide-treated mice compared to those treated with PBS, this difference was not significant (Fig. 4.12A). Interestingly, There was a significantly higher percentage of recently activated CD8⁺ T cells in lixisenatide-treated mice compared to PBS controls ($P = 0.0456$, Fig. 4.12B). Further assessment of these recently activated T cell populations showed that, in spite of this difference in number of recently activated CD8⁺ T cells, there was no significant difference in IFN γ , IL-13 and IL-17 between treatment groups (Fig. 4.13B). There was also no difference in the production of these cytokines in recently activated CD4⁺ T cells (Fig. 4.13A).



4.12: The frequency of recently activated CD8⁺ T cells increases following lixisenatide treatment and *T. muris* reinfection. C57BL/6 mice were infected with low dose (approx. 30 eggs) *T. muris* and infection was allowed to establish for 34 days. Mice were treated with either PBS (control) or lixisenatide by intraperitoneal injection. 3 days after treatment, mice were infected once again with low dose (approx. 30 eggs) *T. muris* infection. Mice were then sacrificed 18 days post-infection and mLN obtained. mLN were stimulated with Cell Stimulation Cocktail (with protein transport inhibitors) overnight, before cells were collected and analysed by flow cytometry. Plotted data shows the percentage of recently activated A) CD4⁺ and B) CD8⁺ T cells. Data (experimental n=4 per group) are presented as mean ± SEM. Each plotted point represents 1 mouse. Data were analysed using unpaired T tests and * = P<0.05.

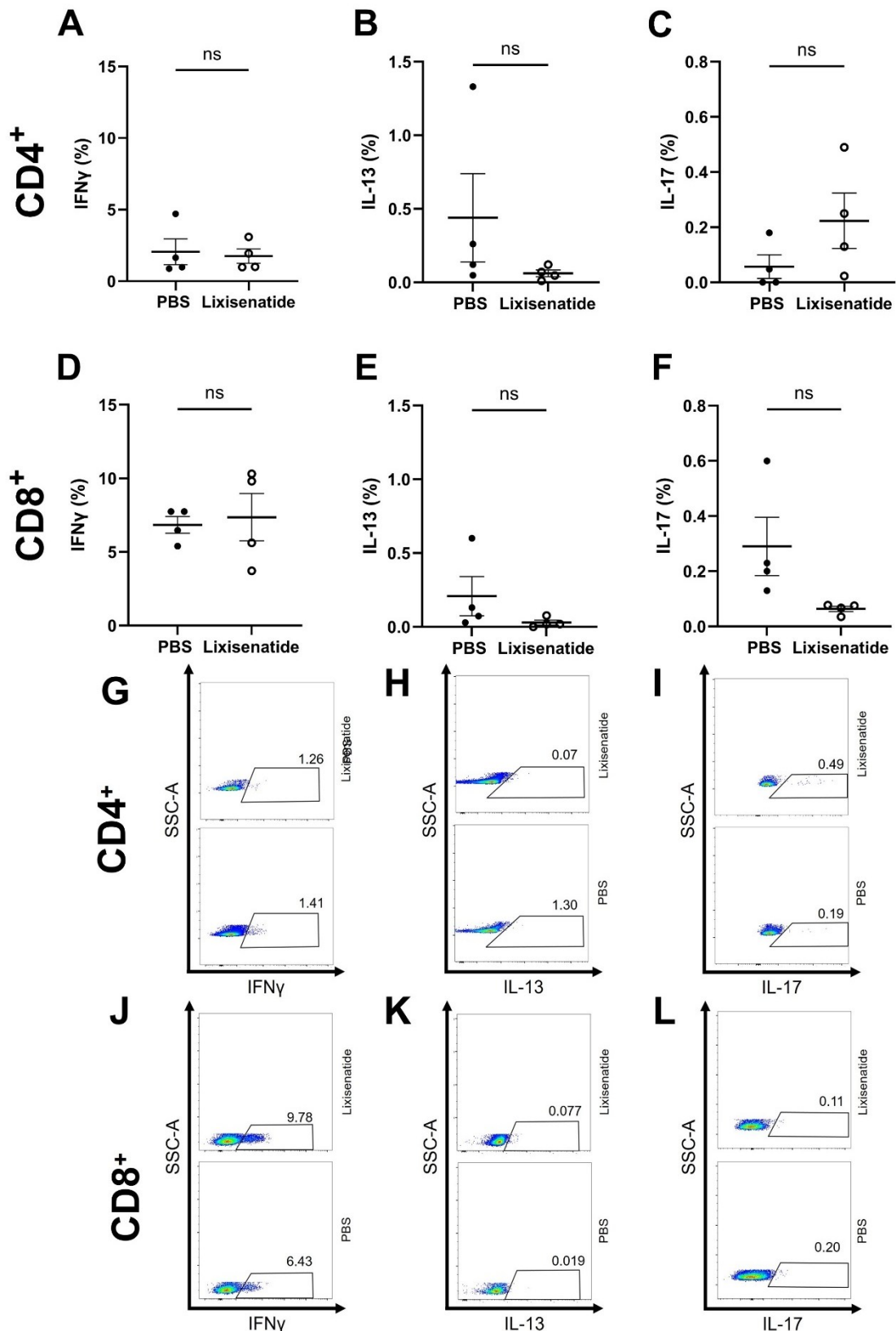


Figure 4.13: Cytokines produced by recently activated CD4⁺ and CD8⁺ T cells are unaffected following lixisenatide treatment and *T. muris* reinfection. C57BL/6 mice were infected with low dose (approx. 30 eggs) *T. muris* and infection was allowed to establish for 34 days. Mice were treated with either PBS (control) or lixisenatide by intraperitoneal injection. 3 days after treatment, mice were

infected once again with low dose (approx. 30 eggs) *T. muris* infection. Mice were then sacrificed 18 days post-infection and mLN obtained. mLN were stimulated with Cell Stimulation Cocktail (with protein transport inhibitors) overnight, before cells were collected and analysed by flow cytometry. Plotted data shows levels of IFN γ , IL-13 and IL-17 produced by A-C) CD4 $^+$ and D-F) CD8 $^+$ T cells, and G-L) show representative flow plots from A-F). Data (experimental n=4 per group) are presented as mean \pm SEM, and each plotted point represents 1 mouse. Data were analysed using unpaired T tests and considered statistically significant where $P < 0.05$.

In order to put these results into the context of infection outcome, the worm burdens of mice from each group were determined by examination of the caecum and proximal colon post-sacrifice (Fig.4.14A). Worm counts showed no significant difference in the total number worm burden at the time of sacrifice in PBS- and lixisenatide-treated mice. Further analysis showed that all worms from the primary infection, which would have matured to adulthood, had been expelled in both treatment groups (Fig.4.14B). Both treatment groups had few immature worms, but there was no significant difference between treatment groups ($P < 0.05$).

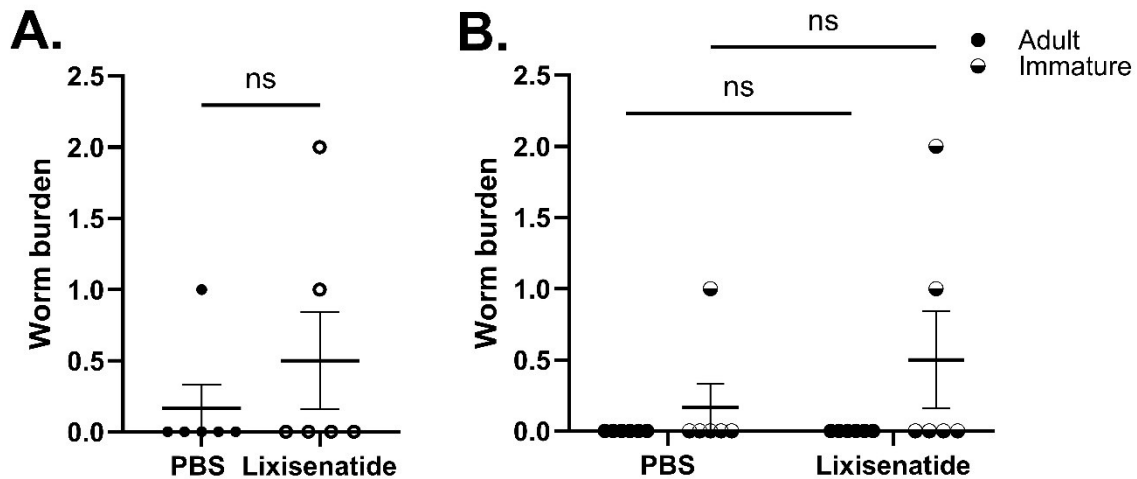


Figure 4.14: Eggs from this passage did not survive past day 51 in control animals meaning treatments were inconclusive. C57BL/6 mice were infected with low dose (~30 eggs) *T. muris* infection by oral gavage. 34 days post-infection mice were treated with PBS (controls) or 10 μ g lixisenatide (treated). 3 days after treatment, mice were re-infected with low dose (~30 eggs) *T. muris*. 18 days after second infection, mice were sacrificed, and caeca and proximal colons were obtained. A) total worms and B) the number of adult and immature worms were counted using a dissecting microscope. Data (experimental $n=6$ per group), and presented as mean \pm SEM, where each point represents 1 mouse. Statistical analyses were completed using A) Mann-Whitney U test and B) two-way ANOVA with Tukey's multiple comparisons test, and results were considered statistically significant where $P < 0.05$.

To further understand these findings, the *T. muris* egg output of each mouse was analysed using a modified McMaster technique (Fig.4.15). Faecal pellets were collected from mice before and after lixisenatide treatment to semi-quantitatively assess infection status at each time point. There was a decrease in faecal egg output in both PBS-treated ($P=0.0143$) and lixisenatide-treated ($P=0.0175$) mice 3 days post-treatment (Fig.4.15A). FEC 11 days after treatment was only significantly lower than pre-treatment in lixisenatide-treated mice ($P=0.0425$) when observing FEC as an average of faecal pellets collected per mouse (Fig.4.15B). When considering FEC per faecal pellet, those collected 11 days post-treatment were not significantly lower than pre-treatment levels in either PBS- or -lixisenatide-treated

mice (Fig.4.15A). There was no significant difference in faecal egg output between treatment groups at any time point.

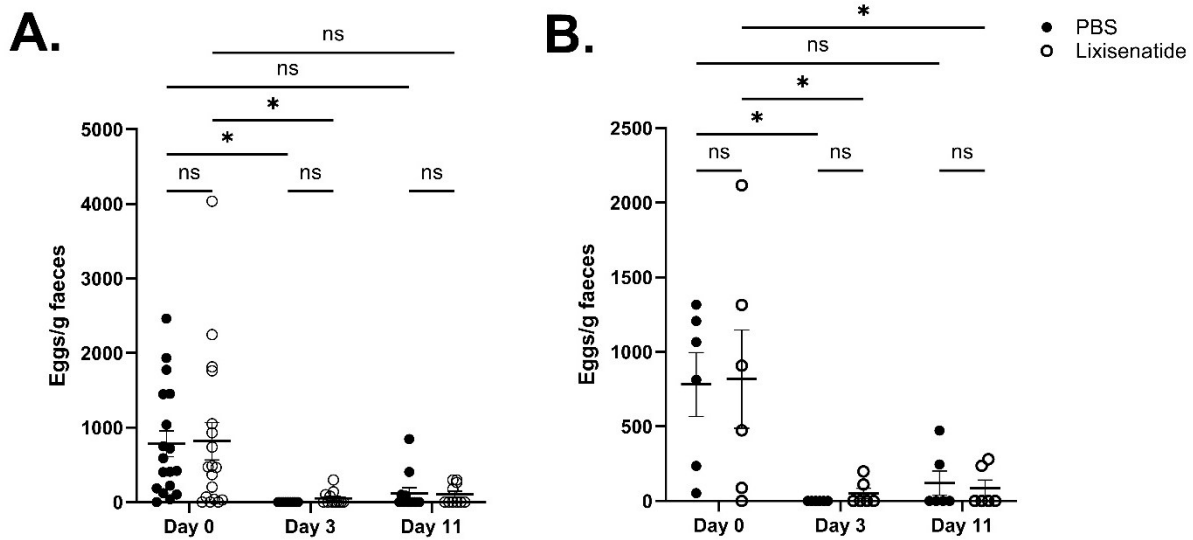


Figure 4.15: Faecal egg counts indicate that worms were expelled from both *PBS-* and *lixisenatide-treated* mice following *lixisenatide* treatment and *T. muris* reinfection. C57BL/6 mice were infected with low dose (~30 eggs) *T. muris* infection by oral gavage. 34 days post-infection (Day 0) mice were treated with PBS (controls) or 10µg *lixisenatide* (treated). 3 days after treatment (Day 3), mice were re-infected with low dose (~30 eggs) *T. muris*. At days 0, 3, and 11 post-treatment, 2-4 faecal pellets were collected from each mouse and *T. muris* eggs were counted using a modified McMaster technique. Data (experimental n=6) are presented as mean ± SEM, where A) each plotted point represents 1 faecal pellet, collected from 6 mice per group, and B) each plotted point represents the average FEC of one mouse. Statistical analyses were completed using two-way ANOVA with Tukey's multiple comparisons test, * = p<0.05

Collectively, these data suggest that the batch of eggs used to establish 'trickle' infection were unable to maintain an infection beyond the initial L4 moult and egg production. Given the lack of local and timely availability of another batch of *T. muris* eggs, an alternative model was used; T cell transfer would be a viable alternative for the investigation of any immunological memory formation following *lixisenatide* treatment.

4.4 *Lixisenatide* treatment decreases worm burden in *T. muris*-infected RAG mice reconstituted with T cells following GLP-1rA treatment

To circumvent the lack of local availability of a viable batch of *T. muris* eggs to repeat the trickle-based reinfection study, adoptive T cell transfer was employed to investigate the protective effects of GLP-1rA treatment of a primary *T. muris* infection against subsequent challenge infection. C57BL/6 mice were infected with low dose (approx. 30 eggs) *T. muris* for 21 days and then treated with PBS or *lixisenatide*. Following treatment, mice were sacrificed, and T cells were obtained and transferred into naïve RAG

mice, which lack adaptive immunity and hence T and B-cells. After 1 week of T cell expansion, these mice were infected with a low dose (approx. 30 eggs) *T. muris* infection.

Serum IgG1 and IgG2a responses were measured in RAG^{-/-} mice which received T cells from PBS- and lixisenatide-treated RAG mice (Fig. 4.16); there was no significant readouts and hence difference between the treatment groups. Mean absorbance readings at each dilution factor were below the negative control value, suggesting neither IgG1 nor IgG2 responses occurring demonstrating that the T cell isolate was not contaminated by B cells.

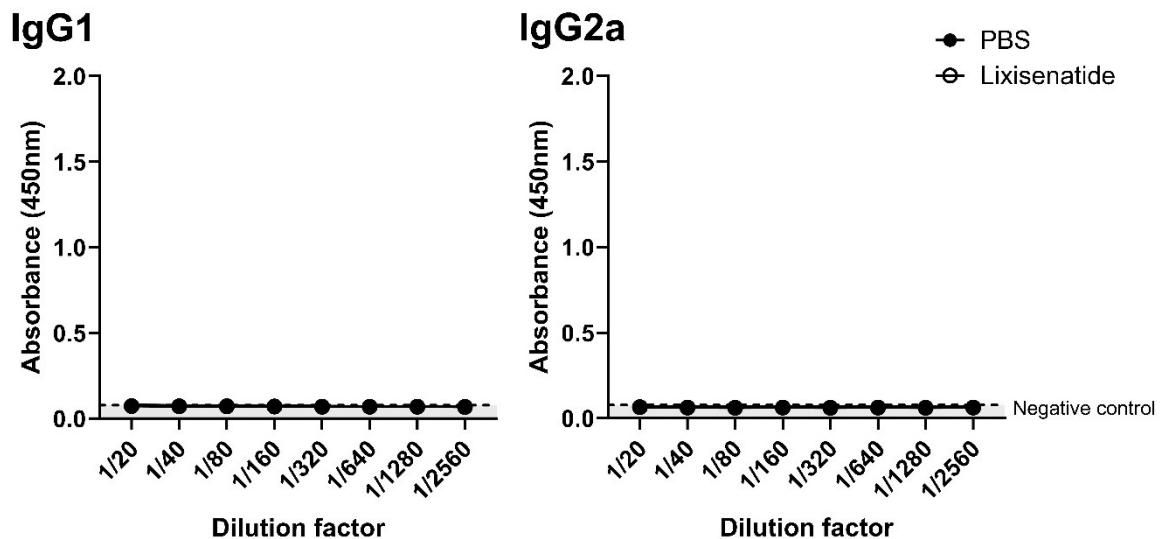


Figure 4.16: Parasite specific IgG1 and IgG2a antibody response of RAG mice reconstituted with CD4⁺ T cells from *T. muris* infected and lixisenatide-treated C57BL/6 mice. C57BL/6 mice were infected with low dose (approx. 30 eggs) *T. muris* and infection was allowed to establish for 21 days. Mice were treated by intraperitoneal injection PBS or with lixisenatide. Upon completion of treatment, mice were sacrificed, and T cells were isolated from mLN and adoptively transferred into RAG mice. After 1 week, these mice were infected with low dose (approx. 30 eggs) *T. muris*, and infection was allowed to progress for 21 days. Serial dilutions of sera from mice with T cells from treated and control mice were incubated with biotinylated rat anti-mouse IgG1 and IgG2a antibodies in antigen coated ELISA plates. Bound antibody was detected using streptavidin peroxidase and TMB substrate, and reaction stopped using sulphuric acid. Absorbance was measured using a Tecan Infinite pro plate reader at 450nm with 540nm reference. Negative control data was obtained from plate wells processed without serum. Data are presented as mean \pm SEM (experimental n=2-3 per group). Statistical analyses were performed using unpaired T tests at each dilution factor and considered statistically significant where $P < 0.05$.

Characteristic changes to caecal crypt and goblet cell structure can be seen in both chronic *T. muris* infection, and *T. muris* expulsion (Klementowicz *et al.* 2012). Dooley (2022) saw no changes in caecal crypt or goblet structure or goblet cell morphology following lixisenatide treatment, however it is unknown whether changes in goblet cell and caecal crypt structure occur following post-treatment

reinfection. Caecal tip sections were stained using alcian-blue-PAS staining for goblet cells, and caecal crypt length, goblet cell frequency and goblet cell size in 20 randomly selected caecal crypt units (CCUs) were measured (Fig. 4.17). Here there was a small trend in goblet cell frequency in mice reconstituted with T cells from lixisenatide-treated infected mice, but this was not significant, as with the crypt length and goblet cell size as compared to transfer of T-cells from PBS treated infected mice.

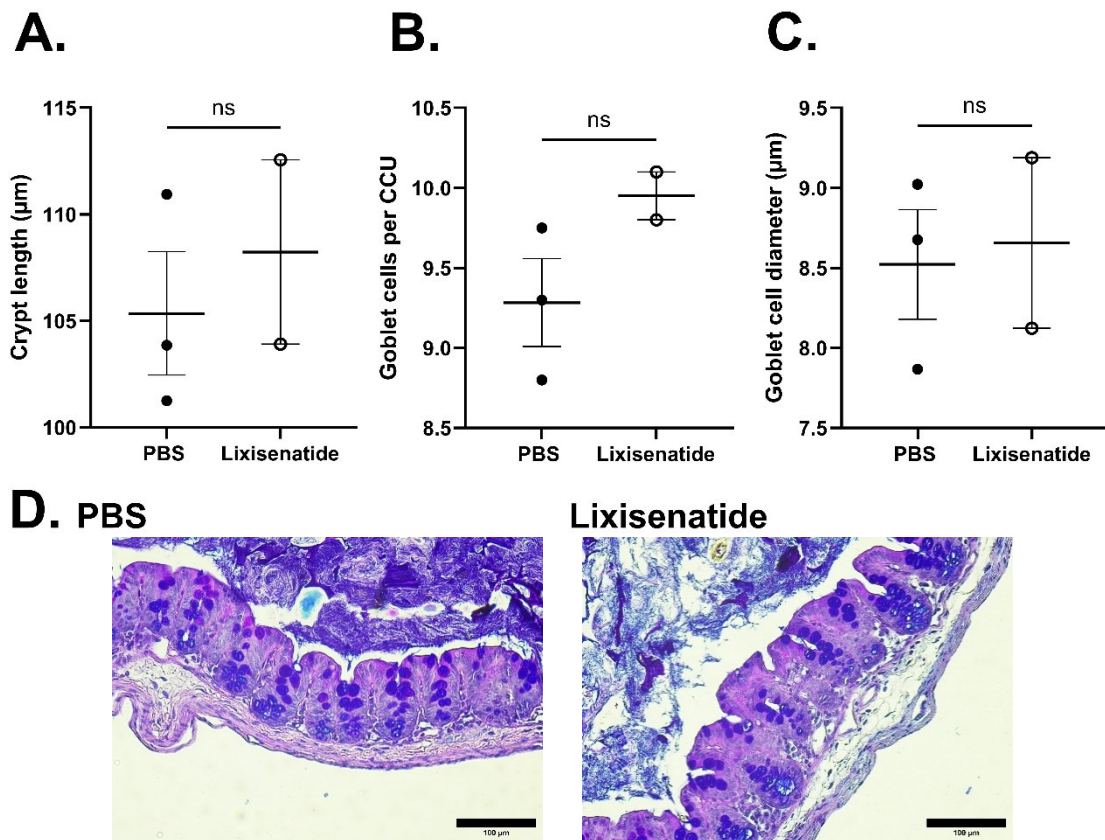


Figure 4.17: Transfer of T-cells from *T. muris* infected and lixisenatide-treated mice to RAG mice does not affect caecal crypt structure or goblet cells following *T. muris* infection. C57BL/6 mice were infected with low dose (approx. 30 eggs) *T. muris* and infection was allowed to establish for 21 days. Mice were treated by intraperitoneal injection with PBS or lixisenatide. Upon completion of treatment, mice were sacrificed, and T cells were isolated from mLN and adoptively transferred into RAG mice. After 1 week, these RAG mice were infected with low dose (approx. 30 eggs) *T. muris*, and infection was allowed to progress for 21 days. At time of sacrifice, caecum samples were obtained. Caecal tip samples were stained using alcian blue-PAS. Crypt length and goblet cell number per caecal crypt unit (CCU) and goblet cell diameter were analysed using ImageJ (A-C) Quantification for each mouse was performed by measuring 20 CCUs and determining the mean (A) crypt length, (B) number of goblet cells and (C) diameter of goblet cells per CCU. (D) Representative images of alcian blue-PAS-stained caecal tip sections in PBS control and lixisenatide treated mice, where bars represent 100 μm . Data are presented as mean \pm SEM where $n=2-3$, where each plotted point represents one mouse. Data were analysed using Mann-Whitney U tests and considered statistically significant where $P < 0.05$.

An increase in epithelial turnover is central to *T. muris* expulsion, and Dooley (2022) showed an increase in epithelial turnover following lixisenatide treatment in *T. muris*-infected C57BL/6 mice. The use of QuCCi mice to observe changes in epithelial turnover was inconclusive, therefore a bromodeoxyuridine (BrdU) pulse-chase experiment was used over a 12-hour period to determine the number of proliferating cells and rate of epithelial turnover. The number of proliferating cells, as measured by positive BrdU staining, was significantly higher ($p=0.0110$) in mice reconstituted with T cells from lixisenatide-treated mice than those from PBS-treated controls (Fig.4.18A). Furthermore, the epithelial turnover over 12 hours was significantly higher ($P=0.0214$) in the lixisenatide group than controls (Fig.4.18B, $P<0.05$)

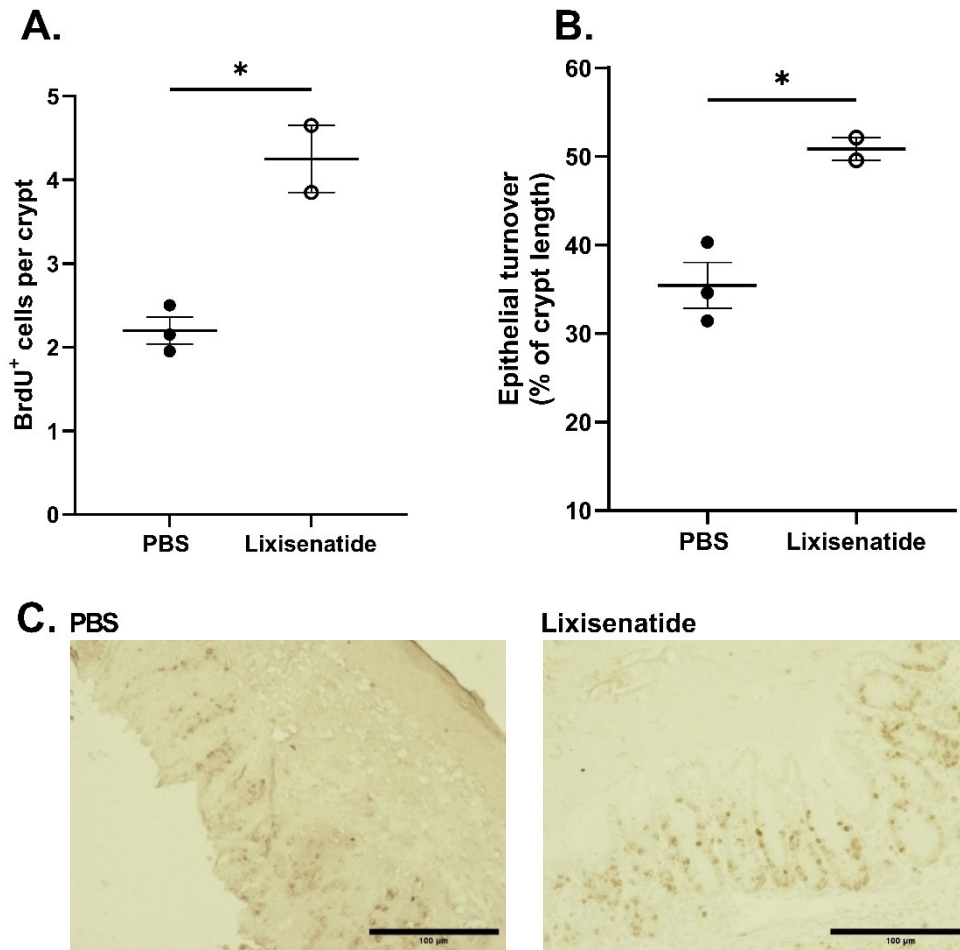


Figure 4.18: Transfer of T-cells from *T. muris* infected and lixisenatide-treated mice to RAG mice significantly increases epithelial turnover following *T. muris* infection. C57BL/6 mice were infected with low dose (approx. 30 eggs) *T. muris* and infection was allowed to establish for 21 days. Mice were treated by intraperitoneal injection with PBS or lixisenatide. Upon completion of treatment, mice were sacrificed, and T cells were isolated from mLN and adoptively transferred into RAG mice. After 1 week, these RAG mice were infected with low dose (approx. 30 eggs) *T. muris*, and infection was allowed to progress for 21 days. At time of sacrifice, caecum samples were obtained. Caecal tip samples were stained using anti-BrdU and A) the number of proliferating cells and B) migration distance assessed by movement of BrdU⁺ cells up the crypt was determined by light microscopy. C) Representative images of BrdU stained caecal tissue of PBS- and lixisenatide-treated mice (D) Representative images of alcian blue-PAS-stained caecal tip sections in PBS control and lixisenatide treated mice. Data (experimental n=2-3 per group) are presented as mean ± SEM, where each plotted point represents 1 mouse. Data were analysed using Mann-Whitney U tests where * = P<0.05.

Flow cytometry was used to observe the T cell response in the mesenteric lymph node (mLN) at the time of sacrifice; T cell-derived IL-13 or IFN γ are central to the mechanisms facilitating worm expulsion or establishment of chronic infection, respectively. The cellularity of the mLN of RAG-/- mice reconstituted with T cells from PBS- and lixisenatide-treated mice was assessed, which showed no

significant difference between treatment groups (Fig.4.19A). Furthermore, there was no significant difference in the number of CD4⁺ T cells between the PBS and lixisenatide groups (Fig.4.19B).

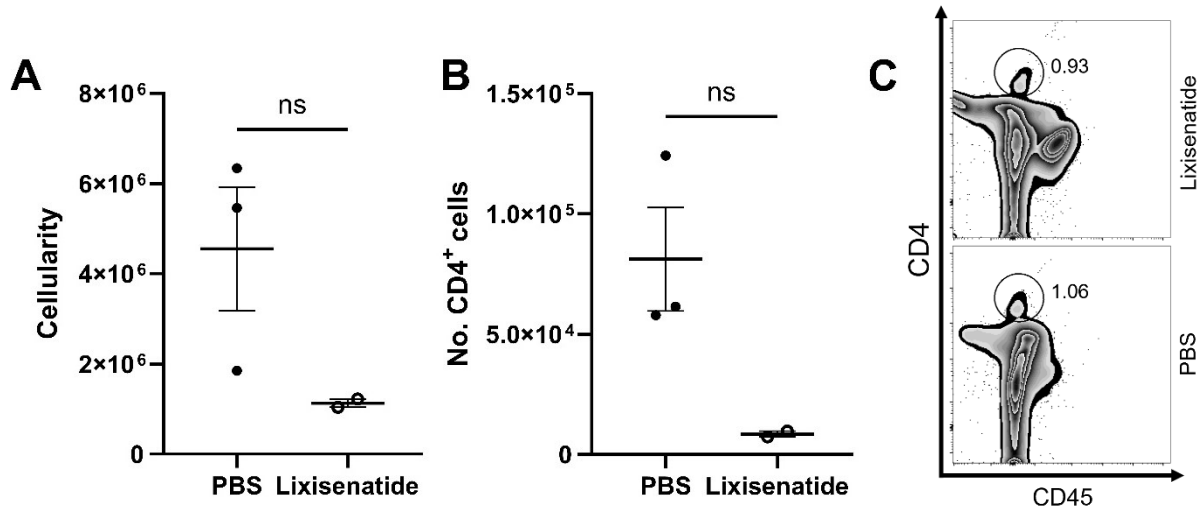


Figure 4.19: Transfer of CD4⁺ T-cells from *T. muris* infected and lixisenatide-treated C57BL/6 mice to RAG mice does not affect cellularity of the mesenteric lymph node following *T. muris* infection. C57BL/6 mice were infected with low dose (approx. 30 eggs) *T. muris* and infection was allowed to establish for 21 days. Mice were treated by intraperitoneal injection with PBS or lixisenatide. Upon completion of treatment, mice were sacrificed, and T cells were isolated from mLN and adoptively transferred into RAG mice. After 1 week, these RAG mice were infected with low dose (approx. 30 eggs) *T. muris*, and infection was allowed to progress for 21 days. Mice were sacrificed 18 days post-infection and mLN obtained. mLN were stimulated with Cell Stimulation Cocktail (with protein transport inhibitors) overnight, before cells were collected and analysed by flow cytometry. A) mLN cellularity was determined using Invitrogen Countess automated cell counter. B) The number of CD4⁺ cells in the mLN at the time of sacrifice. C) Representative flow cytometry plots showing percentage of CD4⁺ cells from (B). Data (experimental n=2-3 per group) are presented as mean ± SEM, where each plotted point represents 1 mouse. Data were analysed using unpaired T tests and considered statistically significant where P<0.05.

The cytokine production of these CD4⁺ T cells was analysed; given the low number of cells present here, the total number of CD4⁺ T cells producing IFN γ , IL-13 and IL-17 was analysed, showing no significant differences between mice with T cells from PBS- and lixisenatide-treated mice (Fig. 4.20).

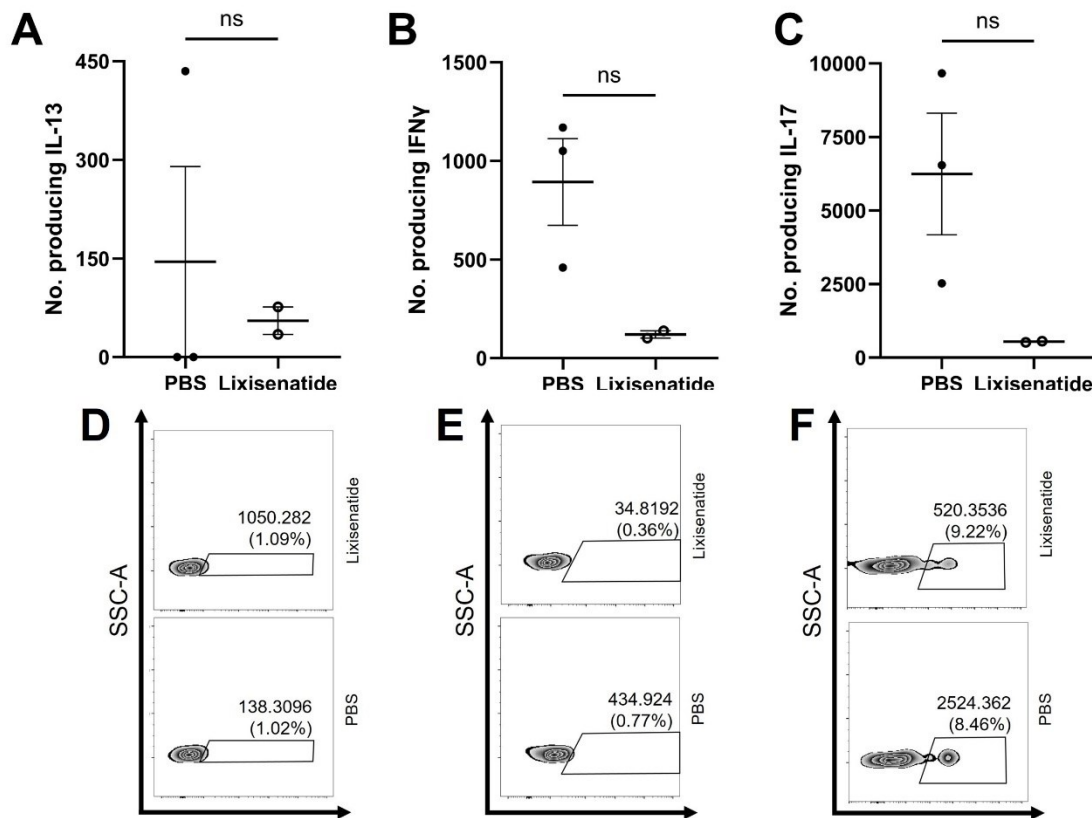


Figure 4.20: Transfer of CD4⁺ T cells from *T. muris* infected and lixisenatide-treated C57BL/6 mice to RAG mice does not alter the number of CD4⁺ cells producing IL-13, IFN γ or IL-17 following *T. muris* infection. C57BL/6 mice were infected with low dose (approx. 30 eggs) *T. muris* and infection was allowed to establish for 21 days. Mice were treated by intraperitoneal injection with PBS or lixisenatide. Upon completion of treatment, mice were sacrificed, and T cells were isolated from mLN and adoptively transferred into RAG mice. After 1 week, these RAG mice were infected with low dose (approx. 30 eggs) *T. muris*, and infection was allowed to progress for 21 days. Mice were sacrificed 18 days post-infection and mLN obtained. mLN were stimulated with Cell Stimulation Cocktail (with protein transport inhibitors) overnight, before cells were collected and analysed by flow cytometry. D), E) and F) show representative flow cytometry plots from A), B) and C), respectively. Plotted data shows the number of CD4⁺ T cells producing A) IL-13, B) IFN γ and C) IL-17. Data (experimental n=2-3 per group) are presented as mean \pm SEM, where each plotted point represents 1 mouse. Data were analysed using Mann-Whitney U tests and considered statistically significant where P<0.05.

To establish the role of effector memory T (TEM) cells in lixisenatide-induced *T. muris* expulsion, the TEM cell populations in the mLN at the time of sacrifice were assessed; despite the mean percentage of TEM cells being higher in mice with T cells from lixisenatide-treated mice than those treated with PBS, this difference was not significant (Fig. 4.21)

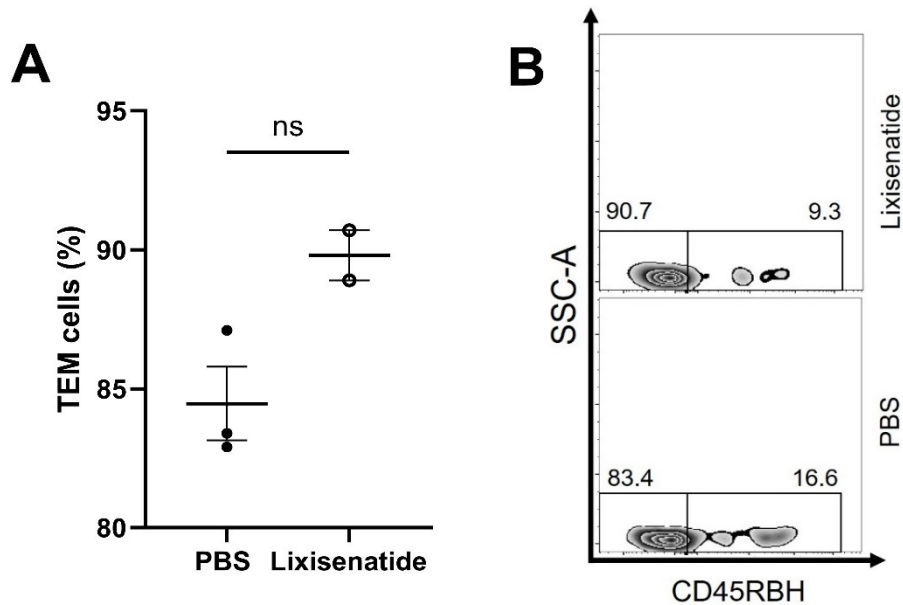


Figure 4.21: Transfer of CD4⁺ T cells from *T. muris* infected and lixisenatide-treated C57BL/6 mice to RAG mice does not alter the number of TEM cells in the mesenteric lymph node following *T. muris* infection. C57BL/6 mice were infected with low dose (approx. 30 eggs) *T. muris* and infection was allowed to establish for 21 days. Mice were treated by intraperitoneal injection with PBS or lixisenatide. Upon completion of treatment, mice were sacrificed, and T cells were isolated from mLN and adoptively transferred into RAG mice. After 1 week, these RAG mice were infected with low dose (approx. 30 eggs) *T. muris*, and infection was allowed to progress for 21 days. Mice were sacrificed 18 days post-infection and mLN obtained. mLN were stimulated with Cell Stimulation Cocktail (with protein transport inhibitors) overnight, before cells were collected and analysed by flow cytometry. Data shows A) the percentage of TEM cells in the mLN and B) representative plots from (A). Data (experimental n=2-3 per group) are presented as mean \pm SEM, where each plotted point represents 1 mouse. Data were analysed using unpaired T tests and considered statistically significant where $P < 0.05$.

To further understand these findings, a modified McMaster technique was used for analysis of *T. muris* egg output of each mouse (Fig.4.22). Faecal pellets were collected from mice 20 days post-infection, prior to sacrifice, to assess faecal egg output. Though there was a small trend in faecal egg output of mice reconstituted with CD4⁺ T cells from lixisenatide-treated mice, this was not significant.

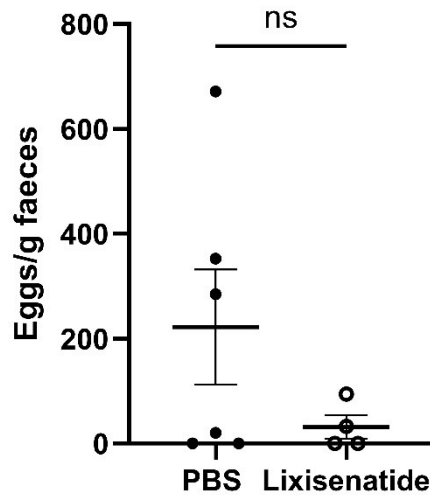


Figure 4.22: Transfer of CD4⁺ T cells from *T. muris* infected and lixisenatide-treated C57BL/6 mice to RAG mice does not alter faecal egg output following *T. muris* infection. C57BL/6 mice were infected with low dose (approx. 30 eggs) *T. muris* and infection was allowed to establish for 21 days. Mice were treated by intraperitoneal injection with PBS or lixisenatide. Upon completion of treatment, mice were sacrificed, and T cells were isolated from mLN and adoptively transferred into RAG mice. After 1 week, these RAG mice were infected with low dose (approx. 30 eggs) *T. muris*, and infection was allowed to progress for 21 days until sacrifice. At day 20 post-infection 2 faecal pellets were collected from each mouse and *T. muris* eggs were counted using a modified McMaster technique. Data (experimental n=4-6) are presented as mean \pm SEM, where each plotted point represents one mouse. Data were analysed using unpaired T tests, and * = P<0.05.

To understand these findings in the context of infection outcome, the worm burden of mice from each group was assessed by examination of the caecum and proximal colon post-sacrifice (Fig.4.23). Worm counts showed a significant decrease in worm burden of mice which received cells from lixisenatide-treated mice compared to PBS-controls (P=0.0368).

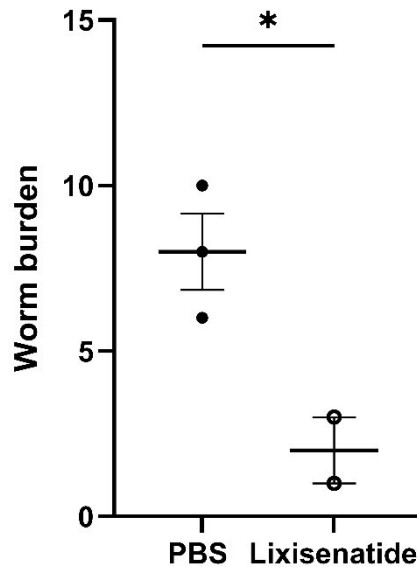


Figure 4.23: Transfer of CD4⁺ T cells from *T. muris* infected and lixisenatide-treated mice to RAG mice induces expulsion of chronic *T. muris* infection in RAG mice reconstituted with T cells from treated mice. C57BL/6 mice were infected with low dose (approximately 30 eggs) *T. muris* and infection was allowed to establish for 21 days. Mice were treated by intraperitoneal injection with lixisenatide. Upon completion of treatment, mice were culled and T cells isolated from serum, adoptively transferred into RAG mice. After 1 week, these mice were infected with low dose (30 eggs) *T. muris*, and infection was allowed to progress for 21 days. Mice were sacrificed and worm burden determined by counting worms present in the caecum and proximal colon. Data (experimental n=2-3 per group) are presented as mean ± SEM, where each point represents 1 mouse. Statistical analyses were completed using a Mann Whitney U test and * = P<0.05

Collectively, these data indicate that lixisenatide treatment induces some protection following *T. muris* reinfection, reducing worm burden upon challenge infection.

4.5 Lixisenatide reduces worm burden in chronic, high-dose *T. muris* infection.

In *T. muris* infection, the number of eggs ingested directly affects the type of immune response to infection; a low-dose infection becomes chronic, facilitated by a T_{H1} response, whereas a high-dose infection induces a T_{H2} response and worm expulsion (Else *et al.* 1994). Bancroft *et al.* 1997 showed that recombinant IL-12 (rIL-12) treatment prior to *T. muris* infection allowed for the establishment of a chronic high-dose infection through driving a T_{H1} response. The efficacy of lixisenatide on a chronic high-dose *T. muris* infection was investigated for the first time.

Serum IgG1 and IgG2a responses were measured in PBS- and lixisenatide-treated mice with a chronic high-dose *T. muris* infection (Fig. 4.24); here there was no significant difference between the treatment groups at any dilution factor, with no IgG1 production and comparable IgG2a production in both groups.

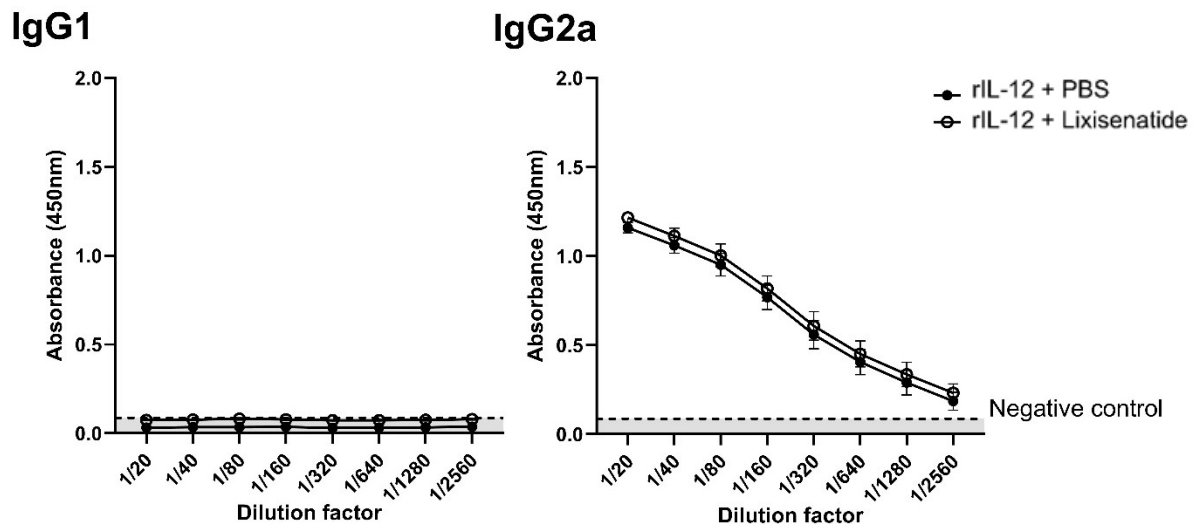


Figure 4.24: Parasite specific IgG1 and IgG2a antibody responses of C57BL/6 mice following chronic high-dose *T. muris* infection and lixisenatide treatment. Mice were treated with 1µg r-IL-12 for 3 days before being infected with high dose (~200 eggs) *T. muris* by oral gavage. Infection was allowed to establish for 34 days before mice were treated with PBS (control) or lixisenatide by intraperitoneal injection for 3 days. 3 days after final treatment, mice were sacrificed, and serum was obtained. Serial dilutions of sera were incubated with biotinylated rat anti-mouse IgG1 and IgG2a antibodies in antigen coated ELISA plates. Bound antibody was detected using streptavidin peroxidase and TMB substrate, and reaction stopped using sulphuric acid. Absorbance was measured using a Tecan Infinite pro plate reader at 450nm with 540nm reference. Negative control data was obtained from plate wells processed without serum. Data are presented as mean ± SEM where experimental n=4 per group. Statistical analyses were performed using unpaired T tests at each dilution factor, and results were statistically significant where P<0.05.

Changes to the structure of the caecal crypt can be seen in both chronic *T. muris* infection and *T. muris* expulsion (Klementowicz *et al.* 2012). Despite no changes in caecal crypt or goblet structure or goblet cell morphology following lixisenatide treatment (Dooley 2022), Histological analysis was used to determine whether changes in goblet cell and caecal crypt structure occur following GLP-1rA treatment of a chronic, high-dose *T. muris* infection. Following sacrifice, caecal tip sections were stained using alcian-blue-PAS staining for goblet cells. Caecal crypt length, goblet cell frequency and goblet cell size of 20 randomly selected caecal crypt units (CCUs) was measured (Fig. 4.25). There were no significant differences in in crypt length, goblet cell frequency and goblet cell size between PBS- and lixisenatide-treated mice.

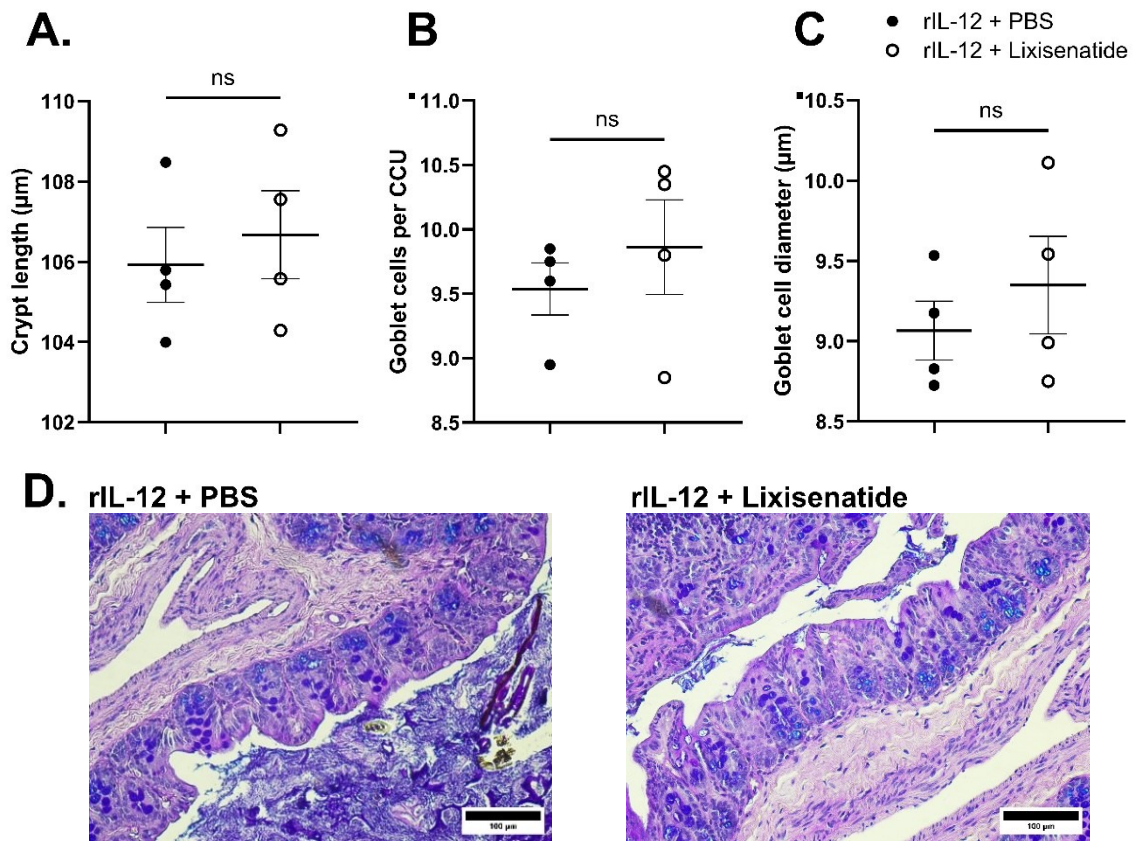


Figure 4.25: GLP-1rA treatment does not affect caecal crypt structure or goblet cells following chronic high-dose *T. muris* infection. Mice were treated with 1 μg r-IL-12 for 3 days before being infected with high dose (~200 eggs) *T. muris* by oral gavage. Infection was allowed to establish for 34 days before mice were treated with PBS (control) or lixisenatide by intraperitoneal injection for 3 days. 3 days after final treatment, mice were sacrificed and caecum samples obtained. Caecal tip samples were stained using alcian blue-PAS. Crypt length and goblet cell number per caecal crypt unit (CCU) and goblet cell diameter were analysed using ImageJ (A-C) Quantification for each mouse was performed by measuring 20 CCUs and determining the mean (A) crypt length, (B) number of goblet cells and C) diameter of goblet cells per CCU. (D) Representative images of alcian blue-PAS-stained caecal tip sections in PBS control and lixisenatide treated mice, where bars represent 100 μm . Data are presented as mean \pm SEM where experimental n=4 per group and each plotted point represents one mouse. Data were analysed using unpaired T tests and considered statistically significant where $P < 0.05$.

Flow cytometry to investigate the immune cell populations present in the mLN following lixisenatide treatment of a chronic, high-dose *T. muris* infection. Analysis of mLN cellularity showed no significant difference between lixisenatide- and PBS-treated mice (Fig.4.26A). Furthermore, the number of CD45⁺ cells in the mLN was not significantly different between treatment groups (Fig. 4.26B).

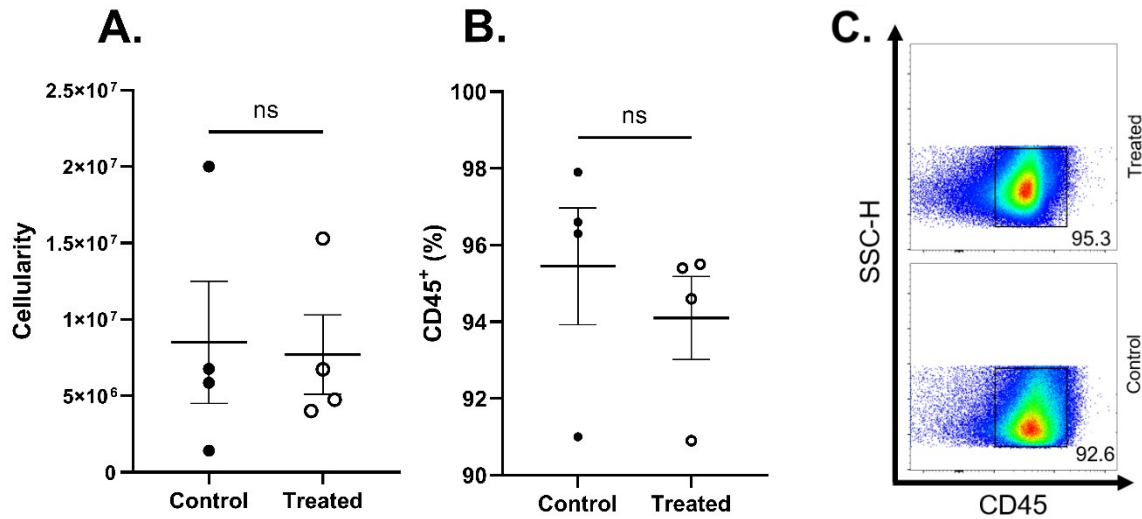


Figure 4.26: Cellularity of the mesenteric lymph node is unaffected by GLP-1rA treatment of a chronic high-dose *T. muris* infection. Mice were treated with $1\mu\text{g}$ r-IL-12 for 3 days before being infected with high dose (~ 200 eggs) *T. muris* by oral gavage. Infection was allowed to establish for 34 days before mice were treated with PBS (control) or lixisenatide by intraperitoneal injection for 3 days. 3 days after final treatment, mice were sacrificed and mLN obtained. mLN were stimulated with Cell Stimulation Cocktail (with protein transport inhibitors) overnight, before cells were collected and analysed by flow cytometry. A) mLN cellularity was determined using Invitrogen Countess automated cell counter. B) Percentage of CD45⁺ cells in the mLN at the time of sacrifice. C) Representative flow cytometry plots from (B). Data are presented as mean \pm SEM where experimental $n=4$ per group. Each plotted point represents 1 mouse. Data were analysed using unpaired T tests and were statistically significant where $P < 0.05$.

The number of T cells and the T cell subsets in the mLN was then analysed; there was no significant difference in the number of CD3⁺ (Fig.4.27A), CD4⁺ (Fig.4.27C) and CD8⁺ (Fig.4.27D) T cells between PBS- and lixisenatide-treated mice.

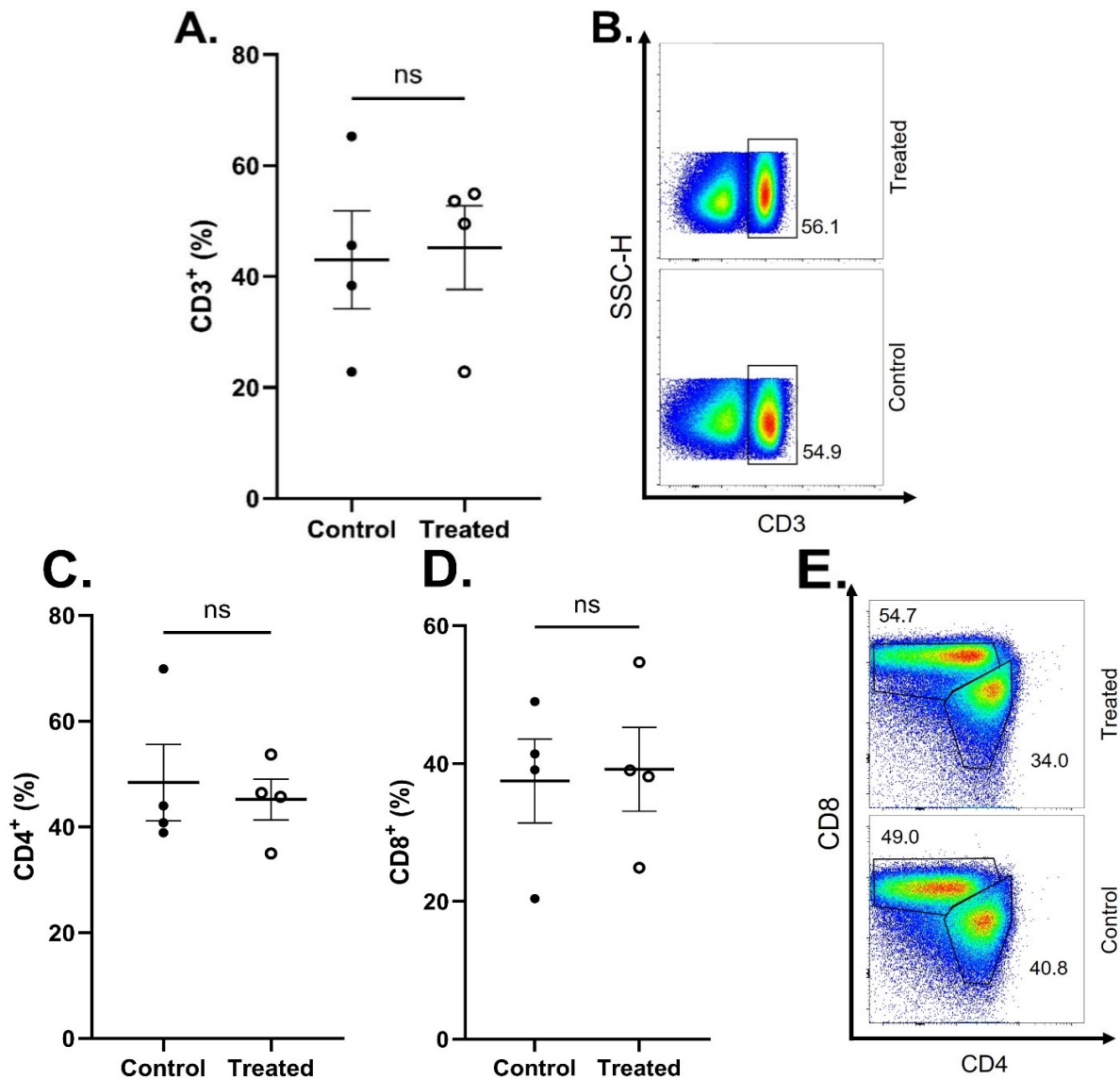


Figure 4.27: The percentage of CD4⁺ and CD8⁺ T cells in the mesenteric lymph node is not altered following lixisenatide-treatment of a chronic high-dose *T. muris* infection. Mice were treated with 1 μ g r-IL-12 for 3 days before being infected with high dose (~200 eggs) *T. muris* by oral gavage. Infection was allowed to establish for 34 days before mice were treated with PBS (control) or lixisenatide by intraperitoneal injection for 3 days. 3 days after final treatment, mice were sacrificed and MLN obtained. MLN were stimulated with Cell Stimulation Cocktail (with protein transport inhibitors) overnight, before cells were collected and analysed by flow cytometry. Plotted data shows the percentage of A) CD3⁺ leukocytes in the MLN with B) representative flow cytometry plots from (A), the percentage of C) CD4⁺ and D) CD8⁺ T cells in the MLN, with E) representative flow cytometry plots from (C) and (D). Data (experimental n=4 per group) are presented as mean \pm SEM where each plotted point represents 1 mouse. Data were analysed using A/C) Mann Whitney U tests D) unpaired T tests and were statistically significant where P<0.05.

Cytokine production by these CD4⁺ and CD8⁺ T cells was assessed (Fig.4.28). Here there was minimal production of IFN γ with less than 5% of CD4⁺ T cells producing IFN γ , and less than 1.5% in CD8⁺ T cells, with no significant difference between lixisenatide-treated mice and PBS controls. IL-17 production by both T cell subsets was minimal (<1%), with no significant difference between treatment groups. Though the number of CD4⁺ and CD8⁺ T cells producing IL-13 was minimal (<1%), There was significantly higher IL-13 production in both CD4⁺ (P=0.0233) and CD8⁺ (0.0336) T cells in lixisenatide-treated mice compared to PBS controls (P<0.05).

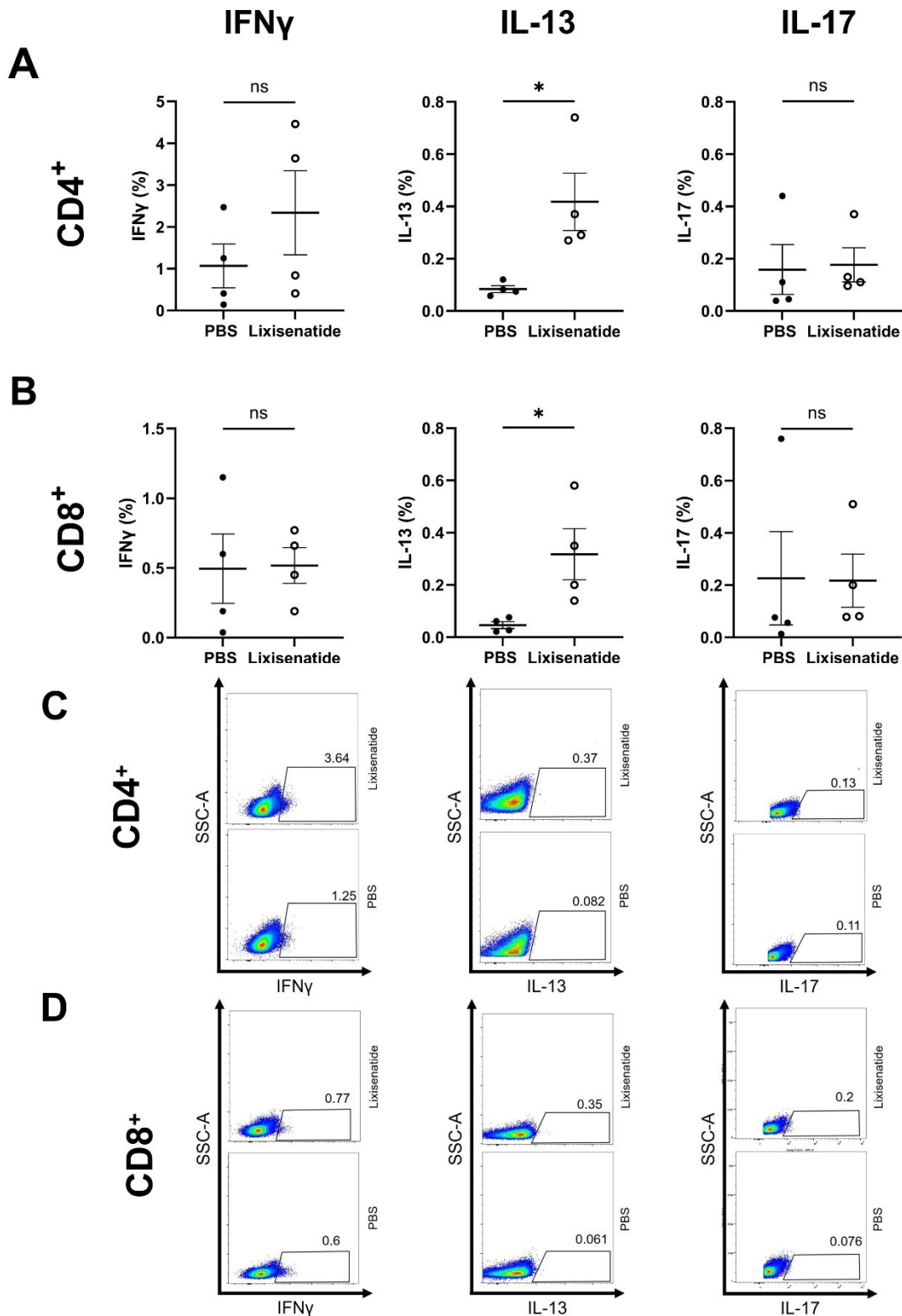


Figure 4.28: The percentage of CD4⁺ and CD8⁺ T cells producing IL-13 increases following GLP-1rA treatment of a chronic, high-dose *T. muris* infection. Mice were treated with 1 μ g r-IL-12 for 3 days before being infected with high dose (~200 eggs) *T. muris* by oral gavage. Infection was allowed to establish for 34 days before mice were treated with PBS (control) or lixisenatide by intraperitoneal injection for 3 days. 3 days after final treatment, mice were sacrificed and MLN obtained. MLN were

stimulated with Cell Stimulation Cocktail (with protein transport inhibitors) overnight, before cells were collected and analysed by flow cytometry. Plotted data shows levels of IFN γ , IL-13 and IL-17 produced by A) CD4⁺ and B) CD8⁺ T cells. Data (experimental n=4 per group) are presented as mean \pm SEM where each plotted point represents 1 mouse. Data were analysed using unpaired T tests and * = p<0.05.

A T_H2-driven increase in epithelial turnover is central to expulsion of *T. muris* from its niche; Dooley (2022) showed that GLP-1rA-driven expulsion of *T. muris* involves an immune-driven increase in epithelial turnover. To investigate the effects of lixisenatide on epithelial turnover in a chronic, high-dose *T. muris* infection, a bromodeoxyuridine (BrdU) pulse-chase experiment over a 12-hour period was used to determine the number of proliferating cells and rate of epithelial turnover. The number of proliferating cells, as measured by positive BrdU staining, was significantly higher in lixisenatide-treated mice than in PBS controls (Fig. 4.29A, P=0.0056). Furthermore, the epithelial turnover over 12 hours was significantly higher in lixisenatide-treated mice as compared to PBS controls (Fig. F.29B, P=0.0004).

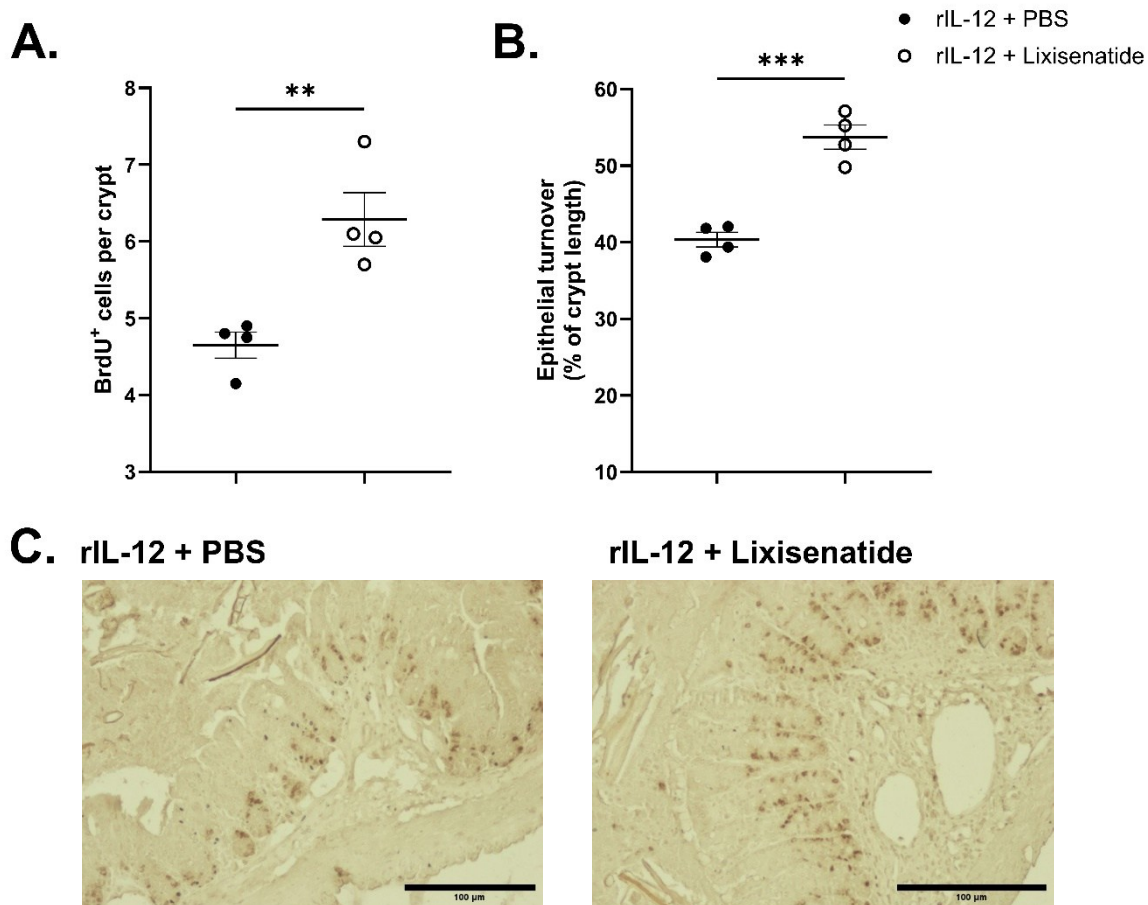


Figure 4.29: GLP-1rA treatment increases epithelial turnover in chronic high-dose *T. muris* infection. Mice were treated with 1μg r-IL-12 for 3 days before being infected with high dose (~200 eggs) *T. muris* by oral gavage. Infection was allowed to establish for 34 days before mice were treated with PBS (control) or lixisenatide by intraperitoneal injection for 3 days. 3 days after final treatment, mice were sacrificed and caecum samples obtained. Caecal tip samples were stained using anti-BrdU and A) the number of proliferating cells and B) migration distance assessed by movement of BrdU⁺ cells up the crypt was determined by light microscopy. C) Representative images of BrdU stained caecal tissue of mice treated with PBS and lixisenatide. (D) Representative images of alcian blue-PAS-stained caecal tip sections in PBS control and lixisenatide treated mice. Data are presented as mean ± SEM where experimental n=4 per group, and each plotted point represents one mouse. Data were analysed using unpaired T tests and ** = P<0.01 *** = p<0.001.

Faecal pellets were collected from mice before and after PBS or lixisenatide treatment and analysed using a modified McMaster technique to assess faecal egg output of each mouse before and after treatment (Fig.4.30). Both lixisenatide- and PBS-treated mice showed comparable faecal egg counts prior to treatment. Following treatment, mice which received PBS showed consistent egg output at each time point. Lixisenatide-treated mice had a lower mean at day 3 and day 5 post-treatment, although this

decrease was not significant as compared to PBS controls. Furthermore, the difference in faecal egg output was not significantly different between treatment groups at any time point.

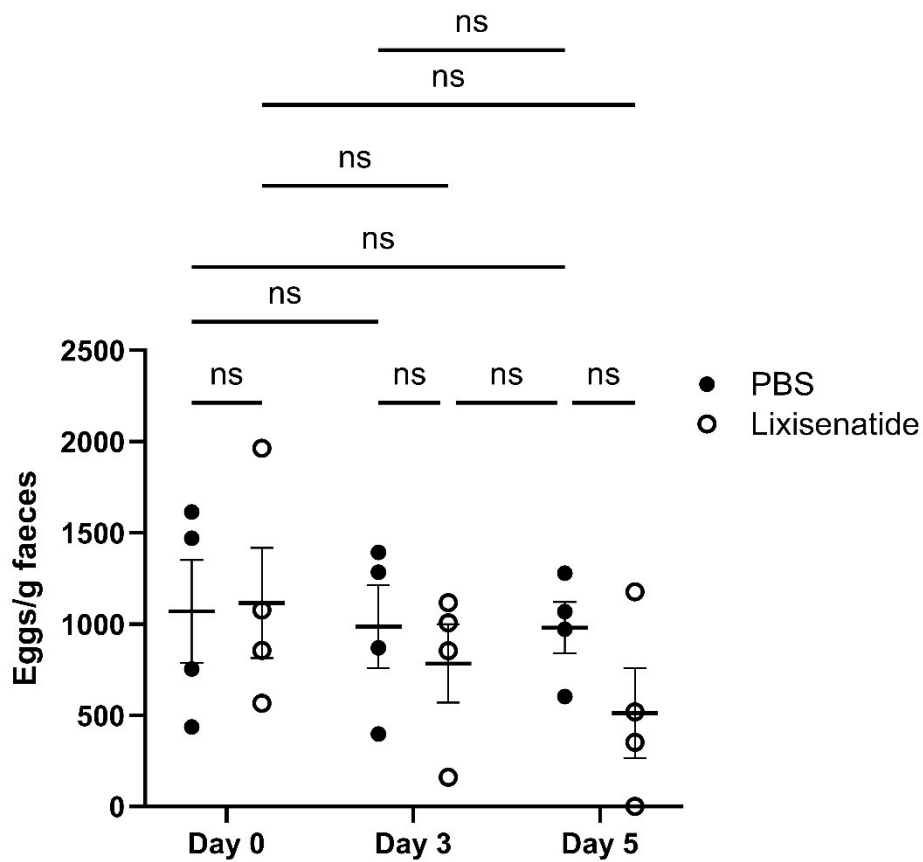


Figure 4.30: Faecal egg output does not appear to be significantly affected by GLP-1rA treatment in high-dose *T. muris* infection. Mice were treated with 1µg r-IL-12 for 3 days before being infected with high dose (~200 eggs) *T. muris* by oral gavage. Infection was allowed to establish for 34 days before mice were treated with PBS (control) or lixisenatide by intraperitoneal injection for 3 days. 3 days after final treatment, mice were sacrificed. 1-2 faecal pellets were collected from each mouse prior to treatment (day 0) and then 3- and 5-days post-treatment and *T. muris* eggs were counted using a modified McMaster technique. Data (experimental n=4 per group) are presented as mean ± SEM where each plotted point represents 1 mouse. Data were analysed using unpaired Two-way ANOVA with Tukey's multiple comparisons test and considered statistically significant where P<0.05.

The worm burdens of mice from each group were determined by examination of the caecum and proximal colon post-sacrifice (Fig.4.31), revealing a significant decrease in the worm burden of mice with a chronic, high-dose *T. muris* infection following lixisenatide treatment (P=0.0402).

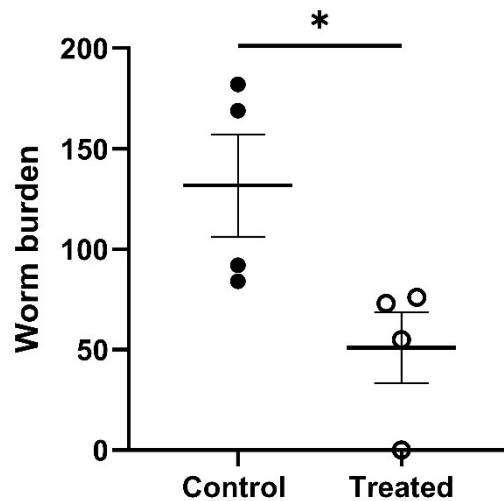


Figure 4.31: Lixisenatide treatment significantly decreases worm burden in mice with chronic high dose *T. muris* infection. Mice were treated with 1µg r-IL-12 for 3 days before being infected with high dose (~200 eggs) *T. muris* by oral gavage. Infection was allowed to establish for 34 days before mice were treated with PBS (control) or lixisenatide by intraperitoneal injection for 3 days. 3 days after final treatment, mice were sacrificed caeca and proximal colons collected. The total number of worms were counted using a dissecting microscope. Data (experimental n=4 per group) are presented as mean ± SEM, where each point represents 1 mouse. Statistical analyses were completed using unpaired T test, where *=P<0.05.

Collectively these data demonstrate that GLP-1rA treatment effectively increase IL-13 cytokine and associated epithelial turnover and excitingly reduces worm burden in a chronic high-dose infection.

5. Discussion

Enteroendocrine cells are transepithelial cells which sense and respond to luminal contents by secreting peptide hormones, such as GLP-1, with functions in appetite regulation, glucose homeostasis and gastrointestinal motility (Gribble & Reimann 2016). More recently, their role in the orchestration of mucosal immunity has gained interest; changes in EEC frequency and function can be seen in intestinal helminth infections, likely due to the close association of helminths with the intestinal epithelium (Worthington *et al.* 2018). This study follows the work of Dooley (2022) which identified GLP-1 receptor agonists as effective in driving expulsion of chronic *T. muris* infection. This study investigates the effect of helminth infection on endogenous GLP-1⁺ EEC development and secretion, and the efficacy and mechanism underpinning GLP-1rA-mediated *T. muris* expulsion.

The intestinal helminth *Trichinella spiralis* significantly increases local secretion of GLP-1 from EECs, which is attenuated by inhibition of bitter taste receptors (TAS2rs). This occurs independently of

changes to GLP-1⁺ EEC abundance, suggesting that these EECs sense helminths, either directly or indirectly, via TAS2rs thereby increasing their secretion of GLP-1 without affecting EEC differentiation. Further experimentation is required to determine the precise mechanisms, such as the precise TAS2r subtype(s) through which EECs sense helminths, and how this increases peptide hormone secretion. Further study would also be useful to establish whether this response is common to a variety of helminths; there was an increase in GLP-1 secretion in organoids cultured with *T. muris* antigen, although this increase was not significant.

Treatment of chronic *T. muris* infection using the GLP-1rA lixisenatide appears to induce some level of protection against challenge infection via CD4⁺ T cells, reducing worm burden upon challenge infection. Furthermore, lixisenatide effectively reduces worm burden in chronic, high-dose *T. muris* infection. Worm expulsion in both cases appears to be driven by an increase in epithelial turnover, independent of changes to crypt and goblet cell structure. Although there were some alterations in cytokines produced, further experimentation is required to fully define the mechanisms by which GLP-1rA treatment drives worm expulsion via increased epithelial turnover.

5.1 Helminth antigen increases GLP-1 secretion without direct influence on GLP-1⁺ EEC frequency.

Previous research has shown alterations in EEC function during helminth infection; *Ascaris suum* and *Trichostrongylus colubriformis* induce increased CCK secretion in livestock (Yang *et al.* 1990; Dynes *et al.* 1998), and GLP-1 and GLP-2 secretion decreases in *Eubothrium crassum* infection in trout (Bosi *et al.* 2005). Peptide hormones are likely to play a key role in intestinal barrier homeostasis; given the role of GLP-1 and GLP-2 as epithelial growth factors (Dube *et al.* 2006; Koehler *et al.* 2015), it is possible that these hormones play a role in helminth-induced epithelial damage repair (Xiao *et al.* 2000). Indeed, the functions of, and mechanisms underpinning helminth-induced changes in EEC function are yet to be elucidated. Here a murine small intestinal organoid platform was used to investigate the effects of helminths on GLP-1⁺ EEC development and function. The initial 'proof of principle' studies demonstrate that this organoid culture technique supports GLP-1⁺ EEC development and reflects the expected small intestinal GLP-1⁺ cell distribution, with GLP-1⁺ cell distribution increasing distally (Baggio *et al.* 2007). Using this platform, GLP-1 secretion was shown to increase significantly in response to *T. spiralis* antigen. Interestingly, culture of small intestinal organoids with *T. spiralis* or *T. muris* antigen had no effect on GLP-1⁺ cell frequency, indicating that this increase in GLP-1 secretion is independent of GLP-1⁺ EEC hyperplasia.

There was a significant increase in GLP-1 secretion from small intestinal organoids cultured with *T. spiralis* antigen compared to controls, and this increase was attenuated in organoids cultured with both *T. spiralis* antigen and the TAS2r inhibitor AITC. There was also a trend in GLP-1 secretion in the presence of *T. muris* antigen, which decreases back to control levels when organoids are cultured with *T. muris* antigen with AITC, although this difference was not significant. Given the small number of

experimental repeats completed using *T. muris* antigen, further experimentation is required to investigate whether GLP-1 secretion does in fact change in response to *T. muris* and, if so, the precise mechanism through which these cells, directly or otherwise, sense intestinal helminths and mediate this change in GLP-1 secretion. For this work, a small intestinal organoid model was used; *T. muris* occupies the caecum and proximal colon during infection (Else *et al.* 2020). Given that GLP-1⁺ EECs are expressed in the proximal large intestine (Grunddal *et al.* 2022), and that the EEC receptor repertoire exhibits spatial specificity along the intestinal tract (Greiner & Bäckhed 2016), it would be of interest to repeat this work using a large intestinal organoid system to elucidate whether *T. muris* exhibits greater effects on GLP-1 secretion from caecal/large intestinal GLP-1 secretion. It would also be of interest to investigate the role of other epithelial cell types in this helminth-driven GLP-1 secretion; it may be that TAS2rs expressed by EECs directly coordinate this response, or perhaps tuft cells orchestrate this increase in GLP-1 secretion through sensing via TAS2rs and downstream signalling to EECs.

It is currently unknown whether helminth-driven increases in GLP-1 secretion are an adaptation by the host or helminth; it is possible that host epithelial cells have adapted to sense helminth antigen to increase GLP-1, however the magnitude of GLP-1 secretion is insufficient in a natural infection to drive worm expulsion. Conversely studies have associated helminth infection with improved metabolic outcomes and lower incidence of T2DM (Tracey *et al.* 2016; Rennie *et al.* 2021). Given incretin role of GLP-1, perhaps helminth-driven modulation of GLP-1 secretion plays a supporting role, with improved host health being mutually beneficial to both helminth and host.

Allyl isothiocyanate (AITC) is a phytochemical abundantly expressed in *Brassicaceae* (Zhao & Miller 2021). Previous studies have demonstrated inhibitory actions of AITC at TAS2rs (Oka *et al.* 2013; Barretto *et al.* 2015; Luo *et al.* 2019), however, there is evidence to suggest that AITC increases GLP-1 secretion through its actions as a TAS2r agonist (Zhao & Miller 2021; Tran *et al.* 2021). The precise interactions between AITC and TAS2rs are yet to be characterised; given the observation that AITC is capable of activating TAS2rs (Zhao & Miller 2021; Tran *et al.* 2021), but can concurrently decrease downstream signalling following activation (Oka *et al.* 2013; Luo *et al.* 2009), it is possible that AITC acts as a high-affinity partial agonist at TAS2rs to outcompete other agonists (Sandilands & Bateman 2016), including parasite-derived molecules. Here, culture of small intestinal organoids with *T. spiralis* antigen with AITC reduces GLP-1 secretion to control levels, potentially identifying these bitter taste receptors as key mediators of helminth-induced GLP-1 secretion. This is consistent with other studies which link TAS2rs with GLP-1 secretion; Yu *et al.* (2015) showed that berberine, the primary active component of the ancient Chinese herb *Coptis chinensis* (Yan *et al.* 2008), induces GLP-1 secretion via activation of TAS2r38. Furthermore, TAS2r inhibition using ATIC abolishes *T. spiralis*-induced tuft cell secretion of IL-25 (Luo *et al.* 2019). Repetition of this work using specific TAS2r inhibitors, such as the TAS2r16, TAS2r38 and TAS2r43 inhibitor probenecid (Greene *et al.* 2011) would allow for the elucidation of the precise receptor subtype(s) involved in parasite-driven GLP-1 secretion. Sweet taste receptors are also known to play a role in GLP-1 secretion from EECs (Jang *et al.* 2007; Steinert *et al.* 2011); further experimentation is required to determine if there is a role for sweet taste receptors in

helminth sensing and helminth-induced peptide hormone secretion. Moreover, further experimentation is required to determine the precise parasite-derived molecules which drive GLP-1 secretion; given that the *T. spiralis* antigen used here is composed of homogenised adult worms, any worm-derived molecule(s) may be acting to drive GLP-1 secretion. Furthermore, it may be that a product of the worms may activate TAS2rs to boost GLP-1 secretion.

Changes in gut microbiota composition can be seen in helminth infections including *T. muris* (Houlden *et al.* 2015; Holm *et al.* 2015) and *T. spiralis* (Kang *et al.* 2021). Furthermore, changes in gut microbiota composition can influence GLP-1 secretion (Zeng *et al.* 2024). In chronic *T. muris* infection there is a marked increase in the abundance of intestinal *Bifidobacterium* and *Lactobacillus* from day 13 and 20 post-infection, respectively (Holm *et al.* 2015); *Lactobacilli* and *Bifidobacterium* are capable of stimulating GLP-1 secretion through the production of short-chain fatty acids which activate G protein-coupled free fatty acid receptors (FFARs) expressed by GLP-1⁺ EECs (Zeng *et al.* 2024; Cheng *et al.* 2024). Given that a small intestinal organoid model was used for this study, observed increases in GLP-1 secretion in response to helminths cannot be attributed to alterations in gut microbiota composition. However, given that the gut microbiota directly influences EEC development and secretion (Chao *et al.* 2025), it would be of interest to investigate whether helminth-induced changes to the composition of the gut microbiota may also influence helminth-driven peptide hormone, including GLP-1, secretion.

5.2 The effect of GLP-1rA treatment on a trickle *T. muris* infection remains inconclusive.

Current treatment of helminth infections relies heavily upon the use of anthelmintic agents, such as mebendazole and albendazole (Hotez *et al.* 2017). In trichuriasis, low cure rates and high rates of reinfection call into question the efficacy of anthelmintics both as reactive treatments and as preventative chemotherapy (PC) in endemic areas (Moser *et al.* 2017). Analyses completed by Hall *et al.* (2009) showed that the annual cost of preventative chemotherapy for children aged 2-14 in 107 developing countries was \$276 million (Hall *et al.* 2009). Meta-analyses estimate that the global prevalence of *T. trichiura* was 7.1%, or around 513 million individuals based on data collected between 2010 and 2023, including a prevalence of 8.14% in children, and ~1.5% (over 100 000 individuals), showing moderate to high intensity infection (Behniafar *et al.* 2024). Data collected prior to 2010 showed a global prevalence of 8.3% (Pullan *et al.* 2014), showing a small decrease in infection rates. However, given the aim of the WHO to 'achieve and maintain elimination of STH morbidity in pre-school and school age children' by 2030 (World Health Organisation 2017), there is low likelihood that adherence to the current WHO PC guidelines will allow for achievement of the STH morbidity goals (Farrell *et al.* 2018). Taken together, these observations emphasize an urgent need for novel treatment options.

Dooley (2020) demonstrated that GLP-1rA treatment of chronic *T. muris* infection effectively induces worm expulsion; Dooley also demonstrated that this treatment does not cause direct toxicity to *T. muris*, with chronic infection persisting in GLP-1r KO mice, and that the adaptive arm of immunity is required for GLP-1rA-induced worm expulsion, with RAG^{-/-} mice unable to expel worms following exendin-4

treatment. Therefore, the potential for this treatment to provide any protection against challenge *T. muris* infection was investigated; high rates of reinfection following treatment limit the efficacy of current treatments against *T. trichiura* (Hotez *et al.* 2017). Alarming rates of AH resistance highlight a critical need for alternative treatments; recent studies in livestock have shown a prevalence of resistance to benzimidazoles of 86% in sheep (Rose Vineer *et al.* 2020). Furthermore, a recent study has estimated that the annual cost of livestock helminth infections to be €1.8 billion in production loss and treatment costs in Europe alone (Charlier *et al.* 2020). Therefore, GLP-1rA-induced immunological memory would be beneficial to individuals living in endemic areas where repeated exposure to *T. trichiura* is commonplace, and to the agriculture industry, in which livestock are afflicted by the deleterious effects of helminth infection, including that of *Trichuris* species, with increasing resistance of *Trichuris* species to current anthelmintic drugs.

To better understand the contributions of GLP-1rA treatment in challenge infection, a trickle infection model was used, characterised by a low-dose infection followed by lixisenatide treatment, and challenge infection. Regrettably, it became apparent that the batch of eggs used for these infections was unable to sustain a long-term infection. Upon assessment of the worm burden of PBS- and lixisenatide-treated mice, all worms from the primary infection had been expelled irrespective of treatment group, with few immature worms from the challenge infection persisting in each group. The presence of immature worms does indicate that GLP-1rA treatment does not cause changes to the microbiota to prevent egg hatching (Hayes *et al.* 2010; Goulding *et al.* 2025). Examination of faecal egg output of mice pre- and post-treatment showed a significant decrease in faecal egg count (FEC) immediately following treatment in both lixisenatide- and PBS- treated mice, indicating that this reduction in FEC and worm burden is treatment-independent. This decrease in FEC is likely to have simply coincided with the death of adult worms, with worms from the secondary infection not yet patent and thus not producing eggs. However, repetition of this study with an alternative *T. muris* egg batch would validate the data obtained here. By day 11 post-treatment, FECs were no longer significantly lower than pre-treatment; it is possible that those worms which persisted reached patency by this time point and began producing eggs. However, the use of FEC as a quantitative measure of worm burden is limited; it is possible that frequency of defecation, or individual female worm egg output differed at each sample collection point.

Antibodies are a strong indicator of the type of immune response occurring to *T. muris*, with IgG1 and IgG2a reflecting a T_H2 and T_H1 response, respectively (Else *et al.* 1993). Parasite-specific antibody ELISA showed a lack of IgG1 and comparable levels of IgG2a in both treatment groups, indicating that both groups were undergoing a T_H1 -dominated response to infection.

Changes in the rate of epithelial turnover are a key determinant in *T. muris* infection outcome, with IL-13-driven increases in turnover causing physical displacement of worms from their niche and thus resistance to chronic infection (Cliffe *et al.* 2005; Oudhoff *et al.* 2016). Given that epithelial turnover returns to naïve levels by day 25 post-infection in both resistant and susceptible mouse strains (Cliffe *et al.* 2005), any increase in turnover following the primary infection in this study will have resolved by

the time of sacrifice. It would be expected to observe an increase in epithelial turnover following lixisenatide treatment; Dooley (2020) showed an increase in epithelial turnover following GLP-1rA treatment, which is consistent with subsequent adoptive transfer and high-dose infection studies. However, there was no significant difference in the number of proliferating cells or epithelial turnover between PBS- and lixisenatide-treated mice following reinfection. Furthermore, there was serum IgG1, indicating a lack of a protective T_H2 response, and no significant differences in crypt structure, goblet cell morphology and abundance, or cytokine production between treatment groups, indicating that worm expulsion in this experiment was due to worm viability rather than GLP-1r-dependent.

Analysis of the cell populations of the mLN showed no significant differences in T cell numbers or $CD4^+$ or $CD8^+$ T cell subsets between PBS- and lixisenatide treated mice. Similarly, there were no significant differences between TEM cell frequency or recently activated $CD4^+$ T cells. IFN γ , IL-13 or IL-17 production by $CD4^+$ and $CD8^+$ T cells, as well as by TEM and recently activated cells, was comparable between treatment groups. There was a significant increase in the proportion of recently activated $CD8^+$ T cells in lixisenatide-treated mice, although no difference in the levels of IFN γ , IL-13 and IL-17 produced by these cells. Dooley (2020) showed that $CD8\alpha^+$ IEL abundance in the large intestine increases in *T. muris* infection, with these cells possessing the transcript for the GLP-1 receptor, although this receptor is not expressed in naïve mice (Yusta *et al.* 2015). Dooley also hypothesised that GLP-1rA treatment may act directly through $CD8\alpha$ TCR $\gamma\delta$ IEL populations to drive worm expulsion. However, it has previously been demonstrated that depletion of $CD8^+$ T cells using anti- $CD8\alpha$ monoclonal antibodies does not alter T_H2 -driven immunity to *T. muris* (Humphreys *et al.* 2004). Further investigation is required to determine if $CD8^+$ T cells do, in fact, play a key role in GLP-1rA-induced *T. muris* expulsion. If the increase in recently activated $CD8^+$ T cells is consistent in repeat experimentation, further analysis of these cells to identify precise cell subtype and expression of a GLP-1rA may indicate a mechanism through which GLP-1rA treatment drives worm expulsion in challenge infection.

5.3 Adoptive transfer of $CD4^+$ T cells from lixisenatide-treated mice provides some protection against challenge *T. muris* infection.

To circumvent the lack of local availability of a viable batch of *T. muris* eggs to repeat this reinfection study, T cell transfer was used to investigate the effects of GLP-1rA treatment on challenge *T. muris* infection. T cells are central to the expulsion of *T. muris*, with a resistant phenotype restored in susceptible athymic nude mice by transfer of splenocytes (Ito *et al.* 1991). $CD4^+$ T cell depletion induces susceptibility in the normally resistant mouse strains, and $CD4^+$ T cell adoptive transfer generates a resistant phenotype in severe combined immunodeficiency (SCID) mice (Else & Grencis 1996). Dooley (2022) showed that despite GLP-1rA treatment effectively clearing *T. muris* in C57BL/6 mice, it was ineffective in RAG $^{-/-}$ mice, indicating that the adaptive arm of immunity is essential in GLP-1rA-mediated worm expulsion. In this study, naïve C57BL/6 mice were infected with a low dose *T. muris* infection, treated using lixisenatide or PBS, and then adoptively transferred $CD4^+$ T cells from these mice into

naïve RAG^{-/-} mice prior to infection. Worm burden was significantly reduced in RAG^{-/-} mice which received T cells from lixisenatide-treated mice compared to PBS controls. Indeed, it is likely, given the short timeframe between treatment of primary infection and isolation of T cells, that this isolate contained considerable numbers of parasite-specific CD4⁺ effector T cells, aiding in reduced worm burden following secondary infection. However, further experimentation using this mode will allow for identification of GLP-1rA-induced parasite-specific memory T cell populations; a long-lived memory response would be beneficial to those living in endemic areas through reduction in worm burden following repeat infection.

Parasite-specific antibody ELISA showed neither IgG1 nor IgG2a in either treatment group, validating that the CD4⁺ T cell isolate was not contaminated by B cells. Flow cytometric analysis of the populations within the mLN showed an increase in the number of effector memory T (TEM) cells, although this was not significant. Given the reduction in worm burden in mice which received T cells from lixisenatide-treated mice, it may have been expected that TEM cells played a role here. It may be possible that repeat experimentation with a greater number of mice would more clearly demonstrate a difference in TEM cell populations, or perhaps this reduction in worm burden occurred independently of TEM cells and was instead the result of the persistence of antigen-specific effector T cells following the primary infection. Though there was a lower mean number of CD4⁺ T cells producing IFN γ and IL-17 in lixisenatide-treated mice, this was not significant. IL-13 production was also not significantly different between treatment groups; the mean number of CD4⁺ T cells producing IL-13 was lower in lixisenatide treated mice, although this was due to a single outlier in the control group. Given the low cellularity of the mLNs across all mice in this study, coupled with the low number of mice used, it would be advisable to repeat this experiment to identify any true alterations in cytokine production here. In general, some increase in IL-13 production would be expected, given that this cytokine is central to *T. muris* immunity (Bancroft *et al.* 1998). Dooley showed that GLP-1rA treatment induces an increased and decreased IL-13 production by CD8 $\alpha\alpha$ IELs and TCR $\gamma\delta$ IELS, respectively. Therefore, repeating this adoptive transfer study using a variety of lymphocyte subsets would allow for further characterisation of the mechanism underpinning GLP-1rA-mediated *T. muris* expulsion and the potential for this treatment to induce immunological memory formation.

Due to low cell counts, analysis of the recently activated (CD69⁺) T cell populations within the mLN were not possible. . The low cellularity here may be due to storage of the mLN following sacrifice, or unfavourable conditions during extraction and culture of mLN cells. Alternatively, given that RAG^{-/-} mice lack mature B and T cells, perhaps a longer period to allow for T cell expansion prior to infection would aid in increasing cell counts and subsequent analysis. Repeating this experiment would allow for validation of these results. In particular, repeat experiments to assess alterations in CD69⁺ populations would provide a useful insight into the role of recently activated T cells, particularly in comparison with that of memory T cell subsets.

In mice reconstituted with CD4⁺ T cells from lixisenatide-treated mice, there was increased epithelial cell proliferation and turnover, which is a well characterised and critical mechanism of worm expulsion in resistant mice (Cliffe *et al.* 2005). Goblet cell hyperplasia is also characteristic of worm expulsion in resistant mice (Noah *et al.* 2009; Shroyer *et al.* 2005; Hasnain *et al.* 2011b). During acute infection, IL-13 also drives upregulation of the GABA- α 3 receptor expression in the caecum, mediating secretion of glycoproteins into the mucus barrier (Hasnain *et al.* 2011b); although there were no changes in caecal crypt structure; further experimentation is required to determine whether hyperplasia-independent alterations to mucous composition, either through changes in mucin production or mucin glycosylation, are induced by GLP-1rA treatment.

Previous studies using lixisenatide in mice have used up to 500ug/kg which, based on an average mouse weight of 30g, would allow for use of up to 17ug lixisenatide (Werner *et al.* 2010). In these studies, lixisenatide at a dose of 10 μ g was used, therefore it would be possible to safely increase the dose to assess if the protective effects of lixisenatide against *T. muris* infection are dose dependent. Furthermore, lixisenatide is a short-acting GLP-1rA with a half-life of only 2-4 hours (Thorkildsen *et al.* 2003; Barnett 2011). More recently, GLP-1rA treatments with modifications to increase their half-life have been developed; semaglutide is a GLP-1 analogue with 94% homology with human GLP-1, but with a half-life of 7 days allowing for weekly administration (Lau *et al.* 2015) for the treatment of T2DM and obesity (Holmes *et al.* 2021; MHRA 2024). Therefore, it is possible that use of a long-acting GLP-1rA such as semaglutide may enhance the protective effects of the treatment against *T. muris* reinfection through prolonged GLP-1r agonism. Moreover, by lowering the number of doses required to treat infection, use of a long-acting GLP-1rA would reduce cost per treatment.

It is well-established that *T. muris* eggs rely upon the presence of specific gut microbiota species for hatching and therefore establishment of infection (Hayes *et al.* 2010). Adoptive transfer was used here, excluding GLP-1rA-induced changes in microbiota composition as the direct cause of decreased worm burden. Similarly, Dooley (2022) showed that treatment of an existing *T. muris* infection using lixisenatide was effective in driving expulsion of an established, chronic infection. GLP-1-dependent changes in gut microbiota composition have been demonstrated in animal models of T2DM and human patients (Zhao *et al.* 2018; Wang *et al.* 2023) and, more recently, studies have revealed that GLP-1r agonism induces changes in the composition of the gut microbiota through interactions at intestinal IEL GLP-1rs (Wong *et al.* 2022). It has been demonstrated that acute semaglutide treatment increases abundance of *E. coli* in the caecum (Kato *et al.* 2021), given that *E. coli* is known to directly facilitate egg hatching (Schärer *et al.* 2023), it is possible that lixisenatide treatment may promote egg hatching through changes in the gut microbiota composition. However, Tsai *et al.* (2021) demonstrated that gut microbiota alterations differ between human patients receiving liraglutide or dulaglutide. The influence of lixisenatide on the composition of the gut microbiota is yet to be characterised; it is possible that lixisenatide treatment alters microbiota composition via GLP-1r expressed by lymphocytes to favour or attenuate *T. muris* egg hatching. In this case, transfer of T cells from lixisenatide treated mice may induce changes in the microbiota of the RAG^{-/-} mice, potentially diminishing egg hatching. Further

experimentation is required to distinguish the effects of GLP-1rA treatment on the host microbiota in the context of challenge helminth infection.

Given the widespread expression of the GLP-1r, it is possible that CD4⁺ T cells are not the sole population mediating GLP-1rA-driven *T. muris* expulsion. To further investigate this, selective depletion of T cell populations could be used to determine their role in GLP-1rA-induced *T. muris* expulsion following challenge infection. It is possible that a combination of immune cell types may induce a more effective and long-lived immune response against challenge infection.

In this experimental model, there was only one week between completion of lixisenatide treatment in the C57BL/6 mice, and administration of infection in the CD4⁺ T cell-reconstituted RAG^{-/-} mice. Therefore, it is likely that a population of CD4⁺ effector T cells from the primary infection persisted and induced expulsion of worms upon 'secondary' infection. Lack of time constraints would have allowed for a longer period between treatment of the primary infection and harvesting and isolation of CD4⁺ T cells prior to adoptive transfer. This would allow for natural clearance of the parasite-specific effector T cell populations and identification of any GLP-1rA-driven parasite-specific memory T cell formation. Alternatively, isolation and adoptive transfer of effector memory T cell populations would reveal whether TEM cells played any role in the reduction in worm burden observed here.

5.4 GLP-1rA treatment reduces worm burden in chronic, high-dose *T. muris* infection.

Parasite dose is a key factor influencing *T. muris* infection outcome; most inbred mouse strains will expel a high-dose (200 eggs) infection, with immunodeficient mice, such as SCID and athymic nude mice facilitating a high-dose infection to chronicity (Antignano *et al.* 2011; Klementowicz *et al.* 2012). Furthermore, although not immunodeficient, AKR mice are susceptible to chronic infection due to the mounting of strong T_h1 responses irrespective of infection dose (Else *et al.* 1992). Recent meta-analysis of the global prevalence and burden of human trichuriasis showed that around 1.5% of those tested worldwide, representing over 100 000 individuals, exhibited a moderate to heavy infection intensity (Behniafar *et al.* 2024). Typically, a high-dose infection in naïve individuals induces a strong T_h2 response and subsequent worm expulsion (Antignano *et al.* 2011; Klementowicz *et al.* 2012). However, priming of BALB/k mice with a low dose infection, followed by anthelmintic treatment, induces a susceptibility to subsequent low- and high-dose infection (Bancroft *et al.* 2001), which provides a useful insight into the establishment of high-intensity infections in humans. Children often bear the heaviest parasite loads (Else *et al.* 2020), with complications including colon perforation (OK *et al.* 2009; Peradotto *et al.* 2021) and *Trichuris* dysentery syndrome, characterised by anaemia, stunted growth and cognitive impairment (Stephenson *et al.* 2000). Here, rIL-12 treatment prior to infection was used as described by Bancroft *et al.* (1997) to establish the efficacy of GLP-1rA in the treatment of a chronic high-dose *T. muris* infection. Lixisenatide treatment reduced *T. muris* worm burden in a chronic, high-dose infection, with one mouse harbouring no adult worms at the time of sacrifice.

AKR mice have previously been utilised to investigate the effects of a T_H1 response and cytokine production on *T. muris* infection; a skew towards T_H1 polarisation in this strain of mouse induces chronic *T. muris* infection irrespective of infective dose (Else *et al.* 1992; Cliffe *et al.* 2005). To circumvent the lack of availability of AKR mice, rIL-12 pretreatment was used to induce a strong T_H1 response to facilitate a high-dose infection to chronicity, as previously described by Bancroft *et al.* (1997). Here, parasite-specific antibody ELISA showed an absence of IgG1 in both treatment groups, with comparable serum levels of IgG2a. This indicates that a strong T_H1 response had been induced in both treatment groups following rIL-12 pretreatment.

Faecal egg counts showed consistent faecal egg output in PBS-treated mice and, although there was a trend in FEC of lixisenatide-treated mice, this was not significant. Despite observation of faecal egg output acting as an excellent diagnostic tool in gastrointestinal helminth infection, its use as a quantitative measure of worm burden is limited. Some studies have shown a reasonable correlation between faecal egg output and *Trichuris* worm burden (Gasso *et al.* 2015), however the frequency of defecation will differ between mice at the time of sample collection and alter parasite egg frequency per faecal pellet. Indeed, the faecal egg output of individual female worms will vary. Furthermore, the ratio of female and male worms present will also affect faecal egg output; in some mice expulsion of worms may deplete male or female populations, thereby reducing the capacity for egg production while worms persist in some mice (Pike 1969, Else *et al.* 2020). Here, FECs were used as a semi-quantitative measure of infection status, to identify whether mice were indeed infected. However, this is still not irreproachable; in the case of persistence of male worms only, faecal egg output would cease but infection would continue.

Here there was no difference in the cellularity of the mLN, nor were there changes in the size of $CD4^+$ or $CD8^+$ T cell populations. There were no significant changes in IFN γ or IL-17 production, however there was significantly higher production of IL-13 from both $CD4^+$ and $CD8^+$ T cells in lixisenatide-treated mice. These data are interesting, as IL-13 production is primarily by $CD4^+$ T cells in *T. muris* infection (Bancroft *et al.* 1998). $CD8^+$ T cells do not typically produce IL-13. However IL-13 production by human type 2 cytotoxic T ($Tc2$) cells, which have been shown to contribute to allergic airway inflammation and disease (Miyahara *et al.* 2004; Gelfand *et al.* 2017) It is possible that GLP-1rA treatment of *T. muris* infection induces expansion of this $CD8^+$ T cell subset, providing an additional source of IL-13 to drive worm expulsion. Repeating this study will validate the increased IL-13 production seen here, in particular that produced by $CD8^+$ T cells, and allow for the identification of the $CD8^+$ T cell subset expressing IL-13.

Interestingly, lixisenatide-treated mice also showed significantly increased numbers of proliferating cells in caecal crypts, as well as increased epithelial turnover. Given the reliance of increased epithelial turnover upon IL-13 in resistant mice (Cliffe *et al.* 2005), it is possible that lixisenatide-driven increases in IL-13 levels may directly increase epithelial cell proliferation and turnover up the epithelial escalator, thus removing worms.

In this experiment mice were sacrificed 3 days after the final lixisenatide treatment; it is possible that a longer period between treatment and sacrifice would allow for further worm expulsion. Furthermore, it would once again be possible to safely increase the lixisenatide dose to assess if the efficacy of GLP-1rA treatment against a chronic high-dose *T. muris* infection is dose dependent. It is possible that use of a long-acting GLP-1rA such as semaglutide may enhance the mechanisms driving worm expulsion; given that the half-life of semaglutide is 7 days (Lau *et al.* 2015), this treatment time may be sufficient for complete expulsion of a chronic high-dose *T. muris* infection.

5.5 GLP-1rA treatment increases intestinal epithelial turnover.

An IL-13-driven increase in intestinal epithelial turnover is a key mechanism in the expulsion of *T. muris* (Cliffe *et al.* 2005; Zaph *et al.* 2014). Previous studies have shown increased epithelial turnover in both susceptible and resistant mice, with a significantly higher rate of turnover in resistant BALB/c mice compared to susceptible AKR mice (Cliffe *et al.* 2005). In susceptible mouse strains, a lower rate of epithelial turnover with increased epithelial cell proliferation and apoptosis drives crypt hyperplasia (Cliffe *et al.* 2007), allowing for adult worms to persist within their niche.

A QuCCi mouse system was first utilised to investigate epithelial cell proliferation and turnover; QuCCi mice are a cell-cycle reporter mouse system in which fluorescence changes during the G1, S, G2/M and G0 stages of the cell cycle (Briggs 2024). Upon examination of intestinal crypts isolated from mice with low dose and high-dose *T. muris* infection using confocal microscopy, there was little staining and elected that this method was not suitable for subsequent experiments (Appendix 1). Therefore, a bromodeoxyuridine (BrdU) pulse-chase experiment was utilised over a 12-hour period to determine the rate of epithelial turnover.

There was a significant increase in the number of proliferating cells and the rate of intestinal epithelial turnover in RAG^{-/-} mice which received T cells from lixisenatide-treated mice following infection compared to PBS controls. There were similar increases following lixisenatide treatment of a chronic high-dose infection. This is consistent with Dooley (2022) who showed an increase in epithelial turnover in C57BL/6 mice with a chronic, low-dose *T. muris* infection following GLP-1rA treatment. There were no significant changes in crypt length in these experiments, so it is possible that an increase in epithelial turnover in the absence of crypt length changes allows for worms to be pushed over the threshold for expulsion.

This consistent increase in epithelial turnover across these experimental platforms, and lack thereof in the original trickle reinfection study indicates that expulsion of worms in this experiment was not treatment dependent.

GLP-1r-agonism is known to alter intestinal crypt growth, however this appears to drive crypt fission rather than crypt cell proliferation (Koehler *et al.* 2015), therefore it is unlikely that lixisenatide treatment accelerates epithelial turnover directly in *T. muris* infection. In resistant mice, critical acceleration in epithelial turnover is IL-13-dependent (Cliffe *et al.* 2005; Oudhoff *et al.* 2016). In mice who received lixisenatide treatment following the establishment of a chronic high-dose infection, there was an increase in IL-13 production from both CD4⁺ and CD8⁺ T cells, indicating that this accelerated epithelial turnover in lixisenatide-treated mice may be IL-13-dependent. However, mice reconstituted with CD4⁺ T cells from *T. muris* infected, lixisenatide-treated mice infected, and subsequently infected with *T. muris* showed an increase in epithelial turnover in the absence of significant changes in IL-13 production. It is possible that, in this adoptive transfer experiment, factors affecting mLN cell viability post-acquisition affected flow cytometric analysis. It is also probable that the low number of experimental repeats affects significance of statistical analyses and identification of outliers. Therefore, repeating this experiment using a larger group of mice would allow for identification of changes in IL-13 production. Indeed, the factors driving this expulsion mechanism may differ between primary infection followed by treatment vs treatment-induced memory responses. It is also possible that GLP-1rA-induced increases in epithelial turnover are not IL-13-dependent; this could be assessed by conducting *T. muris* infection and GLP-1rA treatment in IL-13 KO mice.

5.6 GLP-1rA has no effect on caecal crypt structure.

Across both the adoptive transfer and high-dose infection experiments there was a significant reduction in worm burden in the absence of changes in caecal crypt structure; in resistant mice IL-13-driven worm expulsion is associated with goblet cell hyperplasia and changes to the mucus composition. It may be that GLP-1rA-driven worm expulsion occurs independently of changes to caecal crypt structure, goblet cells and mucous production. Helminth antigen can increase secretory cell secretion of GLP-1 without affecting cell development, therefore it is possible that changes to mucus composition may occur in the absence of goblet cell hyperplasia. In normally resistant mice, a lack of MUC2 delays worm expulsion, and a lack of the normally respiratory-associated mucin, MUC5AC, renders these mice susceptible to chronic infection (Hasnain *et al.* 2010). Conversely, susceptible mice show a lack of MUC5AC coupled with an increase in MUC17 (Hasnain *et al.* 2011b). Interestingly, recent studies have shown that GLP-1rA treatment causes an increase in mucin secretion in humans through direct interaction with GLP-1rs in glandular cells of intestinal Brunner glands (Bang-Berthelsen *et al.* 2016; Grunddal *et al.* 2022). To confirm whether there are any changes in mucin composition associated with GLP-1rA treatment of *T. muris* infection, mucus samples from the caecum and proximal colon could be analysed using qPCR to assess the proportions of critical mucins such as MUC2 and MUC5AC production.

Glycosylation of mucins, in particular the level of mucin sulphation or sialylation, plays a key role in the immune response to helminth infection; upregulation of sulphomucins is associated with protective effects in helminth infections including *Nippostrongylus brasiliensis* and *Strongyloides venezuelensis* (Ishikawa *et al.* 1995; Tsubokawa *et al.* 2009). During infection with *T. muris*, resistant mice show

increased expression of sulphotransferases, driven by the T_H2-associated cytokine IL-13, and hence increased sulphomucin content of intestinal mucus. Conversely, mice susceptible to chronic infection lack sulphomucins and instead show increased expression of sialyltransferases, driven by the T_H1-associated cytokine IFN γ , and hence sialylated mucins, maintaining favourable conditions for chronic infection. Furthermore, worms exposed to sulphated mucins show lower ATP levels and therefore decreased viability than worms exposed to sialylated mucins (Hasnain *et al.* 2017), implicating a direct anti-parasitic role of sulphated mucins during *T. muris* infection. It is possible that GLP-1rA treatment alters glycosylation of mucins, increasing the viscoelastic and protective characteristics of secreted mucus; this could be assessed in future experiments either using high-iron diamine-alcian blue staining as described by Spicer (1969), or by quantification of sulphotransferases using RT-qPCR.

5.7 Limitations

In both the adoptive transfer and high-dose infection studies described here, only female mice were used due to time constraints of this project. Dooley (2022) observed sex-dependent differences in the efficacy of GLP-1rA treatment of low-dose *T. muris* infection, with lower worm burdens exhibited by male mice following identical infection and treatment regimens. The potent androgen dihydrotestosterone (DHT) can skew T cell polarisation towards a type-1 phenotype through IL-18-dependent mechanisms in male IL-4 KO BALB/c mice. Castration of these mice restores a resistant phenotype comparable with their female counterparts with marked reductions in TNF α , IL-6 and IFN γ (Hepworth *et al.* 2010). Furthermore, 17 β oestradiol acts through oestrogen receptor (ER)- α to increase IL-4 and GATA3 expression in CD4⁺ T cells, thus driving a compensatory enhancement of T_H2 responses (Lambert *et al.* 2005; Hamano *et al.* 1998), however this enhancement is not critical to the generation of a T_H2 response in females (Hepworth *et al.* 2010). Furthermore, it has been postulated that sex may alter the efficacy and tolerability of GLP-1rA treatment in patients with T2DM and obesity. Studies have demonstrated sex-dependent differences in HbA1c reduction and accomplishment of glycaemic control following initiation of GLP-1rA treatment (Anichini *et al.* 2013; Quan *et al.* 2016). Female patients also appear to show greater weight loss following commencement of GLP-1rA therapy (Buyschaert *et al.* 2010; Anichini *et al.* 2013). GI adverse effects of these drugs also appear to manifest more frequently in female patients (Petri *et al.* 2018). Taken together, these data demonstrate some level of sexual dimorphism in GLP-1rA treatment, highlighting further the necessity to repeat these experiments using both male and female mice.

In all *in vivo* studies, analyses of immune cell populations and cytokine production were based on the contents of the mLN. Indeed, analysis of the mLN has been critical to increasing our understanding the immune response to *T. muris* infection (Else *et al.* 1991; Dixon *et al.* 2010; Glover *et al.* 2019). Here, analysis of mLN populations alone did not allow for analysis of the tissue-resident immune cell populations local to the parasite niche (Li *et al.* 2025); in all *in vivo* experiments here, caecum and proximal colon samples were utilised for worm counts and histology which were essential to determining infection outcome and changes in epithelial physiology. Given the small number of mice used in each

experiment, there was insufficient tissue for flow cytometric analysis while allowing for an adequate number of experimental repeats to ensure statistical significance. Intestinal IELs are known to express the GLP-1r (Yusta *et al.* 2015) and play a key role in *T. muris* expulsion in resistant mouse strains (Little *et al.* 2005). Therefore, it would be beneficial to characterise IEL populations and activity following lixisenatide treatment of *T. muris* infection. Furthermore, intestinal tissue-resident memory T cells (T_{RM}) are known to play critical roles in GI infection and inflammatory bowel disease (Lyu *et al.* 2022), therefore it would be valuable to analyse this immune cell population in the context of GLP-1rA-mediated immunological memory against *T. muris*. These tissue-resident populations have limited migration ability and therefore were unlikely to be present in the mLN at the time of sacrifice (Edelblum *et al.* 2012; Thompson *et al.* 2019) Using gut digest to isolate immune cells residing in the intestinal epithelium and lamina propria (Lamers *et al.* 2023; Shanmugavadivu *et al.* 2024) and flow cytometry would allow for the characterisation of the immune cells residing in close proximity to the parasite niche. It would be beneficial to repeat these experiments using larger groups of mice, allowing for collection of gut tissues for both worm counts and histology, and analysis of local immune cell populations. Furthermore, repetition of the adoptive transfer study using tissue-resident immune populations, such as intestinal IELs, would allow for the characterisation of the role of IELs in immunological memory against *T. muris* infection.

Flow cytometric analyses were conducted using an established antibody panel, on which fluorescent minus one (FMO) controls had previously been conducted to assist in identification of background fluorescence and setting of appropriate gate boundaries. Furthermore, a previously validated compensation matrix was used here to correct for spectral overlap of fluorophores. However, in future experimentation it would be beneficial to additionally complete antibody isotype controls in order to assess specificity of antibody staining.

5.8 Importance of the work

Soil transmitted helminths are one of the most prevalent infections worldwide, with over 1.5 billion individuals estimated to currently harbour an STH (Palmeirim *et al.*, 2018). These infections are considered to be neglected tropical diseases; given their transmission by the faecal-oral route, they are most common in areas deprived of high-quality sanitation. STH infections are diseases of morbidity rather than mortality, causing greatest morbidity to those harbouring high worm burdens. Children are most prone to severe morbidity, with a high level of intestinal infestation leading to malnutrition, stunted growth and cognitive impairment (Hotez *et al.* 2014; Bethony *et al.*, 2006; Ngwese *et al.*, 2020).

Despite availability of anthelmintic drugs, their efficacy in *T. trichiura* is limited by low cure rates and high rates of reinfection (Speich *et al.* 2014). Furthermore, increasing prevalence of drug-resistant *Trichuris* strains highlights an urgent need for novel therapeutic options (Kenyon *et al.* 2013). Dooley (2020) discovered that GLP-1rA treatment effectively clears low-dose trichuriasis infection in mice. This study builds upon the work of Dooley, investigating the potential for GLP-1rA treatment to induce

immunological protection against challenge infection. The efficacy of GLP-1rAs in chronic high-dose infection was also assessed. Given that this class of drug is well characterised, and it is licensed for use in type 2 diabetes mellitus and, more recently, obesity (Moore *et al.* 2023), their use in helminth infection would involve a rapid, straightforward repurposing of this drug. Protective effects against challenge infection would provide relief to those living in endemic areas, where rapid reinfection makes current treatments obsolete. However, the metabolic impact of GLP-1rA treatment must be considered when repurposing this drug class for the treatment of STH infection; given the role of GLP-1 in satiety and thus weight management, it would be necessary to investigate the effects of acute GLP-1rA treatment on host metabolism and weight management. Given that many with heavy intestinal helminth burden suffer with malnutrition as a result of infection (Mascarini-Serra 2011), reduced appetite would contribute to malnourishment. Indeed, GLP-1rA treatment of obesity is intended as a long-term treatment (NICE 2025c), therefore deleterious effects on host appetite and weight would likely be mitigated by the acute nature of treatment for helminth infection. However, further study is required to establish whether GLP-1rA treatment for acute STH infection, or repeated doses as part of a preventative chemotherapy regimen, would significantly alter host satiety and weight.

For preventative chemotherapy, one dose of albendazole or mebendazole is administered annually, or twice annually (World Health Organisation 2017). For treatment of active STH infection, the NHS recommends treatment twice-daily treatment using mebendazole for 3 days (NHS 2019). Mebendazole costs the NHS £1.34 for a single course of treatment (twice daily for 6 days) of STH (NICE 2025a), costing just £0.22 per dose. On the other hand, liraglutide is prescribed at doses between 0.6mg and 3mg daily for the management of T2DM. Given that GLP-1rA treatments have an indicative cost to the NHS of £127.50 for five 3ml pens containing 6mg/ml lixisenatide (NICE 2025b), the cost per dose here is £0.85-£4.25. Therefore, the cost per dose of liraglutide is between 4 and 19 times higher than that of mebendazole, dependent upon dose.

Determination of the efficacy of this treatment against well-established adult worms would be a critical step to determining the efficacy of GLP-1rA treatment in natural infection; trickle infection, which mirrors how infection would occur naturally, results in the development of partial resistance (Glover *et al.* 2019). In these individuals, T_H2-driven IL-13 drives epithelial turnover which is most effective at removing smaller larval stages in the lower-mid crypt, where epithelial cells move the fastest (Cliffe *et al.* 2005), however adult worms, which are extensively embedded high within the crypts, persist even following anthelmintic treatment (Glover *et al.* 2019). To investigate the efficacy of GLP-1rAs against these adult worms, infection of C57BL/6 mice with a low dose (30 eggs) infection allowed to progress for 48 days before treating with lixisenatide would allow for determination of the efficacy of GLP-1rAs against adult *T. muris*. If effective against these well-embedded adult worms, GLP-1rA treatment of trichuriasis would allow for removal of persistent, anthelmintic-resistant adult worms in individuals in endemic areas.

5.8 Conclusions

Through the study of small intestinal organoids, *T. spiralis* antigen was shown to increase GLP-1 secretion from intestinal EECs, independently of GLP-1⁺ EEC hyperplasia. There was a similar increase in GLP-1 secretion in organoids cultured with *T. muris* antigen; a higher number of experimental repeats may uncover a significant change in GLP-1 secretion driven by *T. muris* antigen. This antigen-dependent increase in GLP-1 secretion was attenuated by broad-spectrum inhibition of TAS2rs, indicating a role of bitter taste receptors in sensing of intestinal helminths and, given the known roles of EECs and GLP-1 in mucosal immunity (Worthington *et al.* 2018), EEC sensing of intestinal helminths via taste receptors, either directly or via another chemosensory epithelial cell type such as tuft cells, may play a role in barrier homeostasis or indeed the immune response to helminth infection.

Lixisenatide treatment has been shown to exhibit protective effects against challenge *T. muris* infection, with a reduction in worm burden in female RAG^{-/-} mice reconstituted with CD4⁺ T cells from C57BL/6 mice with low dose infection and treated with lixisenatide. Indeed, given that T cell isolation occurred only 24 days after the primary infection, it is likely that considerable numbers of antigen-specific effector T cells are present in the RAG^{-/-} mice, aiding in worm expulsion. A longer-term experiment allowing for clearance of these effector cells and establishment of long-lived parasite-specific TEM cells. Indeed, there was an increase in TEM cells in mice which received T cells from lixisenatide-treated mice, compared to PBS controls, though this was not significant here. Repeated experimentation would allow for validation of these results, GLP-1rA treatment may have a direct effect on GLP-1r⁺ CD4⁺ T cells to alter a currently unknown immune factor to induce immunological memory, thereby increasing the rate of intestinal epithelial turnover upon challenge infection to expel worms.

Lixisenatide treatment was found to significantly reduce worm burden in a chronic high-dose infection in female C57BL/6 mice. It appears as though increased production of IL-13 by currently unidentified CD4⁺ and CD8⁺ T cell subsets drives an increase in epithelial turnover to expel worms. Taken together with the findings of Dooley (2022), Therefore, GLP-1rA treatment may induce production of IL-13, or another unknown immune factor, by GLP-1r⁺ IELs and/or CD4⁺ T cells, driving epithelial proliferation and turnover thereby expelling the worms from the epithelium, with the potential for immunological T cell memory formation mediated by CD4⁺ T cells and possibly intestinal IELs also (Fig. 5.1).

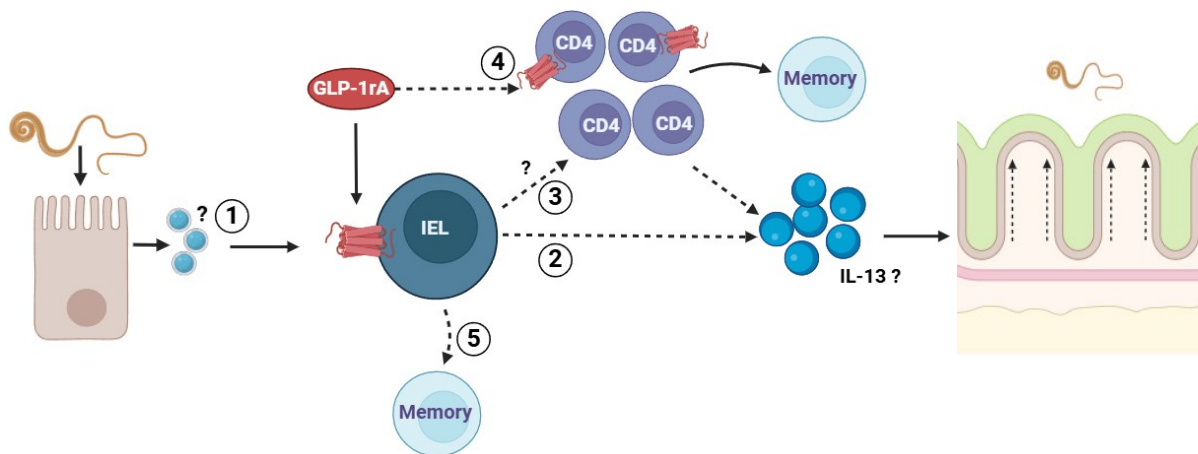


Figure 5.1: Mechanism of GLP-1-driven *T. muris* expulsion. 1) Invasion of the intestinal epithelium by *T. muris* or detection of parasite molecules causes increased GLP-1 release by a pathway that is yet to be identified. IELs then produce IL-13, but this may not be enough to trigger a full response in low dose infection resulting in T_H1 dominance and chronicity. GLP-1rA targets GLP-1^r IELs enough to 2) produce IL-13 or another yet unknown factor, which directly accelerates intestinal crypt epithelial cell proliferation and epithelial turnover, expelling *T. muris* from its intestinal niche. Alternatively, 3) the GLP-1rA-activated IELs may signal to CD4⁺ T cells via a signal transduction pathway which is yet to be identified, driving production of IL-13 and thus epithelial turnover and worm expulsion. 4) Activation by IELs may also drive CD4⁺ T cell surface expression of the GLP-1r, allowing for continued activation by GLP-1rA. Activated CD4⁺ T cells may become long-lived effector memory T cells providing protection against subsequent infection. 5) Activated IELs may also acquire a memory phenotype and aid in protection against challenge infection.

The findings of this project build upon the work of Dooley (2020) who established that GLP-1-1rA treatments are effective in clearing a low-dose *T. muris* infection. The safety and efficacy of this drug class in humans is well-characterised, given their extensive use in the treatment of type 2 diabetes mellitus and weight loss. This would allow for us to rapidly repurpose this drug class for use in helminth infection, decreasing the time before an alternative to anthelmintic drugs becomes available to those afflicted by these neglected tropical infections in endemic countries, thereby increasing quality of life of those currently debilitated by STH infections.

6. Appendix: Exploring the potential use of QuCCi reporter mice to investigate intestinal epithelial turnover in *T. muris* infection

Quiescence and Cell Cycle Indicator (QuCCi) reporter mice utilise the probes p27K-, hCdt1(Cy-) and hGem (1/110) fused to mCerulean, mCherry and mVenus, respectively, in order to discriminate between cells in the G1, S, G2/M and G0 phases of the cell cycle (Briggs 2024). These reporter mice were developed to circumvent the lack of distinction between the S- and G2/M phases, and the G1 and G0 phases in R26Fucci2aR reporter mice (Mort *et al.* 2014). Use of a QuCCi reporter mouse platform was explored for the assessment of lixisenatide induced changes in epithelial turnover in chronic high-dose and trickle *T. muris* infection. Preliminary work using mice with a low dose infection, low dose infection with lixisenatide treatment, and high dose infection (Fig. 6.1), revealed that this platform would not be a suitable platform upon which to quantify epithelial turnover.

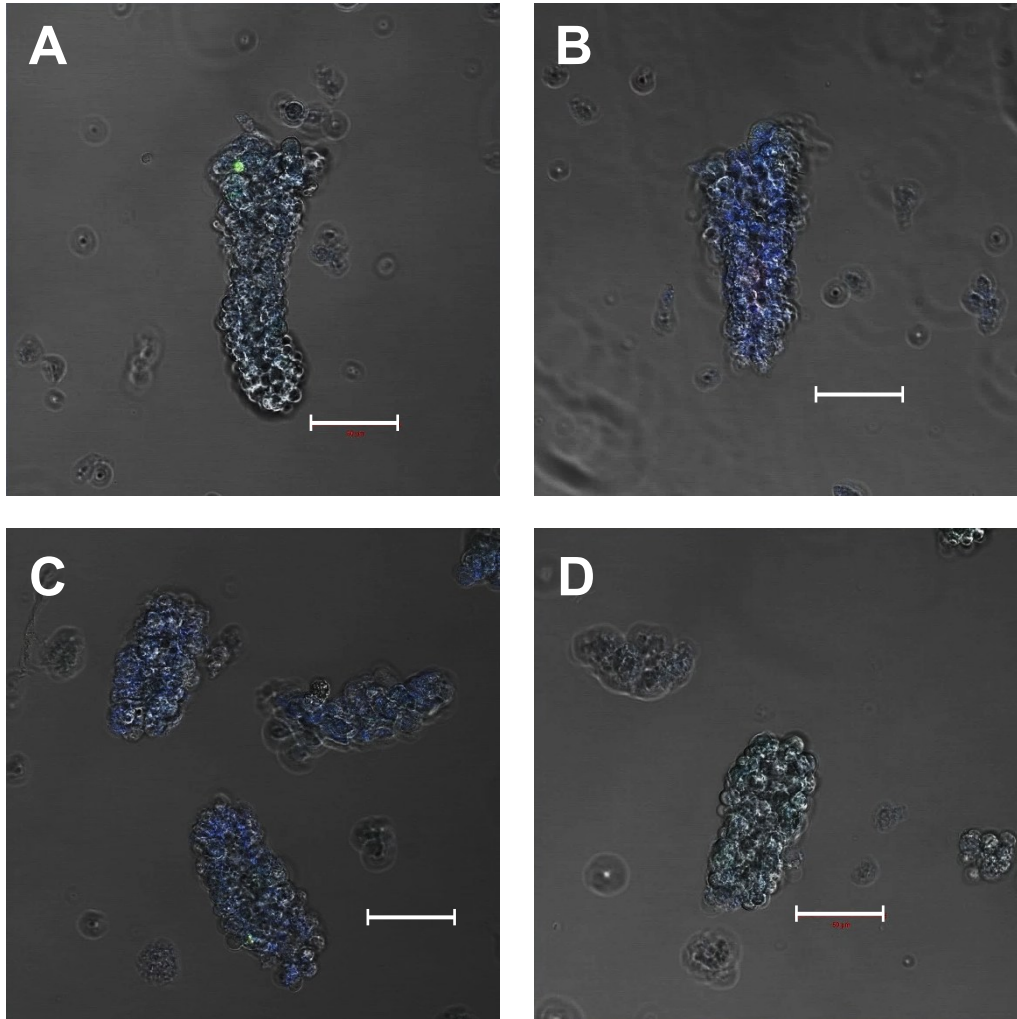


Figure 6.1: Imaging of crypts isolated from QuCCi mice by confocal microscopy is not suitable for assessment for rate of intestinal epithelial turnover. QuCCi mice were administered with PBS, low dose or high dose *T. muris* infection. Mice were sacrificed 34 days post-infection and small intestine was collected. Small intestinal crypts were isolated and assessed by confocal microscopy. Figure shows images of crypts from mice who received A) PBS, B) Low dose infection, C) Low dose infection with lixisenatide treatment, D) High dose infection, where bars represent 50 μ m.

7. References

- Abu-Hamdah R., Rabiee A., Meneilly GS. et al. (2009) Clinical Review: the extrapancreatic effects of glucagon-like peptide-1 and related peptides, *Journal of Clinical Endocrinology and Metabolism*; 94: 1843-52.
- Adegnika AA., Agnandji ST., Chai SK. et al. (2007) Increased prevalence of intestinal helminth infection during pregnancy in a Sub-Saharan African community. *Wiener Klinische Wochenschrift*; 119(23-24): 712-716.
- Alharbi SH. (2024) Anti-inflammatory role of glucagon-like peptide 1 receptor agonists and its clinical implications. *Therapeutic Advances in Endocrinology and Metabolism*. 2024; 15.
- Allen JE. & Maizels RM. (2011) Diversity and dialogue in immunity to helminths. *Nature Reviews Immunology*; 11:375–88.
- Angkasekwina P., Sodthawon W., Jeerawattanawat S., et al. (2017). ILC2s activated by IL-25 promote antigen-specific Th2 and Th9 functions that contribute to the control of *Trichinella spiralis* infection, *PLoS One*; 12: e0184684.
- Anichini R., Cosimi S., Di Carlo A. et al. (2013) Gender difference in response predictors after 1-year exenatide therapy twice daily in type 2 diabetic patients: A real world experience. *Diabetes Metabolic. Syndrome and Obesity*; 6:123–129.
- Anthony RM., Rutitzky LI., UrbanJF. et al. (2007). Protective immune mechanisms in helminth infection. *Nature reviews. Immunology*; 7(12): 975–987.
- Antignano F., Mullaly SC., Burrows K. & Zaph, C. (2011) *Trichuris muris* infection: a model of type 2 immunity and inflammation in the gut, *Journal of visualized experiments*; 51: 2774.
- Baggio LL. & Drucker DJ., (2007) Biology of Incretins: GLP-1 and GIP, *Gastroenterology*; 132: 2131-2157.
- Bancroft AJ., Else KJ., Grecnis RK (1994) Low-level infection with *Trichuris muris* significantly affects the polarization of the CD4 response, *European Journal of Immunology*; 24:3113–3118.
- Bancroft AJ., Else KJ. Sypek JP. et al. (1997). Interleukin-12 promotes a chronic intestinal nematode infection. *European journal of immunology*, 27(4), 866-870.
- Bancroft AJ., McKenzie ANJ., Grecnis RK., et al. (1998) A critical Role for IL-13 in Resistance to Intestinal Nematode Infection, *Journal of Immunology*; 160(7):3453-3461.
- Bancroft AJ., Else KJ., Humphreys NE. et al. (2001). The effect of challenge and trickle *Trichuris muris* infections on the polarization of the immune response, *International Journal for Parasitology* 31(14): 1627–1637.
- Bancroft AJ. & Grecnis RK. (2021) Immunoregulatory molecules secreted by *Trichuris muris*. *Parasitology*; 148(14): 1-7.
- Bang-Berthelsen CH., Holm T.L., Pyke C., et al. (2016) GLP-1 Induces Barrier Protective Expression in Brunner's Glands and Regulates Colonic Inflammation, *Inflammatory Bowel Disease*; 22:2078–2097.
- Barnett AH. (2011) Lixisenatide: evidence for its potential use in the treatment of type 2 diabetes. *Core evidence*, 6, 67–79.
- Barretto RP., Gillis-Smith S., Chandrashekar J. et al. (2015) The neural representation of taste quality at the periphery *Nature*, 517(7534), 373–376.
- Behniafar H., Sepidarkish M., Tadi MJ. et al. (2024) The global prevalence of *Trichuris trichiura* infection in humans (2010-2023): A systematic review and meta-analysis, *Journal of Infection and Public Health*; 17(5): 800-809.
- Bell LV. & Else KJ., (2011). Regulation of colonic epithelial cell turnover byIDO contributes to the innate susceptibility of SCID mice to *Trichuris muris* infection. *Parasite immunology*; 33(4): 244–249.
- Bell RG & Liu WM., (1988). *Trichinella spiralis*: Quantitative relationships between intestinal worm burden, worm rejection, and the measurement of intestinal immunity in inbred mice, *Experimental Parasitology*; 66(1): 44-56.
- Belza A., Ritz C., Sørensen MQ., Holst JJ. et al. (2013) Contribution of gastroenteropancreatic appetite hormones to protein-induced satiety, *American Journal of Clinical Nutrition*; 97: 980-989.
- Bethony J., Brooker S., Albonico M. et al. (2006) Soil-transmitted helminth infections: ascariasis, trichuriasis, and hookworm. *Lancet*: 367(9521): 1521-1532.
- Betts CJ. & Else KJ, (1999) Mast cells, eosinophils and antibody-mediated cellular cytotoxicity are not critical in resistance to *Trichuris muris*, *Parasite Immunology*;21: 45–52.
- Beumer J., Gehart H., & Clevers H. (2020). Enteroendocrine Dynamics - New Tools Reveal Hormonal Plasticity in the Gut, *Endocrine reviews*; 41(5): bnaa018.

- Blackwell NM. & Else KJ. (2002). A comparison of local and peripheral parasite-specific antibody production in different strains of mice infected with *Trichuris muris*. *Parasite Immunology*; 24: 203–211.
- Bogunovic M., Dave SH., Tilstra JS. *et al.* (2007) Enteroendocrine cells express functional Toll-like receptors. *American Journal of Physiology- Gastrointestinal and Liver Physiology*; 292: G1770–G1783.
- Bosi G., Shinn AP., Giari L. *et al.* Changes in the neuromodulators of the diffuse endocrine system of the alimentary canal of farmed rainbow trout, *Onchorhynchus mykiss* (Walbaum), naturally infected with *Eubothrium crassum* (Cestoda), *Journal of Fish Diseases*; 28: 703-711.
- Briggs T., (2024) Development of cell cycle biosensors with improved optical discrimination for use within cell and animal models, PhD, Lancaster University.
- Brown HW. (1927) Studies on the Rate of Development and Viability of the Eggs of *Ascaris lumbricoides* and *Trichuris trichiura* under Field Conditions, *The Journal of Parasitology*; 4(1): 1-15.
- Bundy DA. & Cooper ES. (1989) *Trichuris* and trichuriasis in humans. *Advances in parasitology*; 28: 107-73.
- Bundy DAP., Appleby LJ., Bradley M. *et al.* (2017) *Children and Adolescent Health and Development. Chapter 13: Mass Deworming Programs in Middle Childhood and Adolescence.* [Washington (DC): The International Bank for Reconstruction and Development / The World Bank.
- Buysschaert M., Preumont V., Oriot P. *et al.* (2010) One-year metabolic outcomes in patients with type 2 diabetes treated with exenatide in routine practice, *Diabetes and Metabolism*; 36:381–388.
- Campbell JE. & Drucker DJ., (2013) Pharmacology, physiology and mechanisms of Incretin Hormone Action, *Cell Metabolism*; 17(6): 819-837.
- Campbell L., Hepworth MR., Whittingham-Dowd, J. *et al.* (2019) ILC2s mediate systemic innate protection by priming mucus production at distal mucosal sites, *The Journal of experimental medicine*; 216(12): 2714–2723.
- Capo V. & Despommier DD., (1996) Clinical aspects of Infection with *Trichinella* spp., *Clinical Microbiology Reviews*; 9(1): 47-54.
- Centers for Disease Control and Prevention (2023) *Trichuriasis - Biology.* Global Health, Division of Parasitic Diseases and Malaria. Available at: <https://www.cdc.gov/parasites/whipworm/index.html>
- Centers for Disease Control and Prevention (2024) *Trichinellosis.* Available at: <https://www.cdc.gov/dpdx/trichinellosis/index.html>
- Chai, J. Y., Jung, B. K., & Hong, S. J. (2021). Albendazole and Mebendazole as Anti-Parasitic and Anti-Cancer Agents: an Update. *The Korean journal of parasitology*; 59(3): 189–225
- Chao J, Coleman RA, Keating DJ. *et al.* (2025) Gut Microbiome Regulation of Gut Hormone Secretion, *Endocrinology*; 166(4): bqaf004.
- Charlier J., Rinaldi L., Musella V. *et al.* (2020) Initial assessment of the economic burden of major parasitic helminth infections to the ruminant livestock industry in Europe, *Preventative Veterinary Medicine*; 182: 105103.
- Chaudhuri A., Ghanim H., Vora M., *et al.* (2012) Exenatide exerts a potent anti-inflammatory effect, *Journal of Clinical Endocrinology and Metabolism*; 97: 198–207.
- Cheang JY. & Moyle PM. (2018) Glucagon-Like Peptide-1 (GLP-1)-Based Therapeutics: Current Status and Future Opportunities beyond Type 2 Diabetes, *ChemMedChem*; 13(7): 662–671.
- Chen Z., Luo J., Li J. *et al.* (2021). Interleukin-33 promotes serotonin release from enterochromaffin cells for intestinal homeostasis, *Immunity*; 54: 151–163.e6.
- Cheng Z., Chen J., Zhang Y. *et al.* (2024) *In Vitro* Hypoglycemic Activities of *Lactobacilli* and *Bifidobacterium* Strains from Healthy Children's Sources and Their Effect on Stimulating GLP-1 Secretion in STC-1 Cells, *Foods*;13: 519.
- Cheroutre H., Lambolez F. & Mucida D. (2011) The light and dark sides of intestinal intraepithelial lymphocytes *Nature Reviews Immunology*; 11(7): 445-456.
- Cliffe LJ & Grecis RK (2004) The *Trichuris muris* system: a paradigm of resistance and susceptibility to intestinal nematode infection, *Advanced Parasitology*; 57: 255-307.
- Cliffe LJ., Humphreys NE., Lane TE. *et al.* (2005) Accelerated intestinal epithelial cell turnover: A new mechanism of parasite expulsion. *Science*; 308(5727): 1463-1465.
- Cliffe LJ., Potten CS., Booth CE., & Grecis RK (2007) An increase in epithelial cell apoptosis is associated with chronic intestinal nematode infection, *Infection and immunity*; 75(4): 1556–1564.
- Codina AV., Garcia A., Leonardi D. *et al.* (2015) Efficacy of albendazole:β-cyclodextrin citrate in the

- parenteral stage of *Trichinella spiralis* infection, *International Journal of Biological Macromolecules*; 77: 203-206.
- Coffman RL., Seymour BW., Hudak S. *et al.* (1989) Antibody to interleukin-5 inhibits helminth-induced eosinophilia in mice, *Science (New York, N.Y.)*; 245(4915): 308–310.
- Cooper PJ. Mucosal immunology of geohelminth infections in humans. *Mucosal Immunol.* 2009;2: 288–299.
- Cortes A., Muñoz-Antoli C., Martín-Grau C. *et al.* (2015) Differential alterations in the small intestine epithelial cell turnover during acute and chronic infection with *Echinostoma Caproni* (Trematoda), *Parasites & vectors*; 8: 334.
- Cruz K., Marcilla A., Kelly P. *et al.* (2021). *Trichuris trichiura* egg extract proteome reveals potential diagnostic targets and immunomodulators. *PLoS neglected tropical diseases*; 15(3): e0009221.
- D'Andrea A., Rengaraju M., Valiante NM., *et al.* (1992) Production of natural killer cell stimulatory factor (interleukin 12) by peripheral blood mononuclear cells, *The Journal of Experimental Medicine*; 176(5): 1387-1389.
- Darlan DM., Rozi MF., & Yulfi H. (2021) Overview of Immunological Responses and Immunomodulation Properties of *Trichuris* sp.: Prospects for Better Understanding Human Trichuriasis. *Life(Basel)*; 11(3): 188.
- de Graaf C., Donnelly D., Wootten D. *et al.* (2016) Glucagon-Like Peptide-1 and Its Class B G Protein-Coupled Receptors: A Long March to Therapeutic Successes, *Pharmacological reviews*; 68(4): 954–1013.
- Deacon CF., & Holst JJ., (2009) Immunoassays for the incretin hormones GIP and GLP-1, *Best Practice and Research Clinical Endocrinology and Metabolism*; 23: 425-432.
- DelGiorno KE., Naeem RF., Fang L. *et al.* (2020) Tuft Cell Formation Reflects Epithelial Plasticity in Pancreatic Injury: Implications for Modeling Human Pancreatitis, *Frontiers in Physiology*; 11:88.
- Despommier DD., Gwadz RW. & Hotez PJ. (1995) '*Trichinella spiralis* (Railliet 1896)' In: *Parasitic Diseases*, New York NY: Springer, pp. 32-40.
- Dixit VD., Schaffer EM., Pyle RS. *et al.* Ghrelin inhibits leptin- and activation-induced proinflammatory cytokine expression by human monocytes and T cells, *Journal of Clinical Investigation*; 114: 57-66.
- Dixon H., Little MC., & Else KJ. (2010) Characterisation of the protective immune response following subcutaneous vaccination of susceptible mice against *Trichuris muris*, *International Journal of Parasitology*;40(6): 683-693.
- Dooley M. (2022) Repurposing diabetes drugs for the treatment of intestinal helminth infection, Master's by Research, Lancaster University.
- Drucker DJ. (2018) Mechanisms of Action and Therapeutic Application of Glucagon-like Peptide-1, *Cell metabolism*; 27(4): 740–756.
- Drurey C., Lindholm HT., Coakley G. *et al.* (2022) Intestinal epithelial tuft cell induction is negated by a murine helminth and its secreted products, *Journal of Experimental Medicine*; 219: e20211140.
- Dube PE., Forse CL., Bahrami J. & Brubaker PL. (2006) The essential role of insulin-like growth factor-1 in the intestinal tropic effects of glucagon-like peptide-2 in mice, *gastroenterology*; 131: 589-605.
- Duchesne M., Okoye I. & Lacy P. (2022). Epithelial cell alarmin cytokines: Frontline mediators of the asthma inflammatory response. *Frontiers in immunology*; 13: 975914.
- Dynes RA., Poppi DP., Barrell GD. *et al.* (1998) Elevation of feed intake in parasite-infected lambs by central administration of a cholecystokinin receptor antagonist, *British Journal of Nutrition*; 79: 47-54.
- Edelblum KL., Shen L., Weber CR., *et al.* (2012) Dynamic migration of $\gamma\delta$ intraepithelial lymphocytes requires occludin. *PNAS USA*;109(18):7097-7102.
- Egerod, KL (2012) A major lineage of enteroendocrine cells coexpress CCK, secretin, GIP, GLP-1, PYY, and neurotensin but not somatostatin *Endocrinology*; 153:5782-5795.
- Elkinson S. & Keating GM. (2013), Lixisenatide: first global approval, *Drugs*; 73(4): 383–391.
- El-Salhy M., & Hatlebakk JG. (2016) Changes in enteroendocrine and immune cells following colitis induction by TNBS in rats, *Molecular medicine reports*; 14(6): 4967–4974.
- El-Sayad MH., El-Wakil ES., Moharam ZH. *et al.* (2023) Repurposing drugs to treat trichinellosis: in vitro analysis of the anthelmintic activity of nifedipine and *Chrysanthemum coronarium* extract, *BMC Complementary Medicine and Therapies*; 23: 242.
- Else KJ & Grecis RK (1991) Cellular immune responses to the nematode parasite *Trichuris muris* I.

- Differential cytokine production during acute or chronic infection, *Immunology*; 72: 508-513.
- Else KJ, Hültner L, & Grecnis RK. (1991) Cellular immune responses to the nematode parasite II. Differential induction of Th cell subsets in resistant versus susceptible mice *Immunology*; 75: 232-237.
- Else KJ., Hultner L. & Grecnis RK. (1992) Modulation of cytokine production and response phenotypes in murine trichuriasis, *Parasite Immunology*; 14: 441-449.
- Else KJ., Entwistle GM. & Grecnis RK. (1993) Correlations between worm burden and markers of Th1 and Th2 cell subset induction in an inbred strain of mouse infected with *Trichuris muris*, *Parasite Immunology*; 15(10): 595-600.
- Else KJ, Finkelman FD, Maliszewski CR & Grecnis RK. (1994) Cytokine-mediated regulation of chronic intestinal helminth infection. *Journal of Experimental Medicine*; 179: 347-351.
- Else KJ. & Grecnis RK. (1996) Antibody-independent effector mechanisms in resistance to the intestinal nematode parasite *Trichuris muris*, *Infection and Immunity*; 64(8): 2950-4.
- Else KJ., Keiser J., Holland CV. *et al.* (2020) Whipworm and Roundworm Infections, *Nature Reviews Disease Primers*; 6(1): 44.
- Farrell SH., Coffeng LE., Truscott JE., *et al.* (2018). Investigating the Effectiveness of Current and Modified World Health Organization Guidelines for the Control of Soil-Transmitted Helminth Infections. *Clinical infectious diseases : an official publication of the Infectious Diseases Society of America*, 66(suppl_4), S253-S259.
- Faulkner H., Humphreys N., Renaud JC. *et al.* (1997), Interleukin-9 is involved in host protective immunity to intestinal nematode infection. *European Journal of Immunology*; 27: 2536-2540.
- FDA. (2021). *FDA Approves New Drug Treatment for Chronic Weight Management, First Since 2014.* Available at: <https://www.fda.gov/news-events/press-announcements/fda-approves-new-drug-treatment-chronic-weight-management-first-2014>.
- Ferrick DA., Schrenzel MD., Mulvania T. *et al.* (1995) Differential production of interferon-gamma and interleukin-4 in response to Th1- and Th2- stimulating pathogens by gamma delta T cells *in vivo*, *Nature*; 373 (6511): 255-7.
- Fissiha W., Kinde MZ., (2021) Anthelmintic Resistance and Its Mechanism: A Review, *Infection and Drug Resistance*; 12: 5403-5410.
- Ford CL., Wang Y., Morgan K. *et al.* (2019) Interferon-gamma depresses human intestinal smooth muscle contractility: Relevance to inflammatory gut motility disturbances, *Life Sciences*; 222: 69-77.
- Forgue-Lafitte ME., Fabiani B., Levy PP. *et al.* (2007) Abnormal expression of M1/MUC5AC mucin in distal colon of patients with diverticulitis, ulcerative colitis and cancer, *International Journal of Cancer*; 121: 1543-1549.
- Fox NJ., Smith LA., Houdijk JGM. *et al.* (2018) Ubiquitous Parasites Drive a 33% Increase in Methane Yield from Livestock, *International Journal for Parasitology*; 48: 1017-1021.
- Fröscher W., Gullotta F., Saathoff M. *et al.* (1988) Chronic trichinosis, Clinical, bioptic, serological and electromyographic observations, *European Neurology*; 28:221-226.
- Garside P., Grecnis RK. & Mowat AM. (1992), T lymphocyte dependent enteropathy in murine *Trichinella spiralis* infection, *Parasite immunology*; 14(2): 217-225.
- Gasso D., Feliu C., Ferrer C. *et al.* (2015) Uses and limitations of faecal egg count for assessing worm burden in wild board, *Veterinary Parasitology*; 209(1-2):133-137.
- Genton L. & Kudsk KA (2003) Interactions between the enteric nervous system and the immune system: role of neuropeptides and nutrition, *American Journal of Surgery*; 186: 253-258.
- Gerbe F., van Es JH., Makrini L. *et al.* (2011) Distinct ATOH1 and Neurog3 requirements define tuft cells as a new secretory cell type in the intestinal epithelium. *The Journal of cell biology*; 192(5), 767-780.
- Gerbe F., Sidot E., Smyth DJ. *et al.* (2016) Intestinal epithelial tuft cells initiate type 2 mucosal immunity to helminth parasites, *Nature*; 529: 226-230.
- Giacomin PR., Siracusa MC., Walsh KP. *et al.* (2012) Thymic stromal lymphopoietin-dependent basophils promote Th2 cytokine responses following intestinal helminth infection. *Journal of immunology*; 189(9): 4371-4378.
- Gilbert MP. & Pratley RE. (2020) GLP-1 Analogs and DPP-4 Inhibitors in Type 2 Diabetes Therapy: Review of Head-to-Head Clinical Trials, *Frontiers in endocrinology*; 11: 178.
- Glover M., Colombo SAP., Thornton DJ., & Grecnis RK (2019). Trickle infection and immunity to *Trichuris muris*. *PLoS pathogens*, 15(11), e1007926.
- Gottstein B., Pozio, E. & Nöckler K., (2009) Epidemiology, diagnosis, treatment, and control of trichinellosis, *Clinical Microbiology Reviews*; 22: 127-145.
- Goulding D., Tolley C., Mkandawire TT. *et al.* (2025) Hatching of whipworm eggs induced by bacterial

- contact is serine-protease dependent, *PLOS Pathogens*; 21(1): e1012502.
- Greene TA., Alarcon S., Thomas A., *et al.* (2011) Probenecid inhibits the human bitter taste receptor TAS2R16 and suppresses bitter perception of salicin, *PLoS One*; 6(5):e20123.
- Greiner TU. & Bäckhed F. (2016) Microbial regulation of GLP-1 and L-cell biology, *Molecular Metabolism*; 5: 753-758.
- Grencis RK. (2001). Cytokine regulation of resistance and susceptibility to intestinal nematode infection - from host to parasite. *Veterinary parasitology*; 100(1-2): 45–50.
- Gribble FM., Williams L., Simpson A.K., & Reimann F. (2003) A Novel Glucose-Sensing Mechanism Contributing to Glucagon-Like Peptide-1 Secretion from the GLUTag Cell Line, *Diabetes*; 52: 1147–1154.
- Gribble FM. & Reimann F (2016) Enteroendocrine cells: chemosensors in the intestinal epithelium. *Annual Reviews Physiology*; 78: 277–299.
- Grunddal KV., Jensen ep., Ørskov C. *et al.* (2022) Expression Profile of the GLP-1 Receptor in the Gastrointestinal Tract and Pancreas in Adult Female Mice, *Endocrinology*; 163(1): bqab216.
- Gu Y., Wei J., Yang J. (2013) Protective Immunity against *Trichinella spiralis* Infection Induced by a Multi-Epitope Vaccine in a Murine Model, *PLoS ONE*; 8(10): e77238.
- Habib AM (2012) Overlap of endocrine hormone expression in the mouse intestine revealed by transcriptional profiling and flow cytometry *Endocrinology*; 153:3054-3065.
- Hall A., Horton S. & de Silva N. (2009) The Costs and Cost-Effectiveness of Mass Treatment for Intestinal Nematode Worm Infections Using Different Treatment Thresholds, *PLOS Neglected Tropical Diseases*; 3(3): e402.
- Hamano N., Terada N., Maesako K. *et al.* (1998) Effect of female hormones on the production of IL-4 and IL-13 from peripheral blood mononuclear cells, *Acta Otolaryngologica*; 537: 27-31.
- Hao Y., Zhao X., Yang J. *et al.* (2014) Monoclonal antibody targeting complement C9 binding domain of *Trichinella spiralis* paramyosin impairs the viability of *Trichinella* infective larvae in the presence of complement. *Parasite Vectors*; 7: 313.
- Harris NL. (2017) Recent advances in type-2-cell-mediated immunity: Insights from helminth infection. *Immunity*; 47:1024–1036.
- Hasnain SZ., Want H., Gia JE., *et al.* (2010) Mucin gene deficiency in mice impairs host resistance to an enteric parasitic infection, *Gastroenterology*; 138: 1763-1771.
- Hasnain SZ., Evans CM., Roy M. *et al.* (2011a) Muc5ac: a critical component mediating the rejection of enteric nematodes, *Journal of Experimental Medicine*; 208(5): 893-900.
- Hasnain SZ., Thornton DJ., & Grencis RK. (2011b) Changes in the mucosal barrier during acute and chronic *Trichuris muris* infection, *Parasite Immunol*; 33(1): 45-55.
- Hasnain SZ., Dawson PA., Lourie R. *et al.* (2017) Immune-driven alterations in mucin sulphation is an important mediator of *Trichuris muris* helminth expulsion, *PLoS pathogens*; 13(2): e1006218.
- Hay SI., Abajobir AA., Abate KH., *et al.* (2017) Global, regional, and national disability-adjusted life-years (DALYs) for 333 diseases and injuries and healthy life expectancy (HALE) for 195 countries and territories, 1990-2016: a systematic analysis for the Global Burden of Disease Study 2016. *Lancet*, 390(10100), 1260-134.
- Hayes KS., Bancroft AJ. & Grencis, RK. (2007) The role of TNF-alpha in *Trichuris muris* infection I: influence of TNF-alpha receptor usage, gender and IL-13, *Parasite Immunology*; 29(11): 575-82.
- Hayes K, Bancroft A, Goldrick M. *et al.* (2010) Exploitation of the intestinal microflora by the parasitic nematode *Trichuris muris*. *Science*; 328(5894): 1391–1394.
- He S., Kahles F., Rattik S. *et al.* (2019) Gut intraepithelial T cells calibrate metabolism and accelerate cardiovascular disease, *Nature*; 566 (7742): 115-119.
- Helmbj H., Takeda K., Akira S. *et al.* (2001). Interleukin (IL)-18 promotes the development of chronic gastrointestinal helminth infection by downregulating IL-13. *The Journal of experimental Medicine*, 194(3), 355–364.
- Hepworth MR., Hardman MJ. & Grencis RK., (2010) The role of sex hormones in the development of Th2 immunity in a gender-biased model of *Trichuris muris* infection, *European Journal of Immunology*; 40:406-416.
- Hirasawa A., Tsymaya K., Awaji T. *et al.* (2005) Free fatty acids regulate gut incretin glucagon-like peptide-1 secretion through GPR120, *Nature Medicine*; 11: 90-94.
- Ho LH., Ohno T., Oboki K. *et al.* (2007) IL-33 induces IL-13 production by mouse mast cells independently of IgE-FcepsilonRI signals. *Journal of Leukocyte Biology*; 82: 1481-1490.
- Hogan AE., Gaoatswe G., Lynch L., *et al.* (2014) Glucagon-like peptide 1 analogue therapy directly modulates innate immune-mediated inflammation in individuals with type 2 diabetes mellitus, *Diabetologia*; 57: 781–784.

- Holm JB., Sorobetea D., Kiehlrich P. *et al.* (2015). Chronic *Trichuris muris* Infection Decreases Diversity of the Intestinal Microbiota and Concomitantly Increases the Abundance of *Lactobacilli*. *PloS one*, 10(5), e0125495.
- Holmes P., Bell HE., Bozkurt K. *et al.* (2021) Real-World Use of Once-Weekly Semaglutide in Type 2 Diabetes: Results from the SURE UK Multicentre, Prospective, Observational Study. *Diabetes therapy: research, treatment and education of diabetes and related disorders*; 12(11): 2891–2905.
- Hotez PJ., Bethony J., Bottazzi ME. *et al.* (2005) Hookworm: “The great infection of mankind”, *PLoS Medicine*; 2: e67.
- Hotez PJ., Alvarado M., Basanez MG., *et al.* (2014) The Global Burden of Disease Study 2010: Interpretation and Implications for the Neglected Tropical Diseases. *Plos Neglected Tropical Diseases*, 8(7).
- Hotez PJ. (2017) Global deworming: moving past albendazole and mebendazole. *Lancet Infectious Diseases*; 17(11): 1101-1102.
- Houlden A., Hayes K.S., Bancroft A.J. *et al.* (2015) Chronic *Trichuris muris* infection in C57BL/6 mice causes significant changes in host microbiota and metabolome: Effects reversed by pathogen clearance, *PLoS ONE*;10: e0125945.
- Howitt MR., Lavoie S., Michaud M. *et al.* (2016) Tuft cells, taste-chemosensory cells, orchestrate parasite type 2 immunity in the gut, *Science*; 351: 1329-1333.
- Hurst R.J. & Else K.J. (2013) *Trichuris muris* research revisited: a journey through time, *Parasitology*; 140(11): 1325-39.
- Iftekhhar A., & Sigal M. (2021) Defence and adaptation mechanisms of the intestinal epithelium upon infection, *Microbiology*; 311(3): 151486.
- Ilic N., Gruden-Movsesijan A., Cvetkovic J. *et al.* (2018). *Trichinella spiralis* Excretory-Secretory Products Induce Tolerogenic Properties in Human Dendritic Cells via Toll-Like Receptors 2 and 4, *Frontiers in immunology*; 9: 11.
- Inagaki-Ohara K., Chinen T., Matsuzaki G. *et al.* (2004) Mucosal T cells bearing TCR γ delta play a protective role in intestinal inflammation, *J Immunol*; 173(2): 1390-8.
- Inagaki-Ohara K., Sakamoto Y., Dohi T. & Smith AL. (2011) $\gamma\delta$ T cells play a protective role during infection with *Nippostrongylus brasiliensis* by promoting goblet cell function in the small intestine, *Immunology*; 134(4): 448-58.
- Iqbal J., Wu HX., Hu N. *et al.* (2022). Effect of glucagon-like peptide-1 receptor agonists on body weight in adults with obesity without diabetes mellitus—a systematic review and meta-analysis of randomized control trials. *Obesity reviews: an official journal of the International Association for the Study of Obesity*; 23(6): e13435.
- Ishikawa M., Shi BB., Khan AI. *et al.* (1995) Reserpine-induced sulphomucin production by goblet cells in the jejunum of rats and its significance in the establishment of intestinal helminths, *Parasite Immunology*; 17: 581-586.
- Ito, Y. (1991) The absence of resistance in congenitally athymic nude mice toward infection with the intestinal nematode, *Trichuris muris*: resistance restored by lymphoid cell transfer, *International Journal of Parasitology*; 21(1): 65-9.
- Jang HJ., Kokrashvili Z., Theodorakis MJ. *et al.* (2007) Gut-expressed gustducin and taste receptors regulate secretion of glucagon-like peptide-1, *PNAS USA*; 104(38): 15069–15074.
- Jia X., Cong B., Zhang J. *et al.* (2014) CCK8 negatively regulates the TLR9-induced activation of human peripheral blood pDCs by targeting TRAF6 signaling. *European Journal of Immunology*;44: 489–99.
- Jourdan PM., Lamberton PHL., Fenwick A., & Addiss DG. (2018) Soil-transmitted helminth infections. *Lancet*, 391(10117): 252-265.
- Kang SA., Choi JH., Baek KW. *et al.* (2021) *Trichinella spiralis* infection ameliorated diet-induced obesity model in mice, *International Journal of Parasitology*;51: 63–71.
- Kaplan, R. M. (2004). Drug resistance in nematodes of veterinary importance: a status report, *Trends in Parasitology*; 20: 477–481.
- Karmiris K., Koutroubakis IE., Xidakis C. *et al.* (2006). Circulating levels of leptin, adiponectin, resistin, and ghrelin in inflammatory bowel disease, *Inflammatory bowel diseases*; 12(2): 100–105.
- Kato S., Sato T., Fujita H. *et al.* (2021) Effects of GLP-1 receptor agonist on changes in the gut bacterium and the underlying mechanisms, *Scientific Reports*;11(1): 9167.
- Kenyon F., Dick JM., Smith RI. *et al.* (2013) Reduction in Greenhouse Gas Emissions Associated with Worm Control in Lambs, *Agriculture*; 3: 271-284.
- Khan WI., Richard M., Akiho H., *et al.* (2003) Modulation of Intestinal Muscle Contraction by

- Interleukin-9 (IL-9) or IL-9 Neutralisation: Correlation with Worm Expulsion in Murine Nematode Infections, *Infection Immunity*, 71: 2430-8.
- Kim JJ. & Khan WI. (2013) Goblet Cells and Mucins: Role in Innate Defense in Enteric Infection, *Pathogens*; 2: 55-70.
- Kim KS., Egan JM., & Jang HJ (2014) Denatonium induces secretion of glucagon-like peptide-1 through activation of bitter taste receptor pathways. *Diabetologia*; 57(10): 2117–2125.
- Kissow H., Hartmann B., Holst JJ. & Poulsen, S. S. (2013). Glucagon-like peptide-1 as a treatment for chemotherapy-induced mucositis, *Gut*; 62(12): 1724–1733.
- Klementowicz JE., Travis MA. & Grecis RK. (2012) *Trichuris muris*: a model of gastrointestinal parasite infection, *Seminars in Immunopathology*; 34(6): 815-828.
- Knight PA., Wright SH., Lawrence CE. *et al.* (2000) Delayed expulsion of the nematode *Trichinella spiralis* in mice lacking the mucosal mast cell-specific granule chymase, mouse mast cell protease-1, *Journal of Experimental Medicine*; 192: 1849–1856.
- Kodera R, Shikata K, Kataoka HU, *et al.* (2011) Glucagon-like peptide-1 receptor agonist ameliorates renal injury through its anti-inflammatory action without lowering blood glucose level in a rat model of type 1 diabetes. *Diabetologia*; 54: 965–978.
- Koehler JA., Baggio LL., Yusta B. *et al.* (2015) GLP-1R agonists promote normal and neoplastic intestinal growth through mechanisms requiring Fgf7, *Cell metabolism*; 21(3): 379–391.
- Kondo Y., Yoshimoto T., Yasuda K. *et al.* (2008) Administration of IL-33 induces airway hyperresponsiveness and goblet cell hyperplasia in the lungs in the absence of adaptive immune system: *International Immunology*; 20: 791-800.
- Koyama K. (2013) Evidence for bacteria-independent hatching of *Trichuris muris* eggs, *Parasitology Research*; 112: 1537-1542.
- Koyama K. (2015) Bacteria-induced hatching of *Trichuris muris* occurs without direct contact between eggs and bacteria, *Parasitology Research*; 115: 437-440.
- Kumar V., (2014) Innate lymphoid cells: New paradigm in immunology of inflammation, *Immunology Letters*; 157: 23–37.
- Kyriacou A. & Ahmed AB. (2010) Exenatide Use in the Management of Type 2 Diabetes Mellitus, *Pharmaceuticals (Basel, Switzerland)*; 3(8): 2554–2567.
- Lafferty RA., O'harte FPM., Irwin N. *et al.* (2021) Proglucagon-Derived Peptides as Therapeutics, *Frontiers in Endocrinology*; 12: 689678.
- Lambert KC., Curran EM., Judy BM. *et al.* (2005) Estrogen Receptor Alpha (ERalpha) Deficiency in Macrophages Results in Increased Stimulation of CD4+ T Cells While 17beta-estradiol Acts Through ERalpha to Increase IL-4 and GATA-3 Expression in CD4+ T cells Independent of Antigen Expression, *Journal of Immunology*; 175(9): 5716-23.
- Lamers K., Steele MA & Cangiano LR. (2023) A novel method for isolation and flow cytometry analysis of intraepithelial lymphocytes from colon biopsies, *JDS Communications*; 4(5) 433-437.
- Lamont JT., (1992) Mucus: The Front Line of Intestinal Mucosal Defense; *Annals of the New York Academy of Sciences*; 661:190-201.
- Lau J., Bloch P., Schaffer L., *et al.* (2015) Discovery of the once-weekly glucagon-like peptide-1 (GLP-1) analogue semaglutide, *Journal of Medicinal Chemistry*; 58(18): 7370–80.
- Lebrun LJ., Dusuel A., Xolin M. *et al.* (2023). Activation of TLRs Triggers GLP-1 Secretion in Mice. *International journal of molecular sciences*, 24(6), 5333.
- Lee SH., Jung BK., Park JH. *et al.* (2014). Increased intestinal epithelial cell turnover and intestinal motility in *Gymnophalloides seoi*-infected C57BL/6 mice, *The Korean journal of parasitology*; 52(3): 273–280.
- Lee YS., Park MS., Choung JS., *et al.* (2012) Glucagon-like peptide-1 inhibits adipose tissue macrophage infiltration and inflammation in an obese mouse model of diabetes. *Diabetologia*; 55: 2456–2468.
- Leslie FC, Thompson DG., McLaughlin JT. *et al.* Plasma cholecystokinin concentrations are elevated in acute upper gastrointestinal infections, *QJM: An International Journal of Medicine*; 96(11): 870–871.
- Li CK., Seth R., Gray T. *et al.* (1998) Production of proinflammatory cytokines and inflammatory mediators in human intestinal epithelial cells after invasion by *Trichinella spiralis*. *Infection and immunity*; 66(5): 2200–2206.
- Li J., Xiao C., Li C. & He J. (2025) Tissue-resident immune cells: from defining characteristics to roles in diseases, *Signal transduction and targeted therapy*; 10(1): 12.
- Li S., Ni Z., Cong B. *et al.* (2007) CCK-8 inhibits LPS-induced IL-1beta production in pulmonary

- interstitial macrophages by modulating PKA, p38, and NF-kappaB pathway, *Shock*; 27:678–86.
- Lin HV., Efanov AM., Fang X. *et al.* (2016) GPR142 controls tryptophan-induced insulin and incretin hormone secretion to improve glucose metabolism, *PLoS One*; 11: e0157298.
- Little MC., Bell LV., Cliffe LJ., *et al.* (2005) The characterization of intraepithelial lymphocytes, lamina propria leukocytes, and isolated lymphoid follicles in the large intestine of mice infected with the intestinal nematode parasite *Trichuris muris*. *Journal of Immunology*; 175: 6713–6722.
- Loukas, A., Maizels, RM. & Hotez, PJ. (2021) The yin and yang of human soil-transmitted helminth infections. *International journal for parasitology*; 51(13-14): 1243–1253.
- Luo XC., Chen ZH., Xue JB. *et al.* (2019) Infection by the parasitic helminth *Trichinella spiralis* activates a Tas2r-mediated signaling pathway in intestinal tuft cells, *PNAS USA*; 116(12): 5564–5569.
- Malizia V., Giardina F., Vegvari C. *et al.* (2021) Modelling the impact of COVID-19-related control programme interruptions on progress towards the WHO 2030 target for soil-transmitted helminths *Trans R Soc Trop Med Hyg*; 115 (3): 253-260.
- Lyu Y., Zhou Y. Shen J. (2022) An Overview of Tissue-Resident Memory T Cells in the Intestine: From Physiological Functions to Pathological Mechanisms; *Frontiers in Immunology*; 13: 912393.
- Marx N., Burgmaier M., Heinz P. *et al.* (2010) Glucagon-like peptide-1(1-37) inhibits chemokine-induced migration of human CD4 positive lymphocytes, *Cellular and Molecular Life Sciences* ;67(20): 3549-55.
- Mascarini-Serra L. (2011). Prevention of Soil-transmitted Helminth Infection. *Journal of global infectious diseases*, 3(2), 175–182.
- Massacand JC., Stettler RC., Meier R. *et al.* (2009) Helminth products bypass the need for TSLP in Th2 immune responses by directly modulating dendritic cell function. *PNAS USA*; 106(33), 13968–13973.
- McDermott JR., Bartram RE., Knight PA. *et al.* (2003) Mast cells disrupt epithelial barrier function during enteric nematode infection, *PNAS USA*;100(13):7761-7766.
- McDermott JR., Leslie FC., D'Amato M. *et al.* (2006) Immune control of food intake: enteroendocrine cells are regulated by CD4+ T lymphocytes during small intestinal inflammation, *Gut*;55(4):492-497.
- McDowell MA. & Rafati S. (2014) Neglected Tropical Diseases - Middle East and North Africa Preface, *Neglected Tropical Diseases - Middle East and North Africa*, VII-VIII.
- McGinty JW., Ting HA., Billipp TE. *et al.* (2000) Tuft-cell-derived leukotrienes drive rapid anti-helminth immunity in the small intestine but are dispensable for anti-protist immunity, *Immunity*; 52(3): 528-541.
- McKay DM., Shute A. & Lopes F. (2017) Helminths and intestinal barrier function, *Tissue barriers*, 5(1), e1283385.
- McVay CS., Bracken P., Gagliardo LF. *et al.* (2000) Antibodies to tyvelose exhibit multiple modes of interference with the epithelial niche of *Trichinella spiralis*, *Infection and Immunity*; 68(4):1912–1918.
- MHRA (2024). *MHRA approves GLP–1 receptor agonist semaglutide to reduce risk of serious heart problems in obese or overweight adults*. [online] GOV.UK. Available at: <https://www.gov.uk/government/news/mhra-approves-glp-1-receptor-agonist-semaglutide-to-reduce-risk-of-serious-heart-problems-in-obese-or-overweight-adults>.
- Mitchell PD., Salter BM., El-Gammal A., *et al.* (2016) Glucagon-Like Peptide-1 Receptor expression on human eosinophils and its regulation of eosinophil activation, *Clinical and Experimental Allergy*; 47 (3): 331-338.
- Montesor A., Trouleau W., Mupfasoni D. *et al.* (2017) Preventive chemotherapy to control of soil transmitted helminthiasis averted more than 500 thousand DALYs in 2015. *Transactions of the Royal Society of Tropical Medicine and Hygiene*;111(10):457–463.
- Moore PW., Malone K., VanValkenburg D. *et al.* (2023) GLP-1 Agonists for Weight Loss: Pharmacology and Clinical Implications, *Advances in Therapy*; 40: 723–742.
- Mort R., Ford M., Sakaue-Sawano A., *et al.* (2014) R26Fucci2aR: A global Cre-inducible cell cycle reporter mouse allowing live imaging of cell cycle progression during mouse embryonic development. *Transgenic Research*; 23(5): 855-855.
- Mort RL., Ford MJ., Sakaue-Sawano A. (2014) Fucci2a: a bicistronic cell cycle reporter that allows Cre mediated tissue specific expression in mice, *Cell cycle (Georgetown, Tex.)*; 13(17): 2681–2696.
- Moschovaki Filippidou F., Kirsch AH. Thelen M. *et al.* (2020) Glucagon-like peptide-1 receptor

- agonism improves nephrotoxic serum nephritis by inhibiting T-cell proliferation, *American Journal of Pathology*; 190(2): 400-411.
- Moser W., Schindler C. & Keiser, J. (2017) Efficacy of recommended drugs against soil transmitted helminths: systematic review and network meta-analysis, *BMJ*; 358: J4307.
- Motomura Y., Ghia JE., Wang H. *et al.* (2008) Enterochromaffin cell and 5-hydroxytryptamine responses to the same infectious agent differ in Th1 and Th2 dominant environments, *Gut*; 57(4): 475-481.
- Motomura Y., Khan WI., El-Sharkawy RT. *et al.* (2010) Mechanisms Underlying Gut Dysfunction in a Murine Model of Chronic Parasitic Infection, *American Journal of Physiology Gastrointestinal and Liver Physiology*, 299(6): G1354-G1360.
- Murrell KD. & Pozio E., (2000) Trichinellosis: the zoonosis that won't go quietly, *International Journal for Parasitology*; 30(12-13): 1339-1349.
- Nasr MB., Uusuelli V., Dellepiane S. *et al.* (2024) Glucagon-like peptide 1 receptor is a Tcell-negative costimulatory molecule, *Cell Metabolism*; 36(6): 1302-1319.e12.
- Neill DR., Wong SH., Bellosi A., *et al.* (2010). Nuocytes represent a new innate effector leukocyte that mediates type-2 immunity, *Nature*; 464: 1367-1370.
- Nery Neto JAO., Yariwake VY., Câmara NOS. & Andrade-Oliveira V. (2023) Enteroendocrine cells and gut hormones as potential targets in the crossroad of the gut-kidney axis communication. *Frontiers in pharmacology*, 14: 1248757.
- Ngwese MM., Manouana GP., Moure PAN. *et al.* (2020) Diagnostic Techniques of Soil-Transmitted Helminths: Impact on Control Measures. *Tropical Medicine and Infectious Disease*, 5(2): 93.
- NHS (2019) *Mebendazole*, Available at: <https://www.nhs.uk/medicines/mebendazole/>
- NHS (2024) *Health Survey for England 2022, Part 2: Data tables*. Available at: <https://digital.nhs.uk/data-and-information/publications/statistical/health-survey-for-england/2022-part-2/health-survey-for-england-hse-2022-part-2-data-tables>
- NICE (2025a) Liraglutide, Available at: <https://bnf.nice.org.uk/drugs/liraglutide/>
- NICE (2025b) Mebendazole Medicinal Forms, Available at: <https://bnf.nice.org.uk/drugs/mebendazole/medicinal-forms/>
- Noah TK., Kazanjian A., Whitsett J., *et al.* (2009) SAM pointed domain ETS factor (SPDEF) regulates terminal differentiation and maturation of intestinal goblet cells. *Experimental Cell Research*; 316: 452-465.
- Nozu T., Miyagishi S., Kumei S. *et al.* Glucagon-like peptide-1 analog, liraglutide, improves visceral sensation and gut permeability in rats, *Gastroenterology*; 33(1): 232-239.
- Ok KS., Kim YS, Song JH *et al.* (2009) *Trichuris trichiura* infection diagnosed by colonoscopy: case reports and review of literature, *Korean Journal of Parasitology*: 47(3): 275.
- Oka Y., Butnaru M., von Buchholtz L. *et al.* (2013). High salt recruits aversive taste pathways. *Nature*; 494(7438): 472-475.
- Okumura R. & Takeda K. (2017) Roles of intestinal epithelial cells in the maintenance of gut homeostasis. *Experimental Molecular Medicine*; 49: e338
- Oudhoff MJ., Freeman SA., Couzens AL. *et al.* (2013) Control of the Hippo Pathway by Set7-Dependent Methylation of Yap, *Developmental Cell*; 26(2): 188-194.
- Oudhoff MJ., Antignano F., Chenery AL. *et al.* (2016) Intestinal Epithelial Cell-Intrinsic Deletion of Setd7 Identifies Role for Developmental Pathways in Immunity to Helminth Infection, *PLOS Pathogens*; 12(9):e1005876.
- Owyang AM., Zaph C., Wilson EH. *et al.* (2006) Interleukin 25 regulates type 2 cytokine-dependent immunity and limits chronic inflammation in the gastrointestinal tract, *Journal of Experimental Medicine*; 203: 843-849.
- Palmeirim, MS., Hurlimann, E., Knopp, S. *et al.* (2018) Efficacy and safety of co-administered ivermectin plus albendazole for treating soil-transmitted helminths: A systematic review, metaanalysis and individual patient data analysis. *Plos Neglected Tropical Diseases*, 12(4): e0006458.
- Peradotto M., Rolle E., Zaccaria T. *et al.* (2021) An unpleasant souvenir: endoscopic finding of *Trichuris trichiura* (Nematoda: Trichuridae), *Parasitology International*; 80: 102220.
- Perniss A., Schmidt P., Soutanova A. *et al.* (2021) Development of Epithelial Cholinergic Chemosensory Cells of the Urethra and Trachea of Mice, *Cell and Tissue Research*; 385: 1-15.
- Petersen N., Frimurer TM., Terndrup Pedersen M. *et al.* (2018) Inhibiting RHOA Signaling in Mice Increases Glucose Tolerance and Numbers of Enteroendocrine and Other Secretory Cells in the Intestine, *Gastroenterology*; 155(4): 1164-1176.e2.
- Petri KCC., Ingwersen SH., Flint A. *et al.* (2018) Exposure-response analysis for evaluation of

- semaglutide dose levels in type 2 diabetes. *Diabetes Obesity and Metabolism*; 20:2238–2245
- Pike, E. H. (1969) EGG OUTPUT OF *TRICHURIS MURIS* (SCHRANK, 1788) *Journal of Parasitology*; 55(5):1046-1049.
- Plamboeck A., Holst JJ., Carr RD. & Deacon CF (2005) Neutral endopeptidase 24.11 and dipeptidyl peptidase IV are both mediators of the degradation of glucagon-like peptide 1 in the anaesthetised pig, *Diabetologia*; 48: 1882-1890.
- Potten CS. (1998). Stem cells in gastrointestinal epithelium: numbers, characteristics and death. *Philosophical transactions of the Royal Society of London. Series B, Biological sciences*, 353(1370), 821–830.
- Pozio E., Sacchini D., Sacchi L., *et al.*, (2001). Failure of mebendazole in treating *Trichinella spiralis* infection in humans at the stage of encapsulating larvae. *Clinical Infectious Diseases*; 32: 638-642.
- Pozio, E. (2007) World distribution of *Trichinella* spp. infections in animals and humans. *Veterinary Parasitology*; 149:3-21
- Prangthip P., Tummatorn J., Adisakwattana P. *et al.* (2023) Anthelmintic efficacy evaluation and mechanism of *N*-methylbenzo[d]oxazol-2-amine. *Scientific Reports*; 13: 22840.
- Pullan RL., Smith JL., Jasrasaria R., & Brooker SJ. (2014) Global numbers of infection and disease burden of soil transmitted helminth infections in 2010, *Parasite Vectors*; 7(1): 1-19.
- Qiu Y. & Yang H. (2013) Effects of Intraepithelial lymphocyte-derived cytokines on intestinal mucosal barrier function, *Journal of Interferon and Cytokine Research*; 33(10): 551-562.
- Quan H., Zhang H., Wei W. *et al.* (2016) Gender-related different effects of a combined therapy of Exenatide and Metformin on overweight or obesity patients with type 2 diabetes mellitus, *Journal of Diabetes and Its Complications*; 30: 686–692.
- Rausch S., Midha A., Kuhring M. *et al.* (2018) Parasitic Nematodes Exert Antimicrobial Activity and Benefit from Microbiota-Driven Support for Host Immune Regulation. *Frontiers in Immunology*; 9: 2282.
- Reimann F. & Gribble FM. (2002) Glucose-sensing in glucagon-like peptide-1-secreting cells. *Diabetes*; 51: 2757–2763.
- Rennie C., Fernandez R., Donnelly S. & McGrath KC. (2021) The Impact of Helminth Infection on the Incidence of Metabolic Syndrome: A Systematic Review and Meta-Analysis, *Frontiers in Endocrinology*; 12(12) (728396)
- Rhodin J. & Dalhamn T. (1956) Electron Microscopy of the Tracheal Ciliated Mucosa in Rat, *Zeitschrift für Zellforschung und mikroskopische Anatomie*; 44: 345–412.
- Richard M., Grecis RK., Humphreys NE. *et al.* (2000) Anti-IL-9 vaccination prevents worm expulsion and blood eosinophilia in *Trichuris muris* infected mice. *Proceedings of the National Academy of Sciences of the United States of America*; 97(2): 767-72.
- Rinaman L, Comer J. (2000) Antagonism of central glucagon-like peptide-1 receptors enhances lipopolysaccharide-induced fever. *Autonomic Neuroscience*; 85:98–101.
- Ritzel U., Fromme A., Oettleben M. *et al.* (1997) Release of glucagon-like peptide-1 (GLP-1) by carbohydrates in the perfused rat ileum, *Acta Diabetologica*; 34: 18–21.
- Rode AKO., Buus TB., Mraz V. *et al.* (2022) Induced Human Regulatory T Cells Express the Glucagon-like Peptide-1 Receptor, *Cells*; 11(16): 2587.
- Rose Vineer H., Morgan ER., Hertzberg H. *et al.* (2020) Increasing importance of anthelmintic resistance in European livestock: creation and meta-analysis of an open database, *Parasite (Paris, France)*; 27: 69.
- Ryan H., Flammer PG., Nicholson R., Loe L. *et al.* (2022) Reconstructing the history of helminth prevalence in the UK, *PLoS Neglected Tropical Diseases*; 16(4) e0010312.
- Sandilands EA. & Bateman DN. (2016) Opioids, *Medicine*; 44(3): 187-189.
- Saqui-Salces M., Keeley M., Grosse AS., *et al.* (2011) Gastric tuft cells express DCLK1 and are expanded in hyperplasia. *Histochemistry and Cell Biology*; 136: 191–204.
- Sasaki S., Yoneyama H., Suzuki K. *et al.* (2002) Blockade of CXCL10 protects mice from acute colitis and enhances crypt cell survival, *European Journal of Immunology*; 32(11): 3197-205.
- Schärer A., Biendl S., & Keiser J. (2023) *Trichuris muris* egg-hatching assay for anthelmintic drug discovery and characterization, *International Journal of Parasitology-Drugs and Drug Resistance*; 23:63-70.
- Selleri S. (2008) Induction of pro-inflammatory programs in enteroendocrine cells by the Toll-like receptor agonists flagellin and bacterial LPS, *International Immunology*; 20; 961-970.
- Shanmugavadivu A., Carter K., Zonouzi AP. *et al.* (2024) Protocol for the collection and analysis of the different immune cell subsets in the murine intestinal lamina propria. *Cell Press*; 5(3): 103154.
- Sher A., Coffman RL., Hieny S. *et al.* (1990). Interleukin 5 is required for the blood and tissue

- eosinophilia but not granuloma formation induced by infection with *Schistosoma mansoni*, *PNAS USA*;87(1): 61–65.
- Shiraishi D., Fujiwara Y., Komohara Y. *et al.* (2012) Glucagon-Like Peptide-1 (GLP-1) Induces M2 Polarisation of Human Macrophages via. STAT3 Activation, *Biochemical and Biophysical Research Communications*; 425: 304-308.
- Shires J., Theodoridis E. & Hayday AC., (2001) Biological insights into $\gamma\delta^+$ and TCR $\alpha\beta^+$ intraepithelial lymphocytes provided by serial analysis of gene expression (SAGE), *Immunity*; 15: 419-434.
- Shroyer NF., Wallis D., Venken KJ., *et al.* (2005) Gfi1 functions downstream of Math1 to control intestinal secretory cell subtype allocation and differentiation, *Genes and Development*; 19: 2412–2417.
- Sinha R., Rajesh A., Rawat S. *et al.* (2012) Infections and infestations of the gastrointestinal tract, Part 2: parasitic and other infections, *Clinical Radiology*; 67(5): 495-504.
- Speich B., Ame SM., Ali SM. *et al.* (2014) Oxantel Pamoate-Albendazole for *Trichuris trichiura* Infection, *New England Journal of Medicine*; 370(7): 610-620.
- Steinert RE, Gerspach AC, Gutmann H. *et al.* (2011) The functional involvement of gut-expressed sweet taste receptors in glucose-stimulated secretion of glucagon-like peptide-1 (GLP-1) and peptide YY (PYY), *Clinical Nutrition*; 30: 524-532.
- Stephenson L., Holland C & Cooper E. (2000) The Public Health Significance of *Trichuris Trichiura*, *Parasitology*; 121(S1): S73-S95.
- Sternini C., Anselmi L., & Rozengurt E. (2008) Enteroendocrine cells: a site of “taste“ in the gastrointestinal chemosensing, *Current Opinion in Endocrinology, Diabetes and Obesity*; 15(1):73–78.
- Sugimoto H., Oda S., Otsuki T. *et al.* (2006) Crystal structure of human indoleamine 2, 3-dioxygenase: Catalytic mechanism of O₂ incorporation by a heme-containing dioxygenase, *PNAS USA*;103: 2611–2616.
- Svendsen B. (2015) An analysis of cosecretion and coexpression of gut hormones from male rat proximal and distal small intestine, *Endocrinology*; 156:847-857.
- Svendsen, B. (2016) GLP1- and GIP-producing cells rarely overlap and differ by bombesin receptor-2 expression and responsiveness *Journal of Endocrinology*; 228:39-48.
- Taghipour A., Ghodsian S., Jabbari M. *et al.* (2021) Global prevalence of intestinal parasitic infections and associated risk factors in pregnant women: a systematic review and meta-analysis, *Transactions of the Royal Society of Tropical Medicine and Hygiene*; 115(5): 457-470.
- Thompson EA., Mitchell JS., Beura LK., *et al.* (2019) Interstitial Migration of CD8 Alpha Beta T Cells in the Small Intestine Is Dynamic and Is Dictated by Environmental Cues, *Cell Reports*; 26(11):2859–67.
- Thorkildsen C., Neve S., Larsen BD., *et al.* (2003) Glucagon-like peptide 1 receptor agonist ZP10 A increases insulin mRNA expression and prevents diabetic progression in db/db mice, *Journal of Pharmacology and Experimental Therapeutics*; 307: 490–496.
- Thornton DJ., Rousseau K., McGuckin MA. (2008) Structure and function of the polymeric mucins in air-ways mucus, *Annual Review of Physiology*; 70:459–486.
- Tracey E., McDermott RA. & McDonald MI. (2016) Do worms protect against the metabolic syndrome? A systematic review and meta-analysis, *Diabetes Research and Clinical Practice*; 120: 209-220.
- Tran HTT., Stetter R., Herz C. *et al.* (2021) Allyl Isothiocyanate: A TAS2R38 Receptor-Dependent Immune Modulator at the Interface Between Personalized Medicine and Nutrition, *Frontiers in immunology*; 12: 669005.
- Tsai CY., Lu HC., Chou YH. *et al.* (2021) Gut microbial signatures for glycemic responses of GLP-1 receptor agonists in type 2 diabetic patients: a pilot study, *Frontiers in Endocrinology*; 12: 814770.
- Tsubokawa D., Nakamura T., Goso Y. *et al.*, (2009) *Nippostrongylus brasiliensis*: increase of sialomucins reacting with anti-mucin monoclonal antibody HCM31 in rat small intestinal mucosa with primary infection and reinfection, *Experimental Parasitology*; 123: 319-325.
- Urban JF., Jr, Schopf L., Morris SC. *et al.* (2000). Stat6 signaling promotes protective immunity against *Trichinella spiralis* through a mast cell- and T cell-dependent mechanism. *Journal of immunology*; 164(4): 2046–2052.
- Vallance BA., Matthaehi KI., Sanovic S. *et al.* (2000) Interleukin-5 deficient mice exhibit impaired host defence against challenge *Trichinella spiralis* infections. *Parasite immunology*; 22(10): 487–492.
- von Moltke J., Ji M., Liang HE. & Locksley RM (2016) Tuft-cell-derived IL-25 regulates an intestinal ILC2-epithelial response circuit, *Nature*; 529(7585): 221–225.

- Wang Q., Lin H., Shen C., *et al.* (2023) Gut microbiota regulates postprandial GLP-1 response via ileal bile acid-TGR5 signaling. *Gut Microbes*, 15(2).
- Wang Q., Farhadipour M., Thijs T. *et al.* (2024) Bitter-tasting drugs tune GDF15 and GLP-1 expression via bitter taste or motilin receptors in the intestine of patients with obesity, *Molecular Metabolism*; 88: 102002.
- Watanabe N., Katakura K., Kobayashi A., *et al.* (1988) Protective immunity and eosinophilia in IgE-deficient SJA/9 mice infected with *Nippostrongylus brasiliensis* and *Trichinella spiralis*. *PNAS USA*; 85:4460–2.
- Werner U., Haschke G., Herling AW. & Kramer W. (2010) Pharmacological profile of lixisenatide: A new GLP-1 receptor agonist for the treatment of type 2 diabetes, *Regulatory Peptides*; 164(2-3): 58-64.
- Wong CK., Yusta B., Koehler JA. *Et al.* (2022) Divergent roles for the gut intraepithelial lymphocyte GLP-1R in control of metabolism, microbiota and T cell induced inflammation, *Cell Metabolism*; 34(10): 1514-1531.
- World Health Organisation (2017) *Guideline: Preventative chemotherapy to control soil-transmitted helminth infections in at-risk population groups*, Geneva, Switzerland: World Health Organisation. Available at: <https://www.who.int/publications/i/item/9789241550116>
- World Health Organisation (2024). *Obesity and overweight*. Available at: <https://www.who.int/news-room/fact-sheets/detail/obesity-and-overweight>.
- Worthington JJ., Reimann F. & Gribble, F. (2018) Enteroendocrine cells-sensory sentinels of the intestinal environment and orchestrators of mucosal immunity. *Mucosal Immunology*; 11: 3–20.
- Wright SG., (2012) Protozoan Infections of the Gastrointestinal Tract, *Infectious Disease Clinics of North America*; 26(2): 323-339.
- Xiao Q., Boushey RP., Cino M. *et al.* (2000) Circulating levels of glucagon-like peptide-2 in human subjects with inflammatory bowel disease, *American journal of physiology. Regulatory, integrative and comparative physiology*; 278(4): R1057–R1063.
- Xing Z., Liu S. & He X. (2024) Critical and diverse role of alarmin cytokines in parasitic infections, *Frontiers in cellular and infection microbiology*; 14: 1418500.
- Yan D., Jin C., Xiao XH. *et al.* (2008) Antimicrobial properties of berberines alkaloids in *Coptis chinensis* Franch by microcalorimetry, *Journal of Biochemical and Biophysical Methods*; 70(6): 845-849.
- Yan SW., Cheng YK., Lu QQ. *et al.* (2024) Characterisation of a novel dipeptidyl peptidase 1 of *Trichinella spiralis* and its participation in larval invasion, *Acta Tropica*; 249: 107076.
- Yang S., Gaafar SM & Bottoms GD. (1990) Effects of multiple dose infections with ascaris-suum on blood gastrointestinal hormone levels in pigs, *Veterinary Parasitology*; 37: 31-44.
- Yousefi Y., Haq S., Banksota S. *et al.* (2021) *Trichuris muris* Model; Role in Understanding Intestinal Immune Response, Inflammation and Host Defense, *Pathogens*; 10(8): 925.
- Yu Y., Hao G., Zhang Q. *et al.* (2015) Berberine induces GLP-1 secretion through activation of bitter taste receptor pathways, *Biochemical Pharmacology*; 97(2): 173-177.
- Yusta B., Baggio LL., Koehler J., *et al.* (2015) GLP-1R Agonists Modulate Enteric Immune Responses Through the Intestinal Intraepithelial Lymphocyte GLP-1R. *Diabetes*; 64 (7): 2537–2549.
- Zaph C., Cooper PJ., & Harris N.(2014) Mucosal immune responses following intestinal nematode infection, *Parasite Immunology*; 36(9): 439-452.
- Zarrinpar A., Chaix A., Xu ZZ. *et al.* (2018) Antibiotic-induced microbiome depletion alters metabolic homeostasis by affecting gut signaling and colonic metabolism, *Nature Communications*; 9(1): 2872.
- Zeng Y., Wu Y., Zhang Q., & Xiao X. (2024) Crosstalk between glucagon-like peptide 1 and gut microbiota in metabolic diseases, *mBio*;15: e02032-23.
- Zhang JG., Cong B., Li QX. *et al.* (2011) Cholecystokinin octapeptide regulates lipopolysaccharide-activated B cells co-stimulatory molecule expression and cytokines production *in vitro*; *Immunopharmacology and Immunotoxicology*; 33: 157–63.
- Zhao A., & Miller M., (2021) Isothiocyanates in Brassica Vegetables Induce Glucagon-Like Peptide-1 Secretion in Enteroendocrine Cells Through Intestinal Bitter Taste Receptors, *Current Developments in Nutrition*; 5(S2): 386.
- Zhao L., Zhang F., Ding Z. *et al.* (2018) Gut bacteria selectively promoted by dietary fibres alleviate type 2 diabetes; *Science*; 359(6380): 1151-1156.
- Zhu J., Yamane H., Cote-Sierra J., *et al.* (2006) GATA-3 promotes Th2 responses through three different mechanisms: induction of Th2 cytokine production, selective growth of Th2 cells and inhibition of Th1 cell-specific factors. *Cell Research*; 16(1): 3-10.

Zietek T., & Rath E. (2016) Inflammation Meets Metabolic Disease: Gut Feeling Mediated by GLP-1.
Frontiers in Immunology; 22(7): 154.